2020

The Biology of the Influenza D Virus

Jieshi Yu
South Dakota State University

THE BIOLOGY OF THE INFLUENZA D VIRUS

BY

JIESHI YU

A dissertation submitted in partial fulfillment of the requirements for the

Doctor of Philosophy

Major in Biological Sciences

Specialization in Microbiology

South Dakota State University

2020

DISSERTATION ACCEPTANCE PAGE

Jieshi Yu

This dissertation is approved as a creditable and independent investigation by a candidate for the Doctor of Philosophy degree and is acceptable for meeting the dissertation requirements for this degree. Acceptance of this does not imply that the conclusions reached by the candidate are necessarily the conclusions of the major department.

Feng Li
Advisor Date

Volker Brozel
Department Head Date

Dean, Graduate School Date

This dissertation is dedicated to my advisors, Dr. Feng Li and Dr. Dan Wang who guided and supported me over the years.

ACKNOWLEDGEMENTS

I would especially like to thank my family for giving me the constant love, support, understanding and encouragement. In particular, I would like to thank my parents, my wife, and my sisters. Without your help and support, I wouldn't have achieved so much.

I would like to thank my advisors, Dr. Feng Li and Dr. Dan Wang for guiding me, supporting me, and caring for me, in my life, study and work over the years. You have given me the warmth and comfort like at home though I am in a foreign country. You have set examples of outstanding as researchers, mentors, and instructors.

I would like to thank my committee members Dr. Radhey Kaushik, Dr. Eric Nelson, and Dr. Suzette Burckhard. You provided amazing feedback and helpful guidance throughout the process of my study and research at South Dakota State University.

I would like to thank the former and current Li and Wang Lab members: Dr. Chithra Sreenivasan (a friendly and knowledgeable expert in animal experiments), Dr. Chen Huang, Rongyuan Gao, Sunayana Shyam Jandhyala, Shamiq Aftab, Tirth Uprety, Dr. Ben Hause, Dr. Shaolun Zhai, Dr. Zhao Wang, Dr. Runxia Liu, Hunter Nedland, Busha Hika, Jared Wollman, Kabir Md Imtiazul, and Katherine Meyer for your great help and co-operation in my research work.

I would also like to thank Dr. Bin Zhou and Dr. Zizhang Sheng for your invaluable contributions towards my research projects. I gratefully acknowledge Dr. Steven Lawson, Aaron Singrey, Amanda Zubke and Travis Clement for your help in my animal experiments and research.

I would like to thank my friends Dr. Zhanxin Wang and Zengbin Ma who have always been a huge support and encouragement to me for pursuing higher education abroad. I also wish to express my sincere thanks to Dr. Hexiao Zhang and Dr. Zhiguang Ran who recommended me to study with Dr. Feng Li in South Dakota State University.

CONTENTS

ABBREVIATIONS x

LIST OF FIGURES xii

LIST OF TABLES xiv

ABSTRACT xv

CHAPTER 1. INTRODUCTION 1

1.1 Overview of the four types of influenza viruses 1

1.1.1 Taxonomy and classification 1

1.1.2 Genomes and viral particles of influenza A, B, C, and D viruses 2

1.1.3 General characteristics of the four types of influenza viruses 4

1.2 The biology of the influenza D virus 9

1.2.1 Epidemiology of IDV worldwide 9

1.2.1.1 IDV in North America 9

1.2.1.2 IDV in Europe 12

1.2.1.3 IDV in Asia 16

1.2.1.4 IDV in Africa 18

1.2.2 Pathogenicity and zoonotic potential of IDV 19

1.2.2.1 Pathogenicity of IDV in swine and cattle 19

1.2.2.2 Pathogenicity of IDV in other animals 22

1.2.2.3 Zoonotic potential of IDV 23

1.2.3 Novel biology of IDV 25

1.3 Research Aims 29

1.3.1 Hypothesis 29

1.3.2 Specific Aims 30

CHAPTER 2. THE HEMAGGLUTININ-ESTERASE FUSION GLYCOPROTEIN IS A PRIMARY DETERMINANT OF THE EXCEPTIONAL THERMAL AND ACID STABILITY OF INFLUENZA D VIRUS 31

2.1 Introduction 31

2.2 Methods, results and discussion 33

CHAPTER 3. DEVELOPMENT AND CHARACTERIZATION OF A REVERSE-GENETICS SYSTEM FOR INFLUENZA D VIRUS 42

3.1 Introduction 42

3.2 Results 46

3.2.1 Generation of infectious influenza D/swine/Oklahoma/1314/2011 virus by the reverse-genetics system 46

3.2.2 Replication kinetics of continuously passaged influenza D/OK-RGS viruses at different temperatures 48

3.2.3 Receptor binding of the wild-type D/OK and rescued D/OK-RGS viruses 50

3.2.4 Activity of the IDV RNP complex with PB1-E697K or PB2-L462F mutation 53

3.2.5 Recognition and transcription of the heterotypic promoter sequence by the IDV polymerase complex 57

3.3 Discussion 62

3.4 Materials and methods 67

3.4.1 Cells, viruses, and antibodies 67

3.4.2 Construction of plasmids 67
3.4.3 Transfection and rescue of recombinant viruses 68
3.4.4 Virus replication assay 69
3.4.5 Hemagglutination-based competitive inhibition assay 70
3.4.6 Minigenome replication assay 70
3.4.7 Statistical analysis 71
CHAPTER 4. IDENTIFICATION OF TWO RESIDUES WITHIN THE NUCLEOPROTEIN THAT CRITICALLY AFFECT THE REPLICATION FITNESS OF INFLUENZA D VIRUS 72
4.1 Introduction 72
4.2 Results 75
4.2.1 The D/660 virus was superior to the D/OK virus in replication in different cell lines 75
4.2.2 NP was a key determinant of the replication difference between the D/660 and D/OK viruses 78
4.2.3 Two residues in positions 247 and 381 within the NP protein were key determinants of the replication fitness of IDV 80
4.2.4 Amino acid changes in NP had no effect on IDV RNP activity but might affect virus replication in the late stage of the viral life cycle 83
4.3 Discussion 87
4.4 Materials and Methods 90
4.4.1 Cells and viruses 90
4.4.2 Antibodies and regents 91

4.4.3 Plasmid construction and reverse genetics 91

4.4.4 Viral replication kinetics assay 92

4.4.5 Minigenome replication assay 92

4.4.6 Structural modeling 93

4.4.7 Droplet Digital PCR 93

4.4.8 Statistical analysis 94

CHAPTER 5. CONCLUSIONS AND FUTURE DIRECTIONS 95

LIST OF REFERENCES 98

ABBREVIATIONS

BRD: Bovine respiratory disease

cRNA: Complementary RNA

C/Vic: C/Victoria/2/2012

DMEM: Dulbecco's modified Eagle medium

D/OK: D/swine/Oklahoma/1314/2011

D/660: D/Bovine/Oklahoma/660/2013

GFP: Green fluorescent protein

HA: Hemagglutinin

hAECs: Well-differentiated human airway epithelial cells

HEF: Hemagglutinin esterase fusion

HI: Hemagglutination inhibition

IAV: Influenza A virus

IBV: Influenza B virus

ICV: Influenza C virus

ICTV: International Committee on Taxonomy of Viruses

IDV: Influenza D virus

MDCK: Madin-Darby canine kidney

MOI: Multiplicity of infection

NA: Neuraminidase

NCRs: Non-coding regions

Neu5Gc9Ac: 9-O-acetylated N-glycolylneuraminic acid

Neu5,9Ac_2: N-acetyl-9-O-acetylneuraminic acid

PBS: Phosphate-buffered saline

PEI: Polyethylenimine

Pol I: RNA polymerase I

RBP: Receptor-binding pocket

RGS: Reverse genetics system

RNP: Ribonucleoprotein

SA: Sialic acid

SARS-CoV: Severe acute respiratory syndrome coronavirus

TCID50: 50% tissue culture infective doses

TPCK: Tosylsulfonyl phenylalanyl chloromethyl ketone

LIST OF FIGURES

Figure 1-1. Schematic of IAV/IBV and ICV/IDV……..……3

Figure 1-2. Phylogenetic tree of the HEF gene of IDV at the nucleotide level……14

Figure 1-3. Global distribution of IDV…….……16

Figure 1-4. Schematic illustration of the HA/HEF ……...…27

Figure 1-5. Splicing strategies of influenza viruses for the NS and M segments……29

Figure 2-1. Thermal and pH stability of influenza viruses …….……34

Figure 2-2. HEF is a key determinant of the exceptional acid and temperature stability of IDV ……37

Figure 3-1. Generation of infectious influenza D/swine/Oklahoma/1314/2011 virus by the reverse-genetics system ……47

Figure 3-2. Growth kinetics of continuously passaged influenza D/OK-RGS viruses at different temperatures ……49

Figure 3-3. Receptor-binding properties of the wild-type D/OK virus and the recombinant D/OK-RGS virus ……...……51

Figure 3-4. Activity of the IDV RNP complex with the PB1-E697K or PB2-L462F mutation ……...……54

Figure 3-5. Activities of IDV and ICV RNP complexes with the conserved cognate or noncognate noncoding ends of vRNA segments ……59

Figure 4-1. Replication kinetics of D/660 and D/OK viruses in different cell lines...……77

Figure 4-2. NP determines the replication difference between the D/660 and D/OK viruses.……...…79

Figure 4-3. Two residues in positions 247 and 381 within the NP protein were key determinants of the replication fitness of IDV……82

Figure 4-4. Amino acid changes in NP had no effect on IDV RNP activity but might affect virus replication in the late stage of the viral life cycles…….85

LIST OF TABLES

Table 1-1. General characteristics of the four types of influenza viruses……..……5

Table 1-2. The epidemiology of IDV worldwide…….…..……..…15

Table 1-3. Replication, pathogenicity and transmission of IDV in experimentally infected animals …….19

Table 3-1. Primers used in the RT-PCR and cloning experiments……..……69

Table 3-2. Comparison of the conserved 3’-noncoding ends of the vRNA segments from influenza C and D viruses ……..……70

ABSTRACT

THE BIOLOGY OF THE INFLUENZA D VIRUS

JIESHI YU

2020

Influenza D virus (IDV) was first identified in 2011 from clinically ill pigs in America. In nearly a decade since its discovery, the virus has been detected in multiple animal species in a vast region of the globe and is considered an important cause of concern to animal and human health. IDV utilizes cattle as the primary reservoir. The viral infection can cause mild respiratory disease in cattle and has been indicated as a causative agent of bovine respiratory disease (BRD) complex that is the most common and costly disease affecting the cattle industry. Moreover, outbreaks of IDV in swine and bovine are increasing, and more genetic and serological evidences show that IDV has a potential to adapt to humans.

IDV is unique among four types of influenza viruses. The thermal and acid stability of IDV were examined and directly compared with those of influenza A virus (IAV), influenza B virus (IBV), and influenza C virus (ICV). The results of our experiments demonstrated that only IDV had a high residual infectivity (~2.5 log units of 50% tissue culture infective dose ([TCID50]/ml) after a 60-min exposure to 53°C in solution at a neutral pH, and remarkably, IDV retained this infectivity even after exposure to 53°C for 120 min. Furthermore, the data showed that IDV was extremely resistant to inactivation

by low pH. After being treated at pH 3.0 for 30 min, IDV lost only approximately 20% of its original infectiousness, while all other types of influenza viruses were completely inactivated. Finally, replacement of the hemagglutinin (HA) and neuraminidase (NA) proteins of a temperature- and acid-sensitive IAV with the hemagglutinin-esterase fusion (HEF) protein of a stable IDV through a reverse genetic system largely rendered the recombinant IAVs resistant to high-temperature and low-pH treatments. Together, these results indicated that the HEF glycoprotein is a primary determinant of the exceptional temperature and acid tolerance of IDV. Further investigation into the viral entry and fusion mechanism mediated by the intrinsically stable HEF protein of IDV may offer novel insights into how the fusion machinery of influenza viruses evolve to achieve acid and thermal stability, which as a result promotes the potential to transmit across mammal species.

To better study IDV at the molecular level, a reverse-genetics system (RGS) is urgently needed, but to date, no RGS had been described for IDV. In this study, we rescued the recombinant influenza D/swine/Oklahoma/1314/2011 (D/OK) virus by using a bidirectional seven-plasmid based system and further characterized rescued viruses in terms of growth kinetics, replication stability, and receptor-binding capacity. Our results collectively demonstrated that RGS-derived viruses resembled the parental viruses for these properties, thereby supporting the utility of this RGS to study IDV infection biology. In addition, we developed an IDV minigenome replication assay and identified the E697K mutation in PB1 and the L462F mutation in PB2 that directly affected the activity of the IDV ribonucleoprotein (RNP) complex, resulting in either attenuated or

replication-incompetent viruses. Finally, by using the minigenome replication assay, we demonstrated that a single nucleotide polymorphism at position 5 of the 3' conserved noncoding region in IDV and influenza C virus (ICV) resulted in the inefficient cross-recognition of the heterotypic promoter by the viral RNP complex. In conclusion, we successfully developed a minigenome replication assay and a robust reverse-genetics system that can be used to further study replication, tropism, and pathogenesis of IDV.

Based on the sequences of the hemagglutinin-esterase-fusion (HEF) gene, IDV can be classified into three genetic lineages: D/OK-lineage, D/660-lineage and D/Japan-lineage. The D/swine/Oklahoma/1334/2011 (D/OK) and D/Bovine/Oklahoma/660/2013 (D/660) are the representative strains of the D/OK-, and D/660 -lineages, respectively. We found that the replication of the D/OK virus was approximately 2 $\log_{10}$TCID50/ml lower than that of the D660 virus in different cell lines. Interestingly, by using our reverse genetics system, we generated recombinant chimeric D/OK viruses in that one of each genomic segments was replaced with the segment from the D660 virus, and observed that only the replication fitness of the chimeric D/OK virus with the D660 NP segment was significantly increased. Finally, we identified two positions 247 and 381 within the NP protein were key determinants of the replication difference between the D/OK and D660 viruses. Interestingly, theses amino acid changes in the NP had no effect on IDV RNP activity but may affect virus replication in the late stage of the viral life cycles, which warrants further investigation.

CHAPTER 1. INTRODUCTION

1.1 Overview of the four types of influenza viruses

1.1.1 Taxonomy and classification

Influenza viruses are enveloped, segmented, single-stranded, negative-sense RNA viruses, and belong to the *Orthomyxoviridae* family. Four influenza genera, *Alphainfluenzavirus* (Species: *Influenza A virus*), *Betainfluenzavirus* (Species: *Influenza B virus*), *Gammainfluenzavirus* (Species: *Influenza C virus*) and *Deltainfluenzavirus* (Species: *Influenza D virus*) (*1*), are classified on the basis of antigenic differences in the nucleocapsid protein (NP) and matrix protein (M). Influenza A virus (IAV) can be further divided into subtypes based on the haemagglutinin (HA) and neuraminidase (NA) glycoproteins. To date, 18 different HA subtypes (H1-H18) and 11 different NA subtypes (N1-N11) have been identified in IAV. Three subtypes of IAV, H1N1, H2N2 (circulated from 1957 to 1968) and H3N2, have been found circulated in humans (*2*). Influenza B virus (IBV), according to the major surface HA antigen, can be broken down into two lineages (B/Yamagata and B/Victoria) (*1*). Influenza C virus (ICV) has six evolutionary lineages represented by Taylor/47, Kanagawa/1/76, Yamagata/26/81, Aichi/1/81, Sao Paulo/378/82, and Mississippi/80 (*3*). Influenza D virus (IDV) was first isolated in 2011 (*4*) and officially named in 2016 (*https://www.cdc.gov/flu/about/viruses/types.htm*). IDV can be genetically classified into three lineages: D/OK-, D/660-, and D/Japan-lineages, based on the hemagglutinin-esterase-fusion (HEF) gene (*5*).

1.1.2 Genomes and viral particles of influenza A, B, C, and D viruses

The influenza A and B virus genomes each consist of eight segments, while influenza C and D virus genomes each contain seven segments (Figure. 1-1). The three longest segments of influenza viruses encode the polymerase subunits PB2, PB1 and PA/P3, respectively. In some IAV strains, the PB1 segment can also produce a small accessory protein (PB1-F2) in a +1 alternative reading frame, which can induce apoptosis and play a role in killing host immune cells (*6*). The fourth longest segment of ICV/IDV codes for the only one surface glycoprotein HEF, while IAV and IBV contain two segments (the fourth and sixth segments) encoding two surface glycoproteins HA and NA, respectively (Figure 1-1). The sixth longest segment of IBV (NA) can also encodes the NB matrix protein in a -1 alternate reading frame (*7*). The fifth longest segment of influenza viruses encodes nucleoprotein (NP). The last shortest two segments (M and NS segments) each produce two proteins, M1 and M2 from the M segment, and NS1 and NS2 from the NS segment, respectively, by different expression strategies.

Influenza viruses are enveloped particles with a diameter of 80 to 120 nm. IAV and IBV have two major surface glycoproteins (HA and NA) embedded in the envelope, forming the outer spikes of the virus particle (Figure 1-1). HA recognizes the cellular receptor and fuses the viral membrane to the cellular membrane for the entry, while NA removes the receptor from the cell surface and plays a role in virus release. ICV and IDV have only one spike protein (HEF) in the viral membrane (Figure 1-1). Three functions are combined in HEF protein: receptor binding, membrane fusion and esterase activity as compared to the functions in both HA and NA proteins of IAV and IBV (*8*). In addition

to spike proteins, M2 protein is also embedded into the viral membrane (Figure 1-1), which acts as an ion channel (*9, 10*). M1 protein, serving as a matrix protein, is attached to the inner leaflet of the lipid bilayer (Figure 1-1) (*10*). Inside the enveloped virion, the viral genome segments are coated by the nucleoprotein (NP). NP together with the RNA polymerase components (PB2, PB1, and PA/P3) form the viral ribonucleoprotein complexes (vRNPs) (Figure 1-1) that are essential for transcribing all virally encoded mRNAs and for replicating all viral genome RNA (vRNA) segments. Each vRNA segment exists in the form of a vRNP. It is known that IAV and IBV package eight vRNPs arranged in a "1+7" pattern into their virions (*11, 12*). Interestingly, ICV and IDV also package eight vRNPs arranged in the "1+7" pattern though they only have seven genome segments (*13*). It is still unclear what is the mysterious eighth vRNP observed in the virions of ICV and IDV.

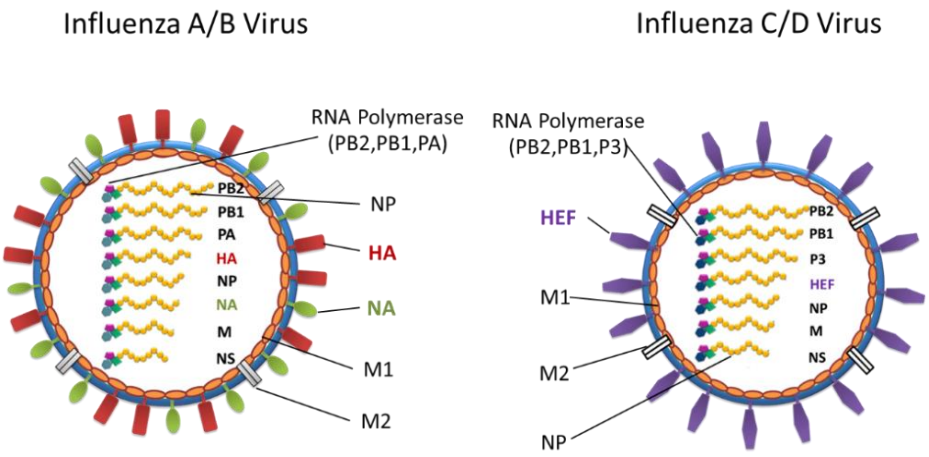

Figure 1-1, Schematic presentation of IAV/IBV and ICV/IDV. Influenza A and B virus particles possess 8 genomic segments (left), while influenza C and D virus particles contain 7 genomic segments (right). The envelope and membrane proteins HEF (ICV/IDV), HA and NA (IAV/IBV),

and M2 overlay the M1 matrix, which enfolds the virion core. Each vRNA segment forms an RNP together with the NP and RNA polymerase proteins (PB2, PB1, and PA/P3).

1.1.3 General characteristics of the four types of influenza viruses

Among the four types of influenza viruses (Table 1-1), IAV is the most common and the most pathogenic, causing seasonal epidemics every year and on some occasions, worldwide pandemics. IAV infects a wide variety of hosts including humans, birds, horses, pigs, dogs and marine mammals (*2, 14*). Waterfowl are the major reservoir of IAV and the amplification host harboring all different subtypes of viruses with the potential reassortment, producing new antigenic variants to which humans do not have pre-existing immunity (*15*). Bird-origin influenza viruses can cross the species barrier and infect humans to cause pandemics. There were three recorded pandemics in the last century, including the 1918 H1N1 Spanish pandemic, the 1957 H2N2 Asian pandemic, and the 1968 Hong Kong pandemic (*16*). In 2009, a novel swine-origin H1N1 influenza virus emerged to cause the first human influenza pandemic of the 21st century (*2*). In addition, various other influenza A viruses of pig- and bird-origin, such as H5, H6, H7, H9, and H10, also have the capacity to infect and spread among humans and, in some cases, result in severe disease and death (*2, 16*). IBV, like IAV, can cause seasonal epidemics in humans but lacks the ability to trigger influenza pandemic. Approximately 25% of the influenza cases are caused by IBV infection, and sometimes IBV can dominate influenza seasons like the 2017-2018 seasonal influenza in Europe (*17*). IBV utilizes human as the primary reservoir (*18*). Although there were cases of IBV crossing over from humans to other species, such as the IBV outbreak in seals in The Netherlands

in 1999, IBV is largely restricted to circulate in humans (*18*). ICV is not thought to cause epidemics and only cause mild clinical symptoms in humans (*19*). The main reservoir of ICV is humans, but it also infects pigs, dogs, and bovines (*20*). IDV uses cattle as the primary reservoir and can be transmitted from cattle to swine (*4*, *21*, *22*). Antibodies specific for IDV were detected in horses, small ruminants, wild boars, camels, and humans especially with cattle exposure (*23-26*), indicating that IDV may have a wide host range and can spread from cattle to humans or other animal species.

Table 1-1. General characteristics of the four types of influenza viruses

	IAV	IBV	ICV	IDV
Severity of illness	++++	++	+	+
Reservoir	Waterfowl	Human	Human	Bovine
Human epidemics	Yes	Yes	No	No
Human pandemics	Yes	No	No	No
Animal hosts	Birds, horses, pigs, dogs, and marine mammals	Seals	Pigs and dogs	Pigs, cattle, goats, sheep, horses and camels
Antigenic changes	Shift and drift	Drift only	Drift only	Drift only
Genome	8 segments	8 segments	7 segments	7 segments
Glycoproteins	HA, NA	HA, NA	HEF	HEF
Receptors	α-2,3 or α-2, 6-linked sialic acids		$Neu5,9Ac_2$	Neu5Gc9Ac and $Neu5,9Ac_2$

Viral attachment to receptors on the host cell surface is the initial step of the virus life cycle. Sialic acid (SA) has been found to serve as a receptor of many important human and animal pathogens, including influenza, parainfluenza, corona, noro, rota, mumps, and

DNA tumor viruses (*8*). SA is the member of the large family molecules derived from neuraminic acid, which is a monosaccharide containing a nine-carbon backbone, ubiquitously expressed in higher vertebrates (*27, 28*). *N*-acetylneuraminic acid (Neu5Ac) and *N*-glycolylneuraminic acid (Neu5Gc) are the most common SAs found on mammalian cell surfaces, both of which are ligands for influenza viruses. SAs are generally attached to glycan chains of glycoproteins or glycolipids via different glycosidic linkages. The most frequent linkage types are α2,3-linkage and α2,6-linkage to a galactose residue. IAV and IBV only recognize α2,3- or α2,6-linked sialic acid moieties as receptors (*8*) (Table 1-1). However, ICV utilizes *N*-acetyl-9-*O*-acetylneuraminic acid (Neu5,9Ac_2) (Table 1-1) that has an additional *O*-acetyl group at C9 position as the receptor, which is independent of α2,3- or α2,6-linkage to the following galactosyl residue (*20*). IDV surface glycoprotein HEF can bind both *N*-acetyl-9-*O*-acetylneuraminic acid (Neu5,9Ac_2) and 9-*O*-acetylated *N*-glycolylneuraminic acid (Neu5Gc9Ac) (Table 1-1) regardless the α2,3- or α2,6-linkage, which indicates IDV uses these 9-O-Ac-SAs as its receptor for entry into the cell (*29, 30*). Almost all viruses attach to the cell membrane via their surface proteins binding to the specific receptors on the host cells. The specificity and affinity of the interaction between influenza virus surface glycoproteins and SA receptors contribute to the viral tissue tropism, host range, pathogenesis, and transmission.

It is generally accepted that avian influenza A viruses preferentially bind to α2,3-linked SAs and replicate in the gastrointestinal tract of the host, while human influenza A viruses have a higher affinity for α2,6-linked SAs that are expressed in the upper

respiratory tract of humans (*2, 31*). Pigs have been shown to express high levels of both α2,3- and α2,6-linked SAs in their respiratory epithelial cells, possibly serving as a mixing vessel that allow for binding of both avian and human influenza viruses (*2, 32*). IBV has a relatively low receptor-binding affinity compared with IAV (*18, 33*). However, more studies are needed to know if the receptor-binding specificity and affinity determine the pathogenicity and restricted host range of IBV. Structure studies show that IDV HEF has an open channel in the receptor-binding pocket (RBP), while in the structurally identical site of ICV HEF, there is a salt bridge (*29*). It has been suggested that the more open receptor binding cavity of IDV HEF contributes to the broader receptor binding and broad tissue tropism of IDV when compared to that of ICV (*22, 29, 30*).

Following attachment, the influenza virus is endocytosed and traffics to the acidic endosomes. The acidic condition facilitates a conformational change in the HA/HEF, exposing the fusion peptide that mediates the fusion of the viral envelop with the endosomal membrane (*34*). At some point, the lower pH activates the M2 ion channel, which as a result, pumps the hydrogen ions from the endosome into the virus particle (*35*). Further acidification of the viral interior causes the disruption of the M1 lattice, which enables the release of the viral RNPs into the host cytoplasm (*34, 36*). After released from the virion, RNPs are transported to the cellular nucleus where all influenza virus RNAs are synthesized. Using the negative-sense vRNA as a template, viral mRNA and complementary RNA (cRNA) are produced. The mRNA is then used for viral protein synthesis in the cytoplasm, and the cRNA templates are used subsequently for generation of more vRNA copies in the nucleus (*34*). The newly synthesized vRNA copies, viral

polymerase (PB2, PB1, PA/P3) and NP are assembled into the new vRNPs. Once assembled, the new vRNPs are then exported from the nucleus with the help provided by NS2 protein (NEP) and eventually destined to the lipid raft domain of the plasma membrane for packaging into assembled and budding progeny influenza virions (*37*). Until now, it remains unclear how influenza virus packages all its different vRNPs into a progeny virion. Following budding driven by concerted action of HA/HEF and M2 proteins from the cell surface of an infected cell, the influenza virus spike proteins continue to bind to the SAs embedded on the plasma membrane. Influenza virus release to extracellular space is dependent on the sialidase activity of NA in IAV and IBV, or the esterase activity of HEF in ICV and IDV (*20*, *37*). To release freshly budded viral particles from the host cells, the NA performs receptor destroying activity to cleave the terminal sialic acid residue from cell-surface glycoproteins and gangliosides, while the HEF utilizes its esterase activity to remove the acetyl group from position C9 of Neu5,9Ac_2 (*20*). From primary virus attachment to progeny virus release, all influenza viruses share similar steps in their replication cycles, but different types of the viruses behave diversely in each step of the life cycles. In this review, I summarize recent advance in influenza D virus research and discuss how novel knowledge we have learned from IDV discriminate it from other types of influenza viruses.

1.2 The biology of the influenza D virus

Since the initial isolation in America in 2011 through the present, influenza D virus (IDV) has emerged as an important concern to animal and human health worldwide. IDV has the exceptional thermal and acid stability, a broad host range and an extensively global distribution. It has been found to utilize cattle as the natural reservoir and amplification host with periodical spillover to other mammalian species. IDV infection can cause mild respiratory illness in cattle and has been implicated as a contributor to bovine respiratory disease (BRD) complex that is the most common and costly disease affecting the cattle industry. On the other hand, outbreaks of IDV in swine and bovine herds have continued to increase, and more evidences suggest that IDV poses a potential risk to humans. In this review, I summarize the epidemiology of IDV followed by discussion of its pathogenicity, zoonotic potential, and unique properties of this novel virus.

1.2.1 Epidemiology of IDV worldwide

1.2.1.1 IDV in North America

In April 2011, a viral isolate with approximately 50% amino acid identity to the human ICV was identified from a clinically-ill pig with influenza-like symptoms in Oklahoma, USA (*4*). It was initially thought to be a new subtype of ICV that circulated in pigs. However, further characterization suggested that the virus was genetically, antigenically and biologically distinct from the human ICV (*21*). This novel virus used a new

mechanism to produce the M1 protein and was unable to productively reassort with the human ICV in cell culture (*21*). Antigenically, no cross-reactivity was detected between antibodies against this new virus and the human ICV in the hemagglutination inhibition (HI) assay (*21*). According to these differences to the human ICV, the International Committee on Taxonomy of Viruses (ICTV) classified this virus as a new genus (*Deltainfluenzavirus,* Species: *Influenza D virus*) of the family *Orthomyxoviridae.*

Although the first IDV was isolated from a diseased pig, subsequent follow-up studies demonstrated that IDV widely spread in cattle (*21*, *38*). Agricultural cattle has not been considered to be susceptible to influenza viruses until the discovery of IDV (*39*). Initial epidemiological investigation of IDV in pigs showed low seropositive rate (9.5%, n=220) (*4*) (Table 1-2). In addition, the percentage of IDV positivity was less than 0.1% by RT-PCR during the routing testing of nasal swabs from pigs, and the isolation of IDV from pigs was also infrequent (*21*). However, higher positive rate (18%, n=48) of IDV was found in a diagnostic testing of nasal swabs from cattle with respiratory disease by RT-PCR (Table 1-2), and viruses were successfully isolated from the 5 of 8 positive samples (*21*). Another surveillance study from the same group found that 10 of the 208 clinical samples (4.8%) submitted for laboratory diagnosis of BRD complex were tested positive for IDV by RT-PCR (Table 1-2), and 6 viruses were isolated from the 10 IDV positive samples (*38*). Moreover, two studies in young calves reported that neonatal cattle showed high levels of maternal antibodies against IDV, 94% and 98% respectively (*40*, *41*). These two studies also suggested that IDV has been present in the US cattle herds (Mississippi and Nebraska) since as early as 2003 (*40*, *41*). A nationwide serosurveillance

of IDV in the United States found an overall 77.5% (n=1992) seropositivity rate in cattle serum samples collected across the country in 2014-1015 (Table 1-2), but the prevalence rates varied from 47.7% to 84.6% among different regions (*42*). Furthermore, seropositive samples were found in 41 of the 42 US states, indicating a widely circulation of IDV in the US cattle population during 2014-2015 (*42*). Two studies, by metagenomic sequencing of samples collected from feedlot cattle in America, Canada, and Mexico, indicated that IDV was detected and significantly associated with BRD (*43, 44*). The widespread presence of IDV and relative ease of the virus isolation in cattle suggested that cattle represent the primary reservoir for this novel influenza virus (*21*).

Interestingly, further surveillance of IDV in North America revealed that multiple nonbovine animal species were susceptible to IDV. A serological survey that was performed to determine if small ruminants (sheep and goats) and poultry (chicken and turkey) were potential hosts to IDV showed that 5.2% (n=557) of sheep serum samples and 8.8% (n=91) goat serum samples were positive for IDV antibodies, while all tested poultry serum samples, collected from the midwest US, were negative for IDV antibodies (*23*) (Table 1-2). In contrast to poultry data reported in this study, a most recent molecular diagnosis study revealed the presence of IDV genomes in poultry farms of Southeast Asia (*45*). Equine was also added into a growing host range of IDV based on a serological surveillance of equine populations through the US. This study showed that an overall 15.7% (n=364) of equine serum samples were positive for antibodies against IDV (*24*) (Table 1-2). In America, feral swine are considered as important vectors for IAV transmission between domestic and wild animals (*46, 47*). The seroprevalence

investigation of IDV in feral swine showed that 57 of 256 (19.1%) samples were IDV seropositive (Table 1-2), which implied that feral swine might play a role in the ecology of IDV (*48*).

Based on the phylogenetic analysis of the nucleotide sequence of the HEF gene, IDV strains circulating in North America belonged to two distinct genetic lineages represented by D/swine/Oklahoma/1334/2011 (D/OK) and D/bovine/Oklahoma/660/2013 (D/660) (*38*) (Figure 1-2). These two lineages currently co-circulate in U.S. cattle populations and frequent reassortments between these two lineages in animals lead to generation of new antigenic variants, which can break through the pre-existing herd immunity and pose a further threat to agricultural animal health.

1.2.1.2 IDV in Europe

The presence of IDV in Europe was first reported in France in 2015, with detection of 6 (4.5%) IDV-positive samples from 134 tested cattle samples during 2011-2014 (*49*) (Table 1-2). Following that report, IDV was found to widely spread throughout other European countries including Italy, Luxembourg, Ireland and United Kingdom (*50-53*) (Table 1-2). The prevalence of IDV in Europe was similar to that in North America, in which the virus and/or its specific antibodies were detected in multiple animal species including cattle, swine, wild boars, sheep and goats, while the highest prevalence of IDV was observed in cattle (*52, 54-57*) (Table 1-2). The serosurveys in Italy, Luxembourg and Ireland revealed the extremely high IDV-seropositive rates in cattle (92.4%, 80.2% and 94.6%, respectively) (*52, 55, 57*) (Table 1-2). In France, IDV was identified from cattle

during 2011-2014, and a recent country-level study showed a high seroprevalence of 47.2% (n=3362) in cattle between 2014 and 2018, which indicated that once IDV was introduced, it might spread efficiently in cattle throughout the country (*49, 56*) (Table 1-2). Compared to the prevalence of IDV in cattle, the seropositivity rate in pigs is lower (Table 1-2), implying that the virus was not widespread but commonly circulated in pigs. To better understand the epidemiology and importance of IDV in the Italian swine population, serological tests were performed on 3698 swine serum samples collected in 2009 and 2015 from the same region. The results showed that in 502 sera collected in 2009, only 3 samples were positive to IDV, while 364 (11.7%) positive samples were detected from a total of 3106 swine sera collected in 2015, suggesting the prevalence of IDV in pigs were steadily increasing over the past several years in Italy (*58*).

Phylogenetic analysis showed that most European IDV strains belonged to the D/OK genetic lineage (Figure 1-2). Unexpectedly, an Italian group recently described the first identification of the D/660 genetic lineage in Europe (*59*). Analyses of the full-genome sequences demonstrated the co-circulation in Italy of the two distinct IDV lineages (*59*). Moreover, a novel reassortant virus was detected in a dairy farm, with the PB2, PB1, NP, P42 and HEF segments from the D/660 genetic lineage and the P3 and NS segments from the D/OK genetic lineage (*59*). These findings highlight the need to continue monitoring the prevalence of IDV in Europe in order to better understand its epidemiology and evolution.

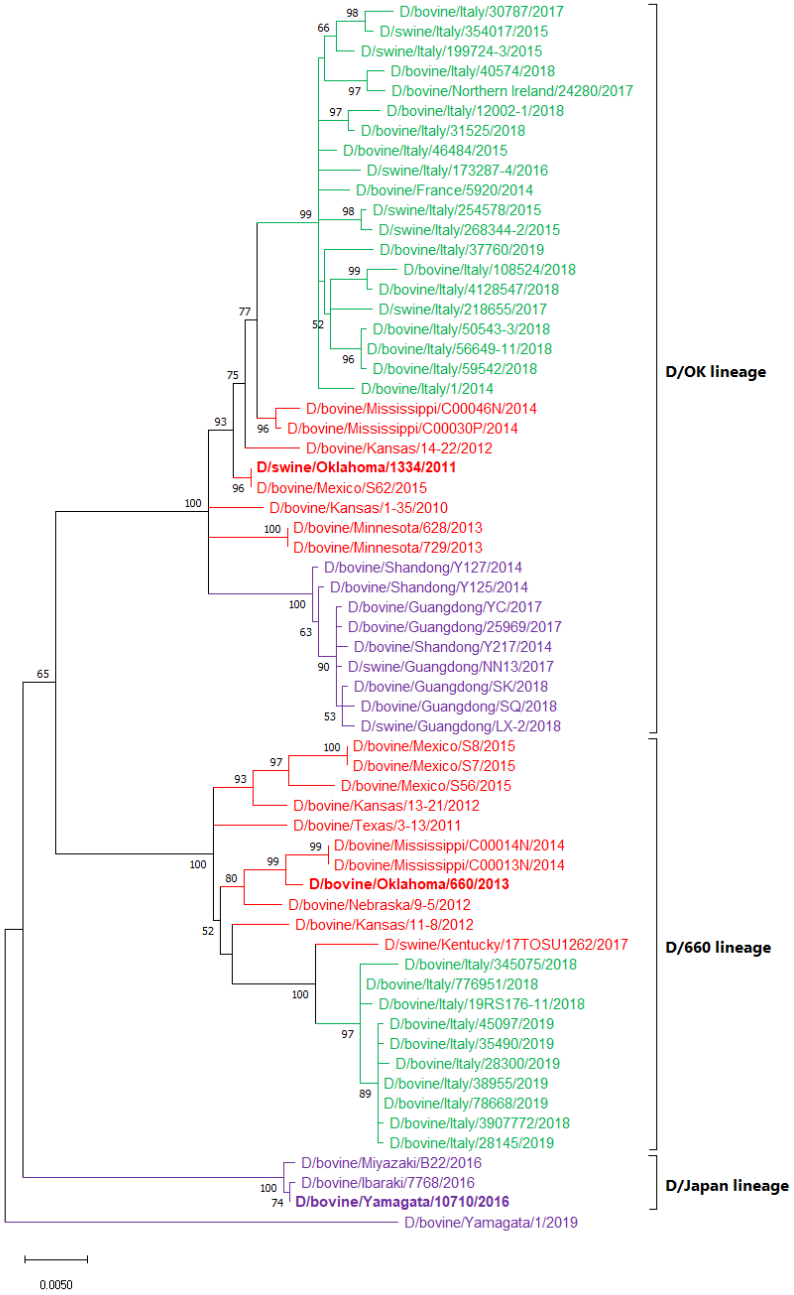

Figure 1-2, Phylogenetic tree for the HEF segment of IDV. Maximum-likelihood analysis in combination with 1000 bootstrap replicates was used to derive tree based on the nucleotide sequences of the HEF. More than 50% of the bootstrap values are shown next to the branches. The scale bars indicate the number of substitutions per site. Red: IDV in North America; Purple: IDV in Asia; Green: IDV in Europe.

Table 1-2. The epidemiology of IDV worldwide

Country (Ref.)	Time	Species	Method	Positive rate: Symptom-Health-Overall		
America (*4*)	2007-2009	Human	HI	--	--	1.3% (n=316)
	2011	Swine	HI	--	--	9.5% (n=220)
America (*21*)	2013	Cattle	RT-PCR	--	--	18.0% (n=48)
America (*38*)	2014	Cattle	RT-PCR	4.8% (n=208)	--	--
America (*23*)	2001-2007, 2014	Sheep	HI	--	--	5.2% (n=557)
		Goat	HI	--	--	8.8% (n=91)
America (*48*)	2012-2013	Feral swine	HI	--	--	19.1% (n=256)
America (*40*)	2013-2014	Neonatal calves	HI	--	94.0% (n=448)	--
	2004-2006	Cow-calf herds	HI	--	13.5%-18.3%	15.9% (n=605) #
	2014	Weaned calves	RT-PCR	23.6% (n=55)	2.4% (n=82)	--
America (*42*)	2014-2015	Cattle	HI	--	--	77.5% (n=1992)
America (*24*)	2015	Equine	HI	--	--	15.7% (n=364) #
America (*41*)	2003-2004	Cattle	HI	--	--	81.9% (n=293)
America (*60*)	2016	Exhibition swine	RT-PCR	--	--	0.07% (n=2862)
America (*25*)	--	Human	HI	--	--	97.0% (n=35)
France (*49*)	2011-2014	Cattle	RT-PCR	--	--	4.5% (n=134)
France (*54*)	2009-2016	Wild boars	HI	--	--	0.5% (n=644)
	2012-2018	Swine	HI	--	--	1.6% (n=2372)
France (*56*)	2014-2018	Cattle	HI	--	--	42.7% (n=3326)
		Ovine	HI	--	--	1.5% (n=1430)
		Caprine	HI	--	--	3.2% (n=625)
Italy (*50*)	2014-2015	Swine	RT-PCR	0.7% (n=150)	--	--
		Cattle	RT-PCR	1.3% (n=150)	--	--
Italy (*61*)	2005-2017	Human	HI	--	--	26.2% (n=1281)
Italy (*58*)	2015-2016	Swine	RT-PCR	2.5% (n=845) #	--	--
	2009,2015	Swine	HI	--	--	10.6% (n=3698) #
Italy (*59*)	2018-2019	Cattle	RT-PCR	10.6% (n=936) #	--	--
Italy (*55*)	2014-2016	Cattle	RT-PCR	5.4% (n=895)	1.1% (n=895)	6.5% (n=895)
	--	Cattle	HI	--	--	92.4% (n=420)
Luxembourg (*52*)	2012-2016	Cattle	HI	--	80.2% (n=450)	--
	2014-2015	Swine	HI	--	--	5.9% (n=287)
	2014-2015	Swine	RT-PCR	--	0.7% (n=427)	--
Ireland (*53*)	2014-2016	Cattle	RT-PCR	5.6% (n=320)	--	--
Ireland (*57*)	2016-2017	Cattle	HI	64.9% (n=1183)	94.6% (n=1219)	--
	--	Swine		--	--	5.8% (n=377)
		Ovine		--	--	4.8% (n=288)
United Kingdom (*51*)	2017-2018	Cattle	RT-PCR	8.7% (n=104)	--	--
China (*62*)	2014	Cattle	RT-PCR	--	0.66% (n=453)	--
China (*63*)	2016	Cattle	RT-PCR	9.7% (n=404) #	1.0% (n=100) #	7.9% (n=504) #
		Swine		31.3% (n=64) #	2.0% (n=50)	18.4% (n=114) #
		Goat		31.8% (n=88) #	0.0% (n=50)	20.3% (n=138) #
Japan (*64*)	2016	Cattle	HI	--	28.6% (n=28)	--
Japan (*65*)	2016-2017	Cattle	RT-PCR	1.7% (n=172)	2.4% (n=205)	2.1% (n=377)
Japan (*66*)	2010-2016	Cattle	HI	--	13.5%-50.0%	30.5% (n=1267)
Turkey (*67*)	2018-2019	Cattle	RT-PCR	4.0% (n=76)	--	--
Ethiopia (*68*)	--	Camel	HI	--	--	57.9% (n=38) #
Togo (*69*)	2017-2019	Cattle	HI	--	--	4.5% (n=399)
		Small ruminants		--	--	3.8% (n=737)
Morocco (*26*)	2012-2015	Cattle	HI	--	--	35% (n=200)
Togo (*26*)	2009,2015	Cattle	HI	--	--	10.4% (n=201)
Benin (*26*)	2012,2014	Cattle	HI	--	--	1.9% (n=207)
Togo (*26*)	2013	Small ruminants	HI	--	--	1.8% (n=340)
Kenya (*26*)	2015	Camel	HI	--	--	99.0% (n=293)

1, "--": data not determined; 2, "#": value calculated by using data from the references.

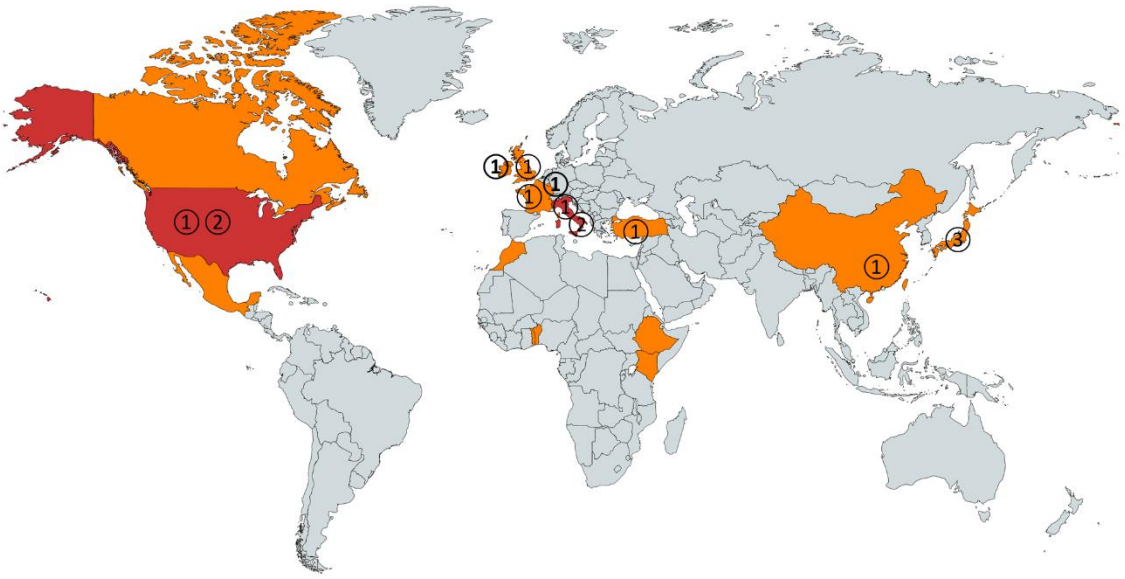

Figure 1-3, Global distribution of IDV by country. Red: IDV positive in humans and animal species; Orange: IDV positive in animal species; Gray: no data or no positives reported. IDV was found in America, Canada, and Mexico in North America; China, Japan and Turkey in Asia; France, Italy, United Kingdom, Ireland and Luxembourg in Europe; Morocco, Togo, Benin, Ethiopia and Kenya in Africa. Circled numbers indicate the reported presence of IDV lineages. ①: D/OK lineage; ②: D/660 lineage; ③: D/Japan lineage.

1.2.1.3 IDV in Asia

IDV in Asia was first reported in 2014 in Shandong, China, with 3 IDV-positive cases out of the 453 samples collected from apparently healthy cattle (*62*) (Table 1-2). A subsequent surveillance study in China showed a high prevalence (> 30%) of IDV in pigs and goats (*63*) (Table 1-2) , which was different from the relatively low prevalence found

in previous studies (*4, 23, 50*). Notably, this study showed that IDV genome was present in serum samples of severely diseased cattle and goats, implying that the virus might enter transiently into the animals' circulatory system and spread to other organs (*63*). Another interesting observation from this study was that IDV was detected in goat rectal swabs, which suggested that IDV might replicate within the intestinal tract similar to IAV and IBV (*63, 70*). IDV genome was also found in buffalo from this study (*63*).

The first identification of IDV in Japan was reported from a cattle herd in the Ibaraki Prefecture in 2016 (*64*). In this study, IDV showed highly contagious property, in which the virus readily spread throughout the herd in a short time once the IDV infection occurred (*64*). Further serological surveys indicated that IDV had been in nationwide circulation in the cattle population of Japan for at least 5 years, with an overall positivity rate of 30.5% (n=1267) (*66*) (Table 1-2). The positivity rates of IDV infection tended to increase with the cattle age when analyzing the seropositive cattle with the age records at the time of collection (*66*). IDV-specific antibodies were detected in samples collected in as early as 2010, suggesting that IDV exposures were present in Japan since at least 2010 (*66*). Most recently, infection of cattle with IDV was also reported for the first time in Turkey (*67*).

Phylogenetic analysis revealed that all IDV strains isolated in China belonged to the D/OK genetic cluster (*63*) (Figure 1-2). Interestingly, IDV circulating in Japan formed a different genetic cluster (termed as D/Japan) from the D/OK and D/660 genetic clusters, suggesting a possibility of unique evolution of IDV in Japan over a long period of time (*5*,

65) (Figure 1-2). Just recently, a new IDV isolate from diseased cattle in Japan was found to be phylogenetically and antigenically distinguished from all previously described IDVs of the 3 known lineages (*71*). Further studies are needed to elucidate prevalence, epidemic status and pathogenicity of this heterologous IDV (*71*).

1.2.1.4 IDV in Africa

IDV has been identified in several continents including North America, Europe and Asia. Recently, a study reported the prevalence of IDV for the first time in Africa, by performing the HI assay on a total of 2083 serum samples from cattle, swine, small ruminants, and dromedary camels in Morocco, Togo, Côte d'Ivoire, Benin, and Kenya during 1991-2015 (*26*). The results showed that IDV antibodies were detected in cattle from Morocco (2012-2015), Togo and Benin (as of 2014), and in small ruminants from Togo (2013) (Table 1-2), suggesting that IDV had been circulating in North and West Africa since at least 2012 (*26*). Significantly, the authors also showed that dromedary camels exhibited extremely high seropositivity (99.0%) for IDV in Kenya (Table 1-2), indicating a new host for IDV (*26*). This was further confirmed by another serological survey in Ethiopia where a high seroprevalence of IDV was also observed in dromedary camels (*68*). Future studies are needed to illustrate the role of camels on the epidemiology, ecology and pathology of IDV. To date, IDV infection has been demonstrated in Morocco, Togo, Benin, and Kenya in Africa by serological evidences, but the virus has not yet been isolated on this continent (*26, 68, 69*).

1.2.2 Pathogenicity and zoonotic potential of IDV

1.2.2.1 Pathogenicity of IDV in swine and cattle

Table 1-3. Replication, pathogenicity and transmission of IDV in experimentally infected animals.

Animal species	Replication	Pathogenicity	Transmissibility
Domestic pigs	Upper respiratory tract	No clinical signs	Contact-transmission
Feral pigs	Both the upper and lower respiratory tracts	No clinical signs	Contact-transmission
Cattle	Both the upper and lower respiratory tracts	Mild respiratory disease	Contact- or aerosol-transmission
Ferrets	Nasal turbinates	No clinical signs	Contact-transmission
Guinea pigs	Both the upper and lower respiratory tracts	No clinical signs	Contact-transmission
Mice	Mainly in upper respiratory tract with a lower extent in the lower respiratory tract	No clinical signs	NA

IDV has a worldwide distribution (Figure 1-3) and can infect multiple animal species (Table 1-2). It was first isolated from pigs with influenza-like illness (*4*). Two surveillance studies reported that IDV RNA was detected in pig lung samples, implying IDV infection in the lower respiratory tract (*58*, *63*). However, domestic pigs experimentally infected with IDV exhibited no clinical signs of illness (*4*) (Table 1-3). In addition, this study revealed that IDV infection was limited to the upper respiratory tract of pigs (*4*) (Table 1-3) . Interestingly, an infection experiment conducted on feral swine showed that IDV was able to replicate in both the upper and lower respiratory tracts

including nasal turbinate, soft palate, trachea, and lung tissues, but no clinical signs were observed (*48*) (Table 1-3). Moreover, IDV viremia was detected in the infected feral swine (*48*). A recent animal study indicated that IDV infection caused lung lesions in pigs with the existence of IAV-specific antibodies (*72*). These different observations regarding the pathogenesis of IDV in swine might be affected by animal types, study conditions, and virus strains. However, all these animal studies pointed out that IDV was transmissible among pigs by direct contact (*4, 48, 72*). Further studies are needed to clarify the pathogenesis and transmission of IDV in swine because diseases sometimes can be readily transmitted from swine to humans and other animal species.

Cattle are the primary reservoir for IDV. Several surveillance studies showed that more IDV RNA was detected in diseased cattle than that in healthy cattle (*40, 43, 63, 73*). The three metagenomic studies performed on cattle with BRD found a positive correlation between BRD and IDV infection (*43, 44, 73*). However, appreciable levels of IDV RNA were also detected in healthy cattle (*40, 52, 57*). To further determine the pathogenesis and transmission of IDV, several experimental studies were conducted on IDV-negative cattle (Table 1-3). These animal studies indicated that IDV could cause mild respiratory disease in experimentally infected cattle (*74-77*). Two of them demonstrated that IDV replicated in both the upper and lower respiratory tracts (*75, 76*). Inflammations characterized by neutrophils were observed in the nasal turbinate (*74*), trachea (*74, 75*), or bronchial lumens (*76*). Importantly, these studies also confirmed that IDV could be transmitted between cattle through direct contact or aerosol (*75, 76*). Overall, cattle, as the natural reservoir of the virus, play an important role in IDV replication and

transmission, which emphasizes the need for continued monitoring and risk assessment of this emerging virus in cattle.

As stated above, IDV was highly associated with BRD that is triggered by complex interactions between host, infectious agents, and environmental factors (*78*). Generally, cattle with stress and under adverse environmental conditions are susceptible to a primary viral infection and the compromised host immunity caused by the viral infection facilitates a secondary bacterial invasion of the respiratory tract, which may lead to severe disease or death in the animals (*77, 78*). Viruses including bovine viral diarrhea virus, infectious bovine rhinotracheitis virus, bovine respiratory syncytial virus, parainfluenza type-3 virus and the newly identified IDV, and bacteria such as *Mannheimia haemolytica* (MHA), *Pasteurella multocida*, *Histophilus somni*, and *Mycoplasma bovis* are considered important pathogens for BRD (*43, 44, 73, 77*). To determine the potential role of IDV in BRD when IDV infection accompanied with a secondary bacterial infection, an animal study was designed on cattle co-infected with IDV and MHA. The results showed that primary IDV infection in cattle did not enhance the disease caused by the secondary MHA infection (*77*). Interestingly, this result was similar to that of an independent mice study, which found that IDV infection in mice did not increase the susceptibility to the secondary *Staphylococcus aureus* infection but was protective against clinical signs of the secondary bacterial infection (*79*). More studies are needed to define synergistic or antagonistic actions behind the opportunistic infection with IDV and determine the underlying mechanisms of IDV pathogenicity in the setting of primary viral infection and secondary bacterial superinfection.

1.2.2.2 Pathogenicity of IDV in other animals

Besides swine and cattle, IDV was found to infect other animal species including sheep, goats, equine, buffalo, and camels in the field (*23, 24, 26, 56, 57, 63, 68*). However, the pathogenicity of IDV in these animals remains unclear. A surveillance study in China reported IDV viremia in 33.8% (n=80) of the goats with severe diseases (*63*). The presence of influenza viremia can be used as an indicator of the level of the disease severity (*80*), but the relatedness requires further validation.

The pathogenicity and transmissibility of IDV was also determined by experimental infection of ferrets, guinea pigs, and mice (Table 1-3). These laboratory animals are widely used in influenza A and B research. No clinical signs of disease were observed in these animals infected with IDVs, respectively (*4, 79, 81, 82*). In ferrets, IDV replicated in nasal turbinates but not in the lower respiratory tract (*4*). The virus could be transmitted to naïve ferrets by direct contact (*4*). In contrast to ferrets, IDV in guinea pigs was detected in both the upper and lower respiratory tracts, and could also be transmitted to the sentinels by direct contact (*82*). IDV replication in mice was observed mainly in the upper respiratory tract but also to a lower extent in the lower respiratory tract (*81*). Importantly, the virus was detected with low titers in mice intestines (*81*), which was in agreement with a recent study that found IDV in rectal swabs of goats (*63*). This enteric tropism of IDV seems to be supported by a studying showing the exceptional acid stability of IDV when compared to other types of influenza. It may be interesting to test

whether IDV can use a fecal-oral transmission route to replicate and transmit among animals.

1.2.2.3 Zoonotic potential of IDV

There are no indications so far that IDV can cause disease in humans. However, IDV is the emerging influenza virus that has a broad host range, which is similar to IAV. As mentioned above, IDV can infect and/or to be transmitted to multiple domestic animals including cattle, pigs, sheep, goats, camels, horses, and poultry, and also to wild species such as feral pigs. In addition, IDV is able to replicate and transmit by direct contact in ferrets and guinea pigs, both surrogate models for influenza virus studies in humans (*4, 82*). Furthermore, IDV showed a broad cellular tropism in the cell culture studies (*4*). A recent study confirmed that IDV was able to efficiently replicate in the well-differentiated human airway epithelial cells (hAECs) that served as an *in vitro* respiratory epithelium model of humans (*83*). This model has been well applied to assess the zoonotic potential of emerging respiratory viruses (*84, 85*). Generally, successful zoonotic infections occur when the pathogens acquire the ability to cross the species barrier and replicate efficiently in a novel host species (*86*). Taken together, these findings suggest that multiple-species-infecting IDV has the great zoonotic potential.

Several serologic studies have demonstrated that IDV-specific antibodies could be detected in humans. An early serosurvey showed that 1.3% (n=316) of the general human population had antibodies against IDV (*4*), while no IDV was detect in patient respiratory

samples by RT-PCR from a later large-scale surveillance study in Scotland (*87*). Notably, a very high seroprevalence of IDV was observed among workers with cattle exposure (34 out of 35 persons had IDV antibodies), as reported in a serological study in Florida, USA (*25*). Recently, a more comprehensive seroprevalence study revealed that IDV antibodies were present and increased over time in the Italian populations from 2005 to 2017 (*61*). The results showed that antibodies against IDV displayed low levels (5.1%-9.8%) in the years 2005-2007, and sharply increased to high levels (37.9%-43.4%) in the years 2008-2010 and (41.0%-46.0%) in the years 2013-2014, followed by a decline in the subsequent years 2011-2012 and 2015-2017 (*61*). Interestingly, this longitudinal study revealed a temporal correlation between IDV prevalence peak in humans and epidemics in domestic pigs in Italy. The prevalence of antibodies against IDV in humans implies that the virus may infect humans and pose a threat to human health.

Interestingly, an aerosol surveillance of respiratory viruses at the Raleigh-Durham International Airport observed that among 4 of the 24 samples positive for known respiratory pathogens, 3 were positive for adenovirus and 1 was positive for IDV (*88*). Similarly, IDV was detected in another molecular surveillance of respiratory pathogens with bioaerosol sampling in a hospital emergency room setting in North Carolina (*89*). Significantly, a more recent study showed that the IDV RNA genome was detected in nasal wash samples of a swine farm worker in Malaysia, Asia (*90*). Although these observations are not enough to indicate the public health threat of IDV, it is considerable that the virus may have spread into the public environment including humans.

1.2.3 Novel biology of IDV

IDV, an emerging type of influenza viruses, with a potential threat to humans, has a broad host range and a global distribution. Moreover, IDV is a new virus with novel biological characteristics among the four influenza genera. IDV was found to be the most stable of the four types of influenza viruses. Only IDV was still infectious after a 15-minute exposure to 53 ℃ in the neutral solution, and surprisingly, it maintained the infectivity even after exposure to 53 ℃ for 2 hours (90). Furthermore, IDV survived after being treated at pH 3.0 for 30 minutes, while all other types of influenza viruses were completely inactivated (90). The recombinant IAV whose HA and NA were replaced with HEF of IDV acquired the ability to resist the high-temperature and low-pH treatments, which was the same as the HEF donor virus (IDV) (*91*). These observations demonstrated that the HEF determined the exceptional thermal and acid stability of IDV. Since the acid stability of HA has been found to impact the host range, infectivity, and transmissibility of IAV (*92*), further studies on the mechanism by which HEF confers the environmental stability to IDV may offer new insights into the interspecies adaptation and transmission of the novel IDV. In addition, this unique property of IDV may partially explain why IDV, but not IAV, IBV or ICV, could be detected in people or patients through the molecular surveillance of respiratory viruses with bioaerosol sampling in the airport or in a hospital emergence room (*88*).

The spike glycoproteins of influenza viruses mediate the viral entry into the host cells via recognition and interaction with the SA receptors. Recent structural and functional studies of the HEF suggested that its unique receptor-binding pocket might contribute to

the broad host range of IDV. The functional form of the spike is a homotrimer (Figure 1-4). The overall structures of IAV and IBV HAs are similar, despite sharing a very low sequence identity of only 20%-30% (*18*). During the viral life cycle, HA is primarily synthesized as a precursor (HA0) that is subsequently cleaved into the globular HA1 subunit and the stalk-like HA2 subunit (*93, 94*). The major domains of the HA protein include the R domain, containing the receptor binding pocket (RBP), the E domain which has a vestigial esterase region, and the F domain, with the fusion peptide that mediates the fusion between the viral and host membrane (*93-95*) (Figure 1-4). HEFs of ICV and IDV have 53% amino acid homology (*4*) and possess a almost identical structure and mode of ligand binding (*20, 29*). Similar to HA, HEF is synthesized as a precursor (HEF0) that is composed of two post-translationally cleavable subunits: the globular head subunit HEF1 and the membrane-near stalk subunit HEF2 (*20, 29*). HEF also can be divided into three domains: the receptor binding domain (R), the esterase domain (E) and the fusion domain (F) (*20, 29*) (Figure 1-4). HEF contains the esterase activity in the E domain while it is degenerated in HA. One interesting difference between ICV HEF and IDV HEF is that IDV HEF protein has an open channel in the RBP, while in the structurally identical site of ICV, there is a salt bridge formed by the positively-charged residue Lysine (K235) and the negatively-charged residue Aspartate (D269) (*29*). The equivalent positions of IDV HEF are T239 and A273 which cannot form the salt bridge interaction (*29*). This subtle difference may indicate that IDV has different receptor-binding properties compared to ICV. Further functional studies demonstrated that IDV HEF was able to efficiently bind both Neu5,9Ac_2 and Neu5Gc9Ac as the receptors, while ICV preferentially bound to Neu5,9Ac_2 as its receptor (*30*). Taken together, the open and

flexible receptor-binding cavity of HEF may allow IDV to recognize more diverse 9-O-acetyl SAs, which further broaden its cell tropism and host range.

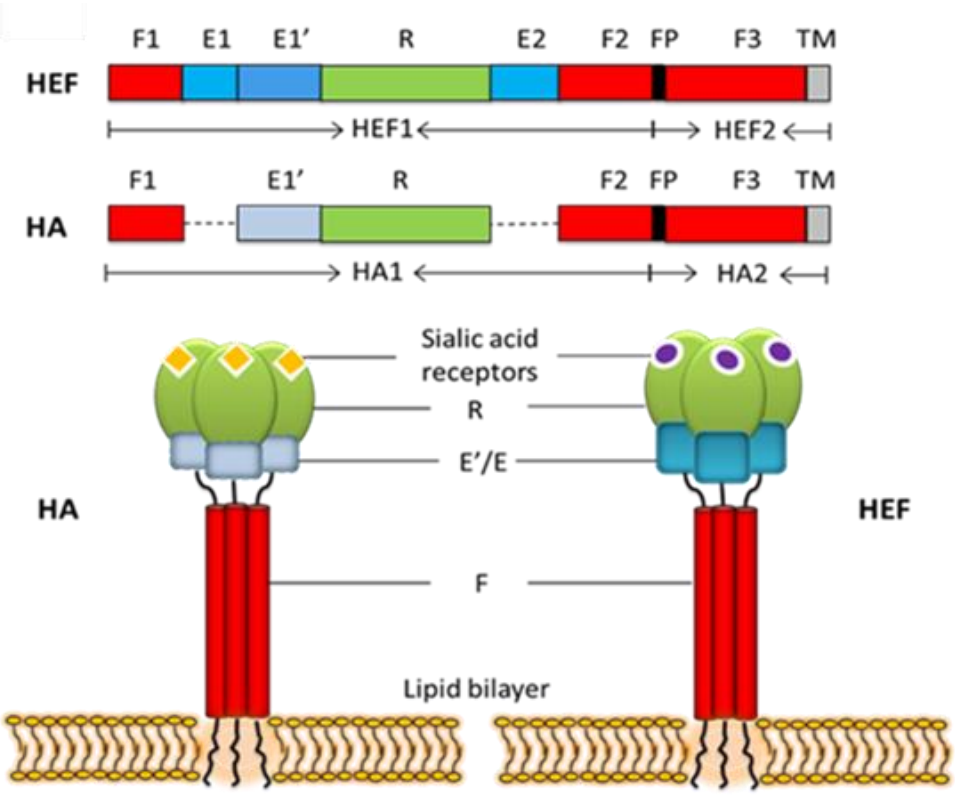

Figure 1-4, Schematic illustration of the HA/HEF. Linear order of the sequence fragments in HA/HEF colored by domains: fusion domain (F1, F2, and F3, red), esterase domain (E1, E1', and E2 in the HEF, blue; only E1' in the HA, gray), receptor domain (R, green), fusion peptide (FP), and transmembrane region (TM).

Influenza viruses have evolved different strategies to produce the viral proteins to maximize the genome coding potential. Splicing has been demonstrated in the NS and/or M segments of influenza viruses. All types of influenza viruses possess a similar mechanism to generate the NS1 and NS2 proteins (*21*, *96*) (Figure 1-5). Generally, the

NS1 protein is encoded by a colinear mRNA transcript from the first initiation codon of the NS segment, while the NS2 protein is encoded by a spliced mRNA transcript from the NS segment, which shares the first portion within the NS1 transcript and switches to the second portion within the 3' end of the NS segment (Figure 1-5). However, each type of influenza viruses uses unique strategy to produce M1 and/or M2 proteins (Figure 1-5). In IAV, M1 protein is made from an unspliced colinear mRNA but M2 protein is synthesized by using a spliced mRNA template (*97*), which is similar to the production of NS1 and NS2 proteins (Figure 1-5). In contrast, the M segment of IBV is not spliced. IBV M1 protein is encoded by a colinear transcript, and M2 protein is generated via a translational stop-start mechanism (*98*) (Figure 1-5). Whereas ICV M1 mRNA needs to be spliced to create a termination codon, while its M2 protein is derived from the proteolytic cleavage of a P42 propeptide encoded by an unspliced colinear mRNA (*99, 100*) (Figure 1-5). IDV uses the proteolytic cleavage strategy similar to that of ICV to generate M2 protein from the P42 protein (*9*), while in contrast to the ICV M segment that generates the M1 protein via splicing that only introduces a termination codon, the splicing of IDV M segment produces additional 4-amino-acid peptide into the preceding exon (*21*). The function of these four amino acids is still unclear. Recently, a study reported that IAV M segment RNA splicing was an important host range determinant (*101*). It would be interesting to speculate that different mechanisms for production of M1 and M2 proteins among four types of influenza viruses may determine the viral evolution and host range, which should be tested experimentally in future studies.

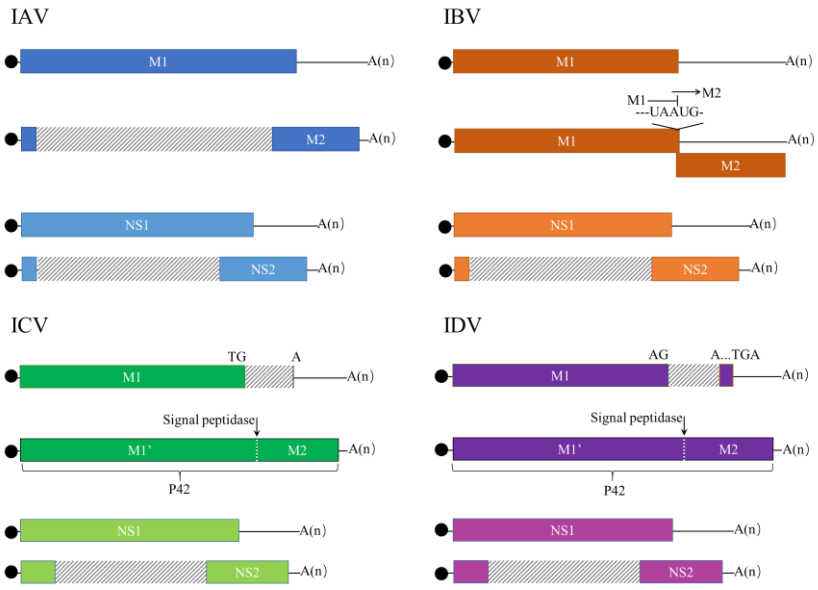

Figure 1-5, Splicing strategies of influenza viruses for the NS and M segments. (*Modified from Andrew M.Q. King, et al., Virus Taxonomy: Ninth Report of the International Committee on Taxonomy of Viruses, 2012, Pages 752-753)*

1.3 Research Aims

1.3.1 Hypothesis

The factors determining the infectivity and transmissibility of influenza viruses could include the viral, host and environmental factors. IAV originally infects waterbirds and can cross the species barrier to infect humans and numerous other animal species. IBV and ICV mainly infect humans. IDV is unique among four types of influenza viruses to utilize cattle as the primary reservoir and can spread to many other agricultural animals. The environment plays an important role in driving IAV persistence and transmission in natural and acquired hosts. **It is unknow how IDV performs in different environments**.

IDV has a worldwide distribution and a broad host range and possesses potential to adapt to humans. IDV shows optimal growth at both 33 ℃ and 37 ℃, unlike its related ICV that is typically replicated well at 33 ℃, which suggests that IDV is not restricted to an elevated temperature for replication. IDV has a broad receptor-binding property. IDV has also evolved a unique strategy to produce the M1 protein. IDV has such important properties but the underlying mechanisms remain unclear, **we ungently need a reverse genetics system to study IDV in molecular level.**

Reverse genetics system is widely used to study viral replication, tropism, and pathogenesis. IDV can be divided into three genetic lineages: D/OK, D/660 and D/Japan. The D/OK virus and the D/660 virus are two lineage-representative IDV strains. Our primary studies showed that the D/660 virus had a higher replication capacity than that of the D/OK virus. Further studies confirmed that the D/660 virus replicated more robust than the D/OK virus in different cell lines, which indicated that the replication difference between the D/660 and D/OK viruses was host cell – independent. **Some viral factors may determine the IDV replication fitness.**

1.3.2 Specific Aims

Project 1: To investigate the thermo and acid stability of influenza viruses.

Project 2: To generate and characterize the reverse genetics system of IDV.

Project 3: To identify genetic determinants of IDV replication fitness.

CHAPTER 2. THE HEMAGGLUTININ-ESTERASE FUSION GLYCOPROTEIN IS A PRIMARY DETERMINANT OF THE EXCEPTIONAL THERMAL AND ACID STABILITY OF INFLUENZA D VIRUS

Jieshi Yu,[a] Busha Hika,[a] Runxia Liu,[a] Zizhang Sheng,[b,c] Ben M. Hause,[d] Feng Li,[a,e,f] Dan Wang,[a,f]

Department of Biology and Microbiology, South Dakota State University, Brookings, South Dakota, USA[a]; Department of Biochemistry and Molecular Biophysics, Columbia University, New York, New York,USA[b]; Department of Systems Biology, Columbia University, New York, New York, USA[c]; Cambridge Technologies,Inc., Worthington, Minnesota, USA[d]; Department of Veterinary and Biomedical Sciences, South Dakota State University, Brookings, South Dakota, USAe; BioSNTR, Brookings, South Dakota, USA[f]

https://doi.org/10.1128/mSphere.00254-17.

Keywords: hemagglutinin-esterase fusion protein, acid stability, influenza virus, thermal stability

2.1 Introduction

Influenza viruses are segmented, single-stranded, negative-sense, enveloped RNA viruses and belong to the Orthomyxoviridae family. Four types of influenza viruses, designated influenza A virus (IAV), influenza B virus (IBV), influenza C virus (ICV), and influenza D virus (IDV), have been identified. The genomes of IAV and IBV consist of eight RNA segments, whereas ICV and IDV have only seven segments. IAV and IBV contain two

major surface glycoproteins: hemagglutinin (HA), which binds to sialylated host cell receptors and mediates membrane fusion, and neuraminidase (NA), which prevents the HA from host cell membrane engagement by cleaving sialic acids from receptors, thereby releasing newly assembled virus particles (*34*). ICV and IDV, however, have only one major surface glycoprotein, the hemagglutinin-esterase fusion (HEF) protein, which performs all above functions, including receptor binding, receptor destroying, and membrane fusion (*4*). IAV infects avian, human, swine, and many other mammalian species, including tigers, seals, dogs, and horses, while IBV and ICV are found principally in humans and rarely infect other species. The recently discovered IDV causes respiratory diseases primarily in cattle and to a lesser extent in pigs. Moreover, serological evidence for IDV infection in small ruminants and humans has been established (*23, 25*). Since the initial isolation of IDV in the United States in 2011, IDV has been reported in China, Mexico, France, Italy, and Japan. Under experimental conditions, IDV is capable of infecting ferrets and guinea pigs and transmitting to naïve animals by direct contact (*4, 82*).

IDV differs from all historically known influenza viruses in that it utilizes cattle as a primary reservoir. Adaptation to cattle may confer some unique features to IDV, which enhance its survival in this particular agricultural animal population. Such inherited characteristics through evolution may make IDV distinguishable from other types of influenza viruses circulating in ducks, pigs, or humans. As a first step toward identifying novel biological traits and better understanding the infection biology of newly emerging

IDV, we directly compared the stability and infectivity of IDV to those of other influenza types following exposure to either high temperatures or low-pH solution. Interestingly, our experiments revealed that IDV was more resistant to high temperatures and highly acidic environments than the other three types of influenza viruses. Significantly, we found that the viral HEF glycoprotein is a primary force in dictating the exceptional stability of IDV infectivity at low pH and high heat.

2.2 Methods, results and discussion

The viruses used in this study are listed in Figure 2-1A, including two IAVs (originated from swine and human), one IBV (from human), one ICV (from human), and two IDVs (from cattle and swine). We started by investigating the effect of temperature on the stability and infectivity of the influenza viruses. Temperature gradients evaluated included 33°C, 37°C, 41°C, 45°C, 49°C, 53°C, 57°C, and 65°C. A temperature of 0°C was included as a control. All the viruses listed in Figure 2-1A were treated under this set of temperatures for 1 h at neutral pH and then incubated on ice for another 30 min. After treatment, the infectivity of these viruses was determined by measuring viral 50% tissue culture infective doses (TCID50s) in MDCK (Madin-Darby canine kidney) cells using the standard protocol (*102, 103*). Viral titers for all tested viruses were not impaired when treated at 33 to 41°C but started to decline at 49°C (Figure 2-1B). The 53°C treatment clearly discriminated IDV D/OK/13 (see Figure 2-1A for the influenza virus strains and influenza virus abbreviations) from the three other types in that IDV retained a high residual infectivity (~2.5 log units of TCID50/ml), while IAV, IBV, and ICV were

completely inactivated. Remarkably, IDV was still infectious when treated at 57°C, and the complete loss of its infectivity was observed only after 1 h of incubation at 65°C.

A.

Strain	Abbreviation	Genus	Origin	Titer ($log_{10}TCID_{50}$/ml)
A/swine/Minnesota/2073/2008	A/MN/08	IAV	Swine	5.9
A/California/07/2009	A/CA/09	IAV	Human	5.8
B/Brisbane/60/2008	B/BR/08	IBV	Human	5.9
C/Johannesburg/1/1966	C/JHB/66	ICV	Human	5.3
D/bovine/Oklahoma/660/2013	D/OK/13	IDV	Bovine	5.4
D/swine/Oklahoma/1334/2011	D/OK/11	IDV	Swine	5.7
A/WSN/1933	A/WSN/33	IAV	Human	6.6
A/WSN/1933-D/swine/ Oklahoma/1334/2011-HEF	A/WSN-D/OK/HEF	Chimeric: IAV's PB1, PB2, PA, NP, M, NS, and IDV's HEF	Human-Swine	6.5

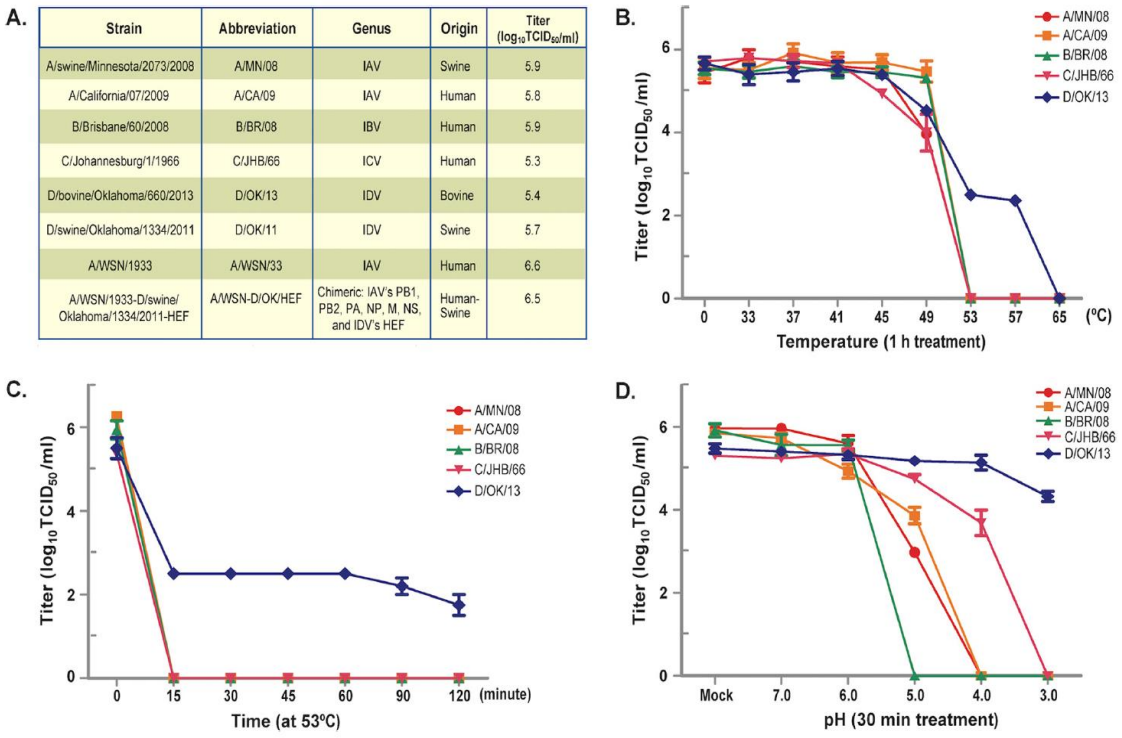

Figure 2-1. Thermal and pH stability of influenza viruses. (A) A list of the influenza viruses used in this study and their infectivity determined as TCID50 per ml in MDCK (Madin-Darby canine kidney) cells. These viruses were replicated in MDCK cells under the same conditions. (B) All viruses were treated in solution under different temperatures for 60 min and incubated for another 30 min in 4°C prior to the infectivity experiment. Note that the virus titers were 5.4 log10 TCID50/ml for A/MN/08, 5.6 log10 TCID50/ml for A/CA/09, and 5.6 log10 TCID50/ml for B/BR/08, which are slightly different from those used for the experiments shown in panels C and D. (C) A/MN/08, A/CA/09, B/BR/08, C/JHB/66, and D/OK/13 were treated in solution under 53°C for different time points and incubated for another 30 min in 4°C prior to the infectivity experiment. (D) A/MN/08, A/CA/09, B/BR/08, C/JHB/66, and D/OK/13 were treated in solution with different pH values for 30 min at room temperature, followed by neutralization and

incubation for another 30 min in 4°C prior to the infectivity experiment. The data presented in this figure are representative of three independent experiments, with each assay sample tested in duplicate. The error bars represent standard deviations and indicate the variations among the experiments.

We next selected the 53°C treatment condition at neutral pH with different time points after incubation (0, 15, 30, 45, 60, and 120 min) to directly study the thermal stability and infectivity of all types of influenza viruses (Figure 2-1C). Significantly, only D/OK/13 was able to tolerate the high temperature of 53°C. All other types of influenza viruses, such as A/MN/08, A/CA/09 (pdm09HIN1), B/BR/08, and C/JHB/66, completely lost their capacity to survive when exposed to 53°C for 15 min (Figure 2-1C). Notably, D/OK/13 was able to maintain about 40% of its infectious titer for 2 h (Figure 2-1C). These results suggested that IDV is the most temperature-stable influenza type of all influenza virus types.

In parallel, we directly studied the stability and infectivity of these viruses (Figure 2-1A) at different pH values ranging from 3.0 to 7.0. For pH trials, 0.2 M sodium acetate-acetic acid buffer was adjusted from pH 3.0 to 7.0 at 1-unit increments with the addition of 10% HCl. A nontreated control (NTC) was also included in the analysis. All pH trials were completed at room temperature for 30 min. Each pH treatment was measured at the start of the study and confirmed at the completion of each trial. In all cases, it did not vary more than 0.2 unit from the starting pH value. Then, treated viruses were pH neutralized with infection medium and incubated for additional 30 min at 4°C followed by measuring their TCID50 in MDCK cells using the same protocol described above. Remarkably,

D/OK/13 was determined to be the most stable influenza virus when treated with a pH of as low as 3.0 (Figure 2-1D). The virus retained about 80% of its original infectivity at pH 3.0, whereas all other types of influenza viruses completely lost their infectivity at a pH of 3.0 (Figure 2-1D). Interestingly, IBV was found to be the most unstable influenza virus and lost its infectivity at pH values below 5.0 (Figure 2-1D), followed by the two IAVs (completely inactivated at pH 4.0). It is interesting to note that ICV, evolutionarily and genetically close to IDV, also acquired appreciable resistance to more acidic environments. For example, despite becoming noninfectious at pH 3.0, ICV retained approximately 60% of its infectivity at pH 4.0. Overall, the ranking in order of the inherent stability at low pH is as follows: IDV > ICV > IAV > IBV. Together, the results of our experiments indicated that IDV is the most stable influenza virus in a low-pH environment.

Premature activation of viral fusion peptide is detrimental to influenza A virus infectivity (*104*). Previous studies have established that pretreating IAV prior to infection of cells by exposing the virus to high temperature or low pH can cause premature exposure of the viral fusion peptide in the HA protein, which leads to an irreversible loss of viral infectivity (*104, 105*). Interestingly, IDV and to a lesser extent ICV, exhibiting a good acid stability (Figure 2-1D), both harbor the HEF protein on the virion surface. The HEF protein in IDV and ICV, like HA in IAV and IBV, mediates virus entry and virus-cell membrane fusion in intracellular endosome compartments in an acidic environment. On the basis of the above analysis, we hypothesize that the viral HEF glycoprotein is a primary determinant of the thermal and acid stability of IDV. To test this hypothesis, the

HA and NA segments of an IAV H1N1 WSN/1933 (A/WSN/33) were replaced with the HEF segment of D/OK/11 (from swine) using the reverse genetic system (Figure 2-2A), and the stability and infectivity of the rescued A/D-HEF chimeric virus were examined and directly compared with its parental viruses (A/WSN/33 and D/OK/11) by the protocol discussed above. As demonstrated in Figure 2-2B, A/WSN/33 (wild type) completely lost its infectivity when treated at 53°C for 15 min. In marked contrast, the A/D-HEF chimera was able to survive and maintain its infectious titer after exposure to 53°C for up to 120 min, which was the same as for wild-type D/OK/11 (the HEF protein donor).

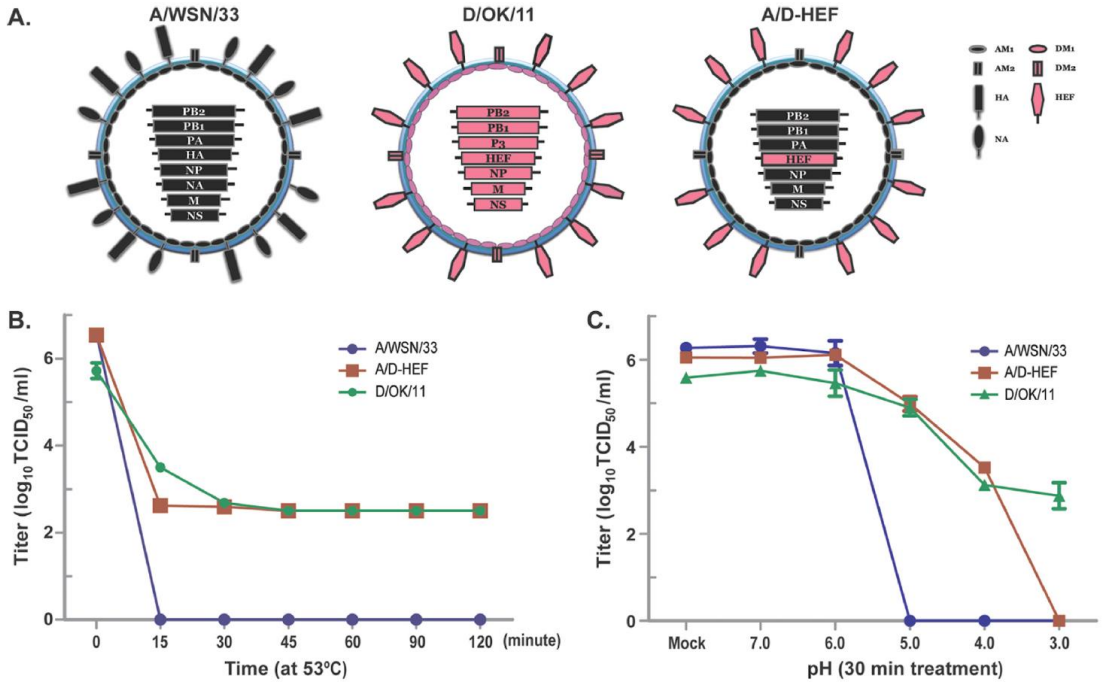

Figure 2-2. HEF is a key determinant of the exceptional acid and temperature stability of IDV. (A) Schematic representation of A/WSN/33, D/OK/11, and chimeric A/D-HEF viruses used in this study. Specifically, we generated a D/OK/11 HEF expression plasmid in the context of pHW2000-derived dual-promoter reverse genetic system (RGS) expression construct of the

A/WSN/33 neuraminidase (NA) segment. The complete HEF cDNA from D/OK/11 is flanked by 183 nucleotides of the 3' NA viral RNA (vRNA) and 157 nucleotides of the 5' NA vRNA, and initiation codons in the 3' NA vRNA are mutated to express HEF protein only. Chimeric A/D-HEF virus was generated through cotransfection of 293T and MDCK cells with the chimeric HEF plasmid together with A/WSN/33-derived PA, PB1, PB2, NP (nucleoprotein), M (matrix), and NS (nonstructural) RGS plasmids. (B) A/WSN/33, IDV D/OK/11, and chimeric A/D-HEF were treated in solution at 53°C for different times, followed by incubation in 4°C for 30 min prior to infection experiments. (C) A/WSN/33, D/OK/11, and chimeric A/D-HEF were treated in solution over a range of pH values from pH 3.0 to 7.0 for 30 min, followed by neutralization and incubation for another 30 min in 4°C prior to the infectivity experiment. The data presented in this figure are representative of three independent experiments, with each assay sample tested in duplicate. The error bars represent standard deviations and indicate the variations among experiments.

Furthermore, following exposure to different pH environments from pH 3.0 to 7.0, the A/WSN/33, like other two IAVs (Figure 2-1D), completely lost its infectivity after exposure to pH 5.0 or below (Figure 2-2C). Remarkably, at pH 5.0, the A/D-HEF chimera lost only about 15% of its infectivity. The chimera still retained more than 50% of its infectivity at pH 4.0 but was completely inactivated only at pH 3.0. Similar to D/OK/13, which originated in cattle (Figure 2-1D), D/OK/11 (swine origin) also survived when held in solution for 30 min at pH 3.0. In summary, these results suggested that the HEF protein is a key factor in determining IDV's exceptional plasticity in response to high-temperature stress and a low-pH environment. It should be noted that the HEF protein, in the context of the A/D-HEF chimeric virus, did not make the chimera fully gain the acid resistance trait as demonstrated in wild-type D/OK/11 (Figure 2-2C) or

D/OK/13 (Figure 2-1D). This discrepancy may be caused by the subtle difference of the density and spatial arrangement of the HEF protein on the virion surface between the chimeric IAV and native IDV, which will be investigated in future studies.

Intriguingly, acquisition of this remarkable physicochemical stability has apparently not inhibited the ability of IDV to spread efficiently in global animal herds. Such stability may give IDV additional advantage in surviving well in harsh environmental conditions, such as heat and low pH. Relating both thermal and acidic stability of IDV to the HEF protein is very similar to recent results with the HA protein of IAV where it was shown that some HA mutations lowering the pH threshold in activation of the HA fusion peptide (i.e., increased acid resistance) evidently rendered the IAVs more resistant to heat (*106-110*). As such, the HA protein of IAV appears to follow IDV in gradually acquiring acidic and thermal stability. Although the mechanism is still largely unknown, it is generally believed that some animal IAVs (swine or poultry) conducting a virus-cell membrane fusion event at a lower pH can transmit more efficiently to humans than those fusing at a higher pH (*111*). Therefore, the increased acid stability and thermostability of HA have been viewed as important requirement, in addition to the receptor binding specificity/affinity, for efficient airborne transmission of IAVs from animals to humans. A recent work also showed that the neuraminidase protein of the 1918 pandemic IAV is relatively stable at low pH, and this low-pH stability is implicated in enhancement of virus replication (*112*). In light of the above facts, further investigation of the molecular mechanism by which naturally stable IDV enters the cell and fuses with the host membrane may offer novel insights into how the fusion machinery of influenza viruses in

general evolves, directed by viral glycoproteins, to achieve higher acid and thermal stability, which as a result promotes the cross-species transmission potential between mammals.

The observation of viral HEF protein conferring exceptional resistance to high temperature and low pH raises several interesting questions with respect to the entry pathway and biology of IDV. First, can acidification artificially transform IDV into a fusogenic stage (i.e., fusion peptide completely exposed)? If so, we would anticipate that low-pH-induced fusogenic IDV would not be infectious. On the basis of our data that the pretreatment of IDV in a low-pH buffer prior to incubation with cells had no substantial effect on viral infectivity, while this treatment completely inactivated IAV, we speculate that low pH is required but not sufficient to trigger complete activation of the IDV fusion peptide, although we cannot rule out the possibility that activation of IDV's fusion activity is pH independent or that IDV HEF conformational changes triggered by low pH leading to viral fusion are reversible (instead of IAV-like irreversible). Second, is there a requirement for cellular acidification in IDV entry? Previous studies have demonstrated that IDV-related ICV requires a low-pH-dependent fusion in cells (*113*, *114*). Interestingly, an earlier ICV fusion characterization study revealed that ICV fused with in vitro-reconstituted liposomes relatively slower than IAV or IBV did (*114*). The time delay in fusion may reflect the more stable nature of the HEF protein of ICV in a low-pH environment, which is demonstrated in our study (Figure 2-1D). On the basis of the results of the above analysis, we speculate that IDV will likely utilize a low-pH dependent endocytosis route, the common pathway for all influenza viruses, to enter the

cell and fuse with the endosomal membrane to initiate infection. Third, what is the primary mechanism employed by IDV to activate the virus-cell membrane fusion event? Here, we propose three models for IDV fusion mechanism. The first test model is that in addition to low pH, receptor binding may play a critical role in priming IDV fusion, a mechanism used by avian sarcoma and leucosis virus (ASLV) (*115*), Jaagsiekte sheep retrovirus (*116*), and hepatitis C virus (*117*). It is interesting to note that ASLV, like IDV, is resistant to inactivation by low pH. The second model is that some cellular factors in acidic intracellular compartments may be required for activation of IDV fusion as observed for Ebola virus and severe acute respiratory syndrome coronavirus (SARS-CoV) (*118, 119*). The third model is that intracellular processing of IDV could trigger some changes in the trimeric structure of the HEF protein, which in turn activates the IDV fusion peptide and drives the virus-cell membrane fusion. This model has been previously suggested for acid-resistant bovine pestivirus in activation of pH-triggered fusion during viral entry (*120*). Further investigation of these hypothetical models is needed to achieve a better understanding of the entry and fusion mechanisms mediated by the intrinsically stable HEF protein of IDV. Such information may offer novel insights into how the fusion machinery of influenza viruses in general evolves to achieve the acid and thermal tolerance, which as a result promotes the potential to transmit across mammal species.

CHAPTER 3. DEVELOPMENT AND CHARACTERIZATION OF A REVERSE-GENETICS SYSTEM FOR INFLUENZA D VIRUS

Jieshi Yu,[a] Runxia Liu,[a] Bin Zhou,[b,c] Tsui-wen Chou,[c] Elodie Ghedin,[c] Zizhang Sheng,[d] Rongyuan Gao,[a] Shao-lun Zhai,[e] Dan Wang,[a,f,g] Feng Li[a,f,g]

[a]Department of Biology and Microbiology, South Dakota State University, Brookings, South Dakota, USA. [b]Influenza Division, National Center for Immunization and Respiratory Diseases, Centers for Disease Control and Prevention, Atlanta, Georgia, USA. [c]Center for Genomics and Systems Biology, Department of Biology, New York University, New York, New York, USA. [d]Zuckerman Mind Brian Behavior Institute, Columbia University, New York, New York, USA. [e]Animal Disease Diagnostic Center, Institute of Animal Health, Guangdong Academy of Agricultural Sciences, Guangdong Key Laboratory of Animal Disease Prevention, Guangdong Open Laboratory of Veterinary Public Health, Guangzhou, China. [f]BioSNTR, Brookings, South Dakota, USA. [g]SD-CBRC, Brookings, South Dakota, USA.

https://doi.org/10.1128/JVI.01186-19.

Keywords: influenza D virus, reverse-genetics system

3.1 Introduction

Influenza viruses are enveloped, segmented, single-stranded, negative-sense RNA viruses that belong to the Orthomyxoviridae family. Four influenza types, A, B, C, and D are

classified on the basis of antigenic differences in the nucleoprotein (NP) and the matrix protein (M). Among these four types, influenza A virus (IAV) is the most common and the most pathogenic, causing seasonal epidemics every year in the Northern and Southern hemispheres and periodic pandemics (*121*). Despite lacking the ability to trigger pandemics, influenza B virus (IBV) also causes annual epidemics frequently associated with deaths in people (*18*). Influenza C virus (ICV) is generally not associated with annual influenza epidemics and gives rise to only mild respiratory infections in humans (*20*). Influenza D virus (IDV) was first isolated in 2011 (*4*) and officially named in 2016 (https://www.cdc.gov/flu/about/viruses/types.htm). Soon after its discovery, similar viruses were successively identified from swine and/or cattle in North and Central America, Asia, Europe, and Africa ((*23, 40, 41, 43, 49, 50, 52, 53, 58, 62-64*)). It was shown that IDV utilizes cattle as a primary reservoir and amplification host, with periodical spillover to other mammalian hosts (*21, 22*). In addition to swine and bovines, antibodies against IDV were detected in sera from small ruminants (goats and sheep), horses, camels, and humans (especially cattle workers) (*22-26, 41*). Significantly, a more recent study showed that the IDV genome was detected in nasal wash samples of a swine farm worker in Malaysia, Asia (*90*). Furthermore, molecular surveillance of respiratory viruses with bioaerosol sampling in the Raleigh-Durham International Airport found that among 4 (17%) of the 24 samples positive for known respiratory pathogens, 1 was positive specifically for IDV (*88*). It should be noted that none of the 24 samples tested positive for influenza A, B, and C viruses. Using a similar approach, one study detected IDV in hospital visitors in North Carolina (*89*). In addition to these epidemiological studies, several clinical studies were performed in cattle, showing that IDV replication

can damage the structure of epithelial cells lining the respiratory tract and cause mild respiratory disease in infected animals (*4, 75, 76*). Considering the worldwide distribution and broad host range of IDV and its potential to adapt to humans, it is necessary to further characterize this novel influenza virus at the molecular level.

Unlike the genomes of IAV and IBV that consist of eight segments, ICV and IDV contain only seven genome segments. The three longest segments of IDV encode the polymerase subunits PB2, PB1, and P3, which form a heterotrimer to catalyze the transcription and replication of the viral genome RNA (vRNA). Transcription of vRNA to mRNA starts with the "cap-snatching" reaction, a process during which capped RNAs are bound by the cap-binding domain of the PB2 subunit and cleaved by the endonuclease of the P3 subunit; actual RNA synthesis is performed by the PB1 subunit that forms the core structure of the heterotrimeric RNA polymerase complex (*22, 122*). The fourth segment produces a major surface glycoprotein, the hemagglutinin-esterase fusion (HEF), which harbors viral receptor-binding, receptor-destroying, and membrane fusion activities (*4, 29*). The fifth segment encodes the nucleoprotein (NP), which, together with the vRNA and the polymerase complex, forms the ribonucleoprotein (RNP) complex. Each vRNA segment forms an RNP complex, and the RNP is the fundamental unit for vRNA transcription and replication (*29*). The sixth segment encodes the matrix proteins DM1 and DM2, and the DM2 protein exhibits the ion channel activity (*9*). The last segment produces two nonstructural proteins, NS1 and NS2. To date, the biological function of the individual proteins of IAV has been well studied, while very limited work has been performed to characterize functions of IDV proteins.

Reverse genetics is one of the most powerful tools to study the biological properties and molecular characteristics of influenza viruses. But until now, no system for the rescue of IDV has been reported. Over the past 20 years and more, several plasmid-based systems for the rescue of recombinant IAV, IBV, and ICV have been successfully developed (*123-133*). To rescue an influenza virus in the unidirectional system, plasmids with the human RNA polymerase I (Pol I) promoter and the hepatitis delta virus ribozyme sequence or the mouse Pol I terminator are used to generate vRNA-like transcripts and are cotransfected with four other helper plasmids expressing PB2, PB1, PA/P3, and NP (*128, 129, 131*). In the bidirectional system, viral cDNA is inserted between the human Pol I promoter and the murine Pol I terminator, and the entire Pol I transcription unit is flanked by the bovine growth hormone (BGH) polyadenylation site or the simian virus 40 (SV40) late mRNA polyadenylation signal and the cytomegalovirus (CMV) Pol II promoter (*123, 130, 133*). Plasmids with the Pol I-Pol II transcription units allow the generation of both vRNA and mRNA from one viral cDNA template via the two different orientations. A modified system has been made to reduce the number of plasmids required for virus generation. This system combines multiple Pol I transcription units on one plasmid and allows the efficient generation of IAV in Vero cells (*126*). Finally, to overcome the limitation of species specificity of the Pol I transcription system, a T7 RNA polymerase-driven reverse-genetics system (RGS) was developed for efficient rescue of influenza viruses in human, avian, and canine cells (*132*).

Here, we describe the first RGS for IDV. By using a bidirectional seven-plasmid-based system, we generated recombinant influenza D/swine/Oklahoma/1314/2011 (D/OK) viruses. Their biological characteristics were evaluated in detail, and our analyses showed that RGS-rescued viruses had replication and receptor-binding properties similar to those of wild-type viruses in cell culture. We also developed a minigenome replication assay for IDV. This assay was successfully used to identify determinants of the activity of the IDV RNP complex essential for viral replication. In summary, we have successfully developed a minigenome replication assay and reverse-genetics system, and these tools can be used to further investigate the biology, tissue tropism, and transmission of IDV.

3.2 Results

3.2.1 Generation of infectious influenza D/swine/Oklahoma/1314/2011 virus by the reverse-genetics system

The cDNAs of the seven genomic segments (PB2, PB1, P3, HEF, NP, M, and NS) of influenza virus D/swine/Oklahoma/1314/2011 (D/OK) were amplified by reverse transcription-PCR (RT-PCR) and cloned individually into the bidirectional vector pHW2000 (Figure 3-1A). The pHW2000 vector contains the human Pol I promoter and the murine Pol I terminator that direct the precise synthesis of vRNA from one strand, flanked by the truncated CMV promoter and the BGH poly(A) signal that direct viral mRNA transcription from the opposite strand (*123*) (Figure 3-1A). The seven plasmids encoding each of the genomic segments of D/OK virus were cotransfected into cocultured HEK-293T (293T)–Madin-Darby canine kidney (MDCK) cells. Five days

after transfection, supernatants were collected and inoculated onto fresh MDCK cells. Three to five days after inoculation, infectious virus was detected only when all seven plasmids were present (data not shown). No virus was detected in the control group in which the plasmid encoding the PB2 segment was excluded. These results indicated that the infectious virus was generated from cloned plasmids following transfection.

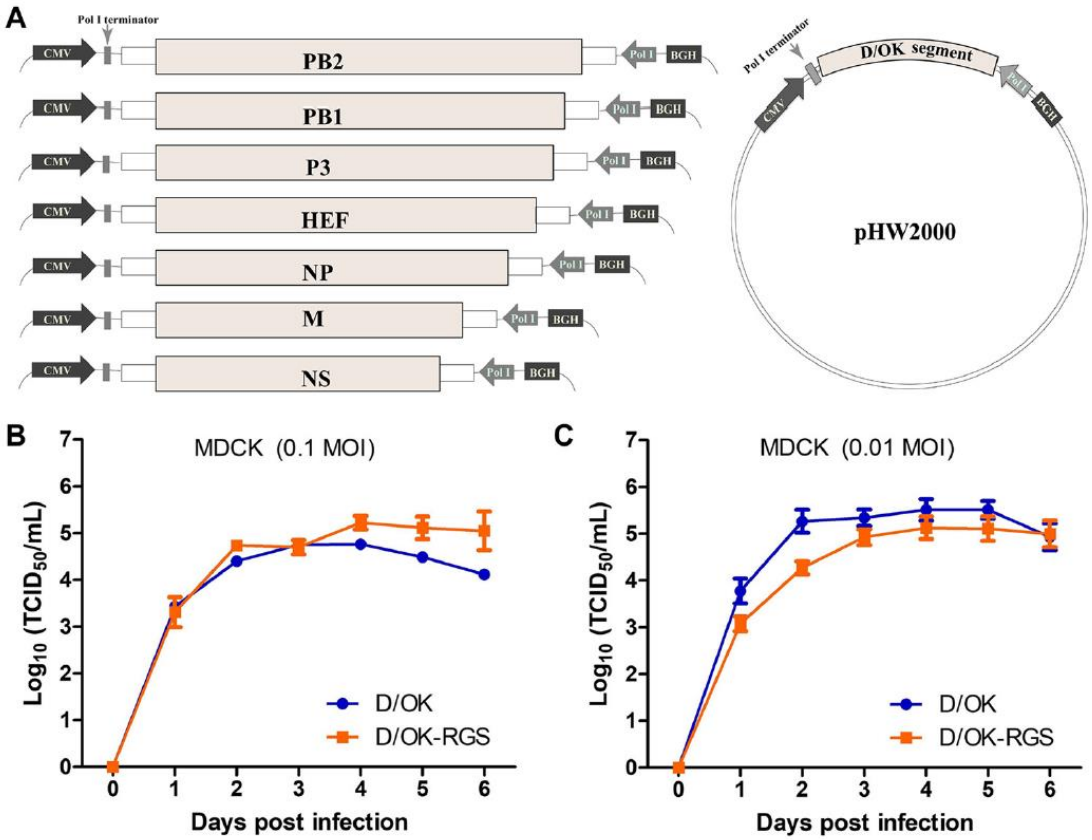

Figure 3-1. Generation of infectious influenza D/swine/Oklahoma/1314/2011 virus by the reverse-genetics system. (A) Schematic representation of the bidirectional seven-plasmid-based reverse-genetics system for IDV. The seven IDV cDNA segments were cloned into the pHW2000 vector (*123*). Each of the cDNA segments was flanked by the human Pol I promoter and the murine terminator. The RNA Pol I transcription unit was flanked by the truncated CMV promoter and the bovine growth hormone (BGH) poly(A) signal. (B and C) Growth kinetics of the wild-

type D/OK and the rescued D/OK-RGS viruses. MDCK cells were infected with the D/OK or D/OK-RGS virus at a MOI of 0.1 (B) or an MOI of 0.01 (C). Samples of supernatants were collected at the indicated times, and virus titers were then determined in MDCK cells by a TCID50 assay. The data presented in panels B and C are representative of results from three independent experiments, with each experiment analyzing samples in duplicate.

To determine whether there is any difference in replication between wild-type D/OK virus and rescued D/OK-RGS virus, we studied the growth kinetics of these viruses in MDCK cells. The cells were infected with the viruses at multiplicities of infection (MOIs) of 0.1 and 0.01. Samples of supernatants were collected every 24 h from day 0 to day 6, and virus titers were then determined by a 50% tissue culture infective dose (TCID50) assay. The wild-type D/OK virus and the rescued D/OK-RGS virus showed similar growth kinetics in MDCK cells infected at a MOI of 0.1 (Figure 3-1B) or a MOI of 0.01 (Figure 3-1C). Taken together, these data led us to conclude that the influenza D/OK virus was successfully rescued by the reverse-genetics system presented here.

3.2.2 Replication kinetics of continuously passaged influenza D/OK-RGS viruses at different temperatures

To ensure that rescued viruses from the transient transfection of 293T-MDCK cell cocultures with IDV RGS plasmids are stable in terms of infectivity during the course of serial passages, we conducted five more passages in MDCK cells using the RGS-derived virus and then analyzed their infectivity using the TCID50 assay. As shown in Figure 3-2A, similar virus stock titers were observed for D/OK-RGS viruses from passage 1 (P1)

to P5, ranging from 5.62 x10^4 TCID50/ml to 3.80 x 10^5 TCID50/ml. This result indicates that viruses rescued from our IDV RGS are stable and that the developed genetic system can be further exploited to study IDV infection biology.

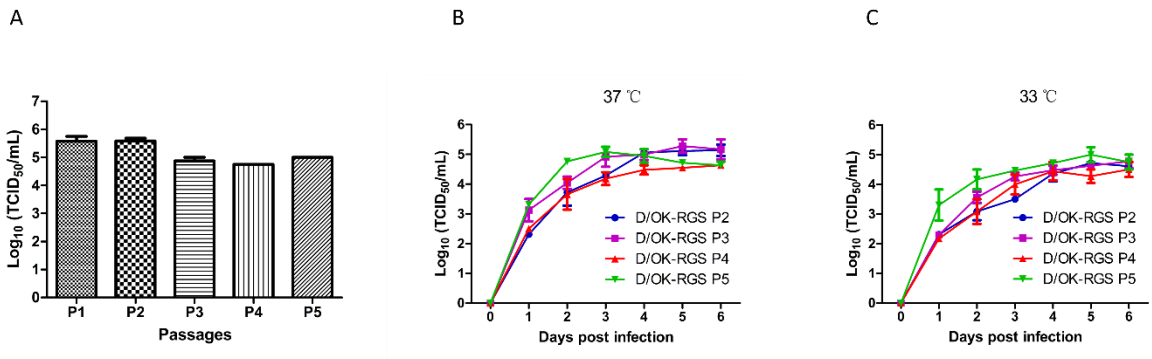

Figure 3-2. Growth kinetics of continuously passaged influenza D/OK-RGS viruses at different temperatures. (A) MDCK cells were infected with D/OK-RGS virus at an MOI of 0.01. After 5 days of infection, culture supernatants were collected and used for the next passage in MDCK cells. Virus titers at the indicated passages were determined by a TCID50 assay. (B and C) MDCK cells were infected with different passages of D/OK-RGS virus at an MOI of 0.01, followed by further incubation at 37°C (B) or 33°C (C). Samples of supernatants were collected at the indicated days and then titrated by a TCID50 assay. The data presented are representative of results from three independent experiments, with each experiment analyzing samples in duplicate.

Influenza D virus differs substantially from the related human influenza C virus (ICV) in temperature-restricted replication. Specifically, IDV replication is permissive at both 33°C and 37°C, while ICV replication is largely restricted to 33°C. Next, we determined whether RGS-derived viruses replicated in the same manner as the parental virus at both temperatures. As summarized in Figure 3-2B and C, different passages of D/OK-RGS

viruses (P2 to P5) replicated efficiently at both 33°C and 37°C, although the overall replication efficiency of these viruses was slightly lower at 33°C than at 37°C (Figure 2-3B and C). Furthermore, the serially passaged D/OK-RGS viruses showed similar growth kinetics at either 33°C or 37°C (Figure 3-2B and C). These data collectively show that IDV RGS-derived viruses, similar to the parental virus, replicate efficiently at both 33°C and 37°C, which further supports the utility of IDV RGS in future mechanistic studies toward elucidating a genetic basis of the temperature-mediated restriction that separates IDV from its related ICV.

3.2.3 Receptor binding of the wild-type D/OK and rescued D/OK-RGS viruses

Viral attachment to receptors on the host cell surface is the initial step of the virus life cycle. Sialic acids (SAs) have been found to serve as receptors for influenza viruses. N-acetylneuraminic acid (Neu5Ac) and N-glycolylneuraminic acid (Neu5Gc) are the most common SAs found on mammalian cell surfaces, both of which are ligands for influenza viruses. SAs are generally attached to glycan chains on glycoproteins or glycolipids via different glycosidic linkages. The most frequent linkage types are α-2,3 and α-2,6 linked to a galactose residue. IAV and IBV recognize α-2,3- or α-2,6-linked sialic acid moieties as receptors (*8*). However, ICV utilizes N-acetyl-9-O-acetylneuraminic acid (Neu5,9Ac2), which has an additional O-acetyl group at the C-9 position as the receptor; this is independent of the α-2,3- or α-2,6-linkage to the following galactosyl residue (*20*). A recent study shows that the IDV HEF protein can bind both Neu5,9Ac2 and 9-O-acetyl-N-glycolylneuraminic acid (Neu5Gc9Ac), regardless the α-2,3- or α-2,6-linkage, which

indicates that IDV uses 9-O-Ac-SAs as its receptor (*29*). The chemical structures of these SAs are shown in Figure 3-3A.

A

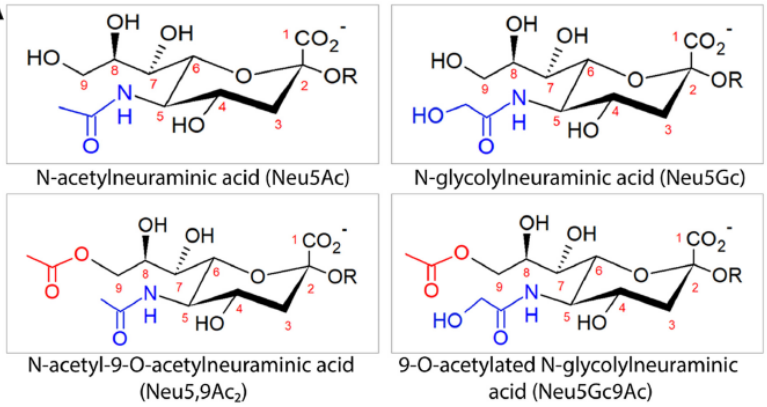

B

Neu5,9Ac$_2$ (ng/μL)	0	8	32	128	512	1024
D/OK virus	+	+	+	–	–	–
D/OK-RGS virus	+	+	+	–	–	–
PBS	–	–	–	–	–	–

"-": HA activity negative, "+": HA activity positive

C

Neu5Gc9Ac (ng/μL)	0	8	32	128	512	1024
D/OK virus	+	+	+	+	–	+
D/OK-RGS virus	+	+	+	+	–	+
PBS	–	–	–	–	–	+

"-": HA activity negative, "+": HA activity positive

Figure 3-3. Receptor-binding properties of the wild-type D/OK virus and the recombinant D/OK-RGS virus. (A) Chemical structures of sialic acids that serve as receptors for influenza viruses. (B and C) Inhibition of viral hemagglutination by receptor analogs. The receptor analog Neu5,9Ac$_2$ (B) or Neu5Gc9Ac (C) at the indicated concentrations was added to the virus containing 4 HA units. Mixtures were incubated for 30 min at room temperature. Aliquots of turkey RBCs were then added to the mixtures, and results were read after 30 min at room temperature. PBS was used

as a negative control. Note that "-" indicates no hemagglutination, while "+" denotes evident hemagglutination. The data presented in panels B and C are representative of results from four independent experiments, with each experiment analyzing samples in duplicate.

To further investigate whether the RGS-derived IDV resembles the parental virus in its receptor-binding profile, we used the traditional hemagglutination (HA) assay-based competitive inhibition approach to determine their receptor-binding properties, replacing antibody with synthetic receptor analogs. The viruses were incubated with the receptor analogs at various concentrations ranging from 0 to 1,024 ng/µl. Both D/OK and D/OK-RGS viruses were capable of agglutinating turkey red blood cells (RBCs) in the presence of lower concentrations of receptor analogs (Figure 3-3B and C). However, the HA activity of both viruses was completely inhibited in the presence of Neu5,9Ac_2 at concentrations of 128 ng/µl and above (Figure 3-3B) or in the presence of Neu5Gc9Ac at a concentration of 512 ng/µl (Figure 3-3C). Because the nonspecific reaction (agglutination) occurred between RBCs and higher concentrations of Neu5Gc9Ac, no HA inhibition was observed for both viruses in the presence of 1,204 ng/µl Neu5Gc9Ac (Figure 3-3C). In summary, the results suggested that the wild-type D/OK and rescued D/OK-RGS viruses had the same capacity to interact with the sialic acid receptors Neu5,9Ac_2 and Neu5Gc9Ac. The data presented here are important, as they further confirm the utility of our reported IDV RGS in future studies toward illustrating the molecular and chemical details of IDV receptor binding and entry.

3.2.4 Activity of the IDV RNP complex with PB1-E697K or PB2-L462F mutation

During the course of IDV RGS development, we identified two key mutations (PB1-E697K and PB2-L462F) that prevented us from successfully rescuing infectious virus particles. These two mutations were likely introduced by reverse transcription or PCR. These mutations have not been observed in natural IDV isolates. Here, we took advantage of these two coincident mutations and used them to assess the robustness of the newly developed IDV RGS. As demonstrated in Figure 4-4B, we found that the PB1-E697K mutation caused attenuation of viral replication, while the PB2-L462F mutation rendered the virus replication incompetent. To find out the underlying mechanisms, we developed a minigenome replication assay to investigate whether the PB1-E697K or PB2-L462F mutation directly affects the activity of the IDV RNP complex. We synthesized a reporter plasmid, pUC57$_{mini}$-D/OK-HEF-Reporter, that contains the green fluorescent protein (GFP) reporter gene located between the 5'- and 3'-end sequences of the viral cRNA of the D/OK HEF segment and flanked by the Pol I terminator and the human RNA Pol I promoter (Figure 4-4A). This reporter plasmid was cotransfected with plasmids encoding PB2, PB1, P3, and NP into 293T cells. The cellular RNA Pol I bound to the Pol I promoter to produce a reporter transcript that mimics the HEF vRNA, and the incoming viral polymerase complex then recognized the HEF terminal regions (viral promoter sequence) on the reporter transcript, initiating mRNA production for the expression of the GFP reporter. The GFP reporter was qualitatively detected by fluorescence microscopy (Figure 4-4C), while its expression level was quantitatively analyzed by both Western blotting (Figure 4-4D) and fluorescence-activated cell sorter (FACS) analysis (Figure 4-4E).

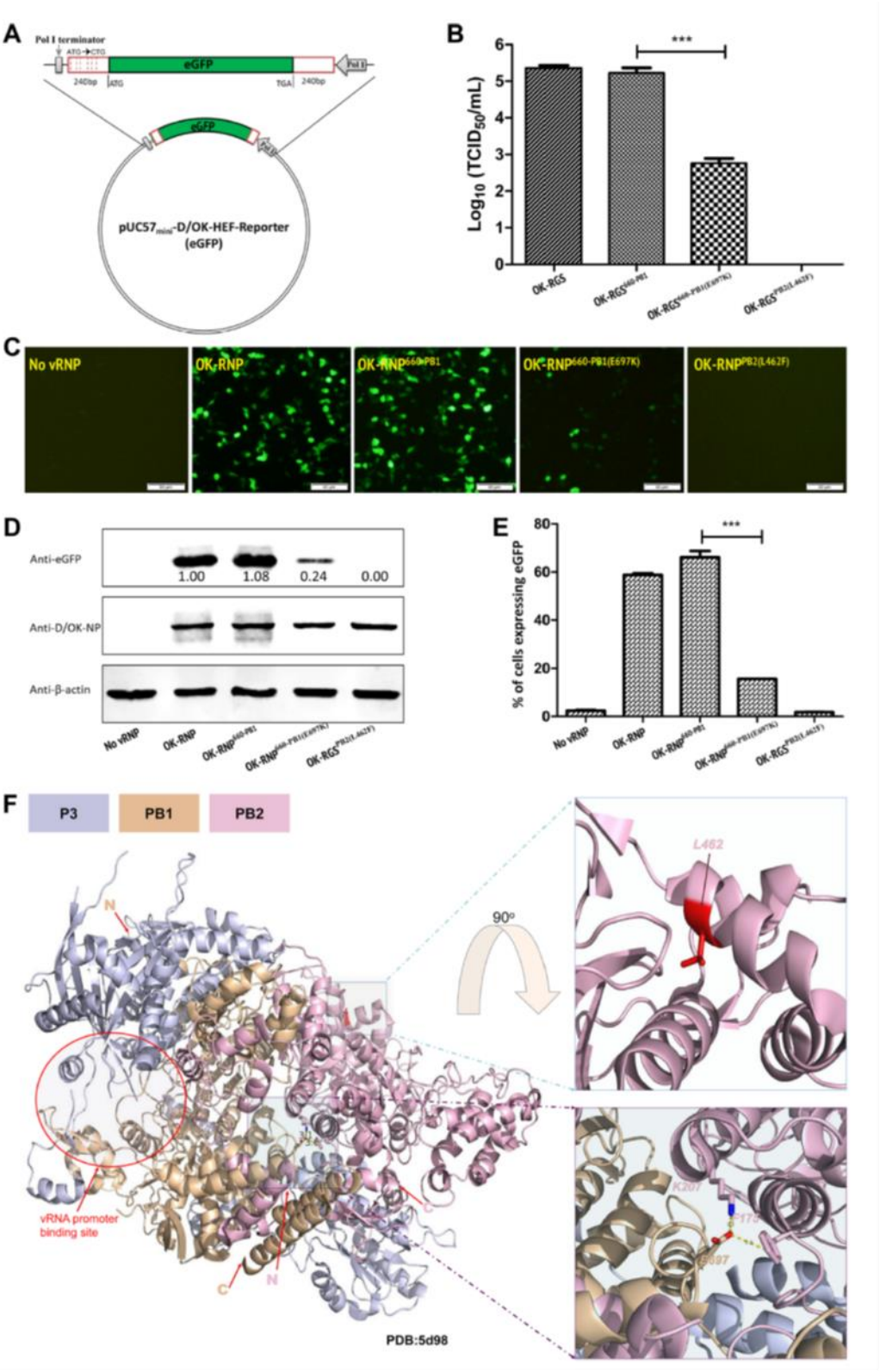

Figure 3-4. Legend in the next page

Figure 3-4. Activity of the IDV RNP complex with the PB1-E697K or PB2-L462F mutation. (A) Schematic diagram of the pUC57mini-D/OK-HEF-Reporter plasmid. This reporter plasmid contains the GFP reporter gene inserted between the D/OK-HEF cRNA 5= and 3= ends and then flanked by the Pol I terminator and the human RNA Pol I promoter. All ATG codons before the GFP translation initiation codon in the construct were mutated to CTGs; thus, the translation of GFP utilized its own start codon. (B) Virus titers for PB1-E697K and PB2-L462F mutants were determined by a TCID50 assay. Note that IDV OK-RGS$^{660\text{-}PB1}$ is identical to IDV OK-RGS except for the PB1 segment derived from IDV D/660. (C to E) Activity of the IDV wild-type RNP complex or the RNP complex with the PB1-E697K or PB2-L462F mutation was measured by a minigenome replication assay. In this assay, the GFP reporter plasmid and the wild-type or mutant plasmids encoding IDV RNP complex components were cotransfected into HEK-293T cells. At 48h post-transfection, cells were collected, and the GFP reporter was detected and analyzed by fluorescence microscopy (C), Western blotting (D), and FACS analysis (E). NP or β-actin was also detected by Western blotting, which was set up as a transfection or loading control, respectively. Note that densitometry of Western blot bands was quantified by using ImageJ software (https://imagej.nih.gov/ij/). Specifically, the density of the GFP band (i.e., surrogate of viral RNP activity) was first normalized by the value obtained with the input transfected NP control (i.e., to gauge the transfection variability). Relative viral RNP activity was determined by setting the level of the wild-type "OK-RNP" group to 1.00. (F) Mutations PB1-E697K and PB2-L462F are localized on the complex structure of RNA polymerase from ICV (PDB accession number 5D98). The structure of RNA polymerase was downloaded from the PDB (https://www.rcsb.org/) and was shown in PyMOL. The data presented in panels B to E are representative of results from three independent experiments, with each experiment analyzing samples in duplicate. eGFP, enhanced GFP.

We analyzed the activity of the IDV RNP complex with the PB2-L462F or PB1-E697K mutation by using the minigenome replication assay. Interestingly, no green fluorescence was observed when wild-type PB2 was replaced by the mutated PB2-L462F segment (Figure 4-4C). In support of this observation, the expression of GFP was below the detection level as either measured by Western blotting (Fig. 4D) or quantified by FACS analysis (Figure 4-4E). These results indicated that the L462F mutation on PB2 severely abolished the activity of the IDV RNP complex. For the PB1-E697K mutation that was observed only in the influenza virus D/bovine/Oklahoma/660/2013 (D/660) PB1 segment during our initial effort in the development of the IDV RGS, we first determined whether the wild-type D/660 PB1 segment could replace its counterpart (D/OK PB1) in the minigenome replicon assay. As demonstrated in Figure 4-4C to E, the substitution had no detectable effect on D/OK RNP activity. Interestingly, the RNP activity, as indicated by GFP reporter levels, was significantly decreased when wild-type D/OK PB1 was replaced with the mutant D/660 PB1-E697K segment (Figure 4-4C to E), indicating an essential role of PB1 E697 in viral genome replication of IDV. In summary, the PB2-L462F and PB1-E697K mutations, encountered during initial IDV RGS development, can lead to either replication-incompetent or replication-attenuated virus, likely caused by their direct effect on the activity of the IDV RNP complex.

To further investigate the underlying mechanisms by which PB1-E697K and PB2-L462F mutations impair RNP complex activity, we took advantage of the recently resolved structure of the RNA polymerase complex from ICV (PDB accession number 5D98) in the absence of promoter RNA (*134*) to structurally visualize the location of these two

mutations. Since the PB1 and PB2 proteins show high sequence similarity between ICV and IDV (*4*), and the corresponding positions are absolutely conserved in ICV, we assumed that the IDV RNA polymerase complex could adopt a structure similar to that of ICV and that structural modeling could offer mechanistic insight into mutation-associated replication defects. Our analysis showed that PB1 E697 most likely binds PB2 through hydrogen bonding to PB2 K207 (3.1 Å between E697 OE1 and K207 NZ atoms) and also forms an anion-pi interaction with PB2 F175 (~3.6 Å between E697 OE1 and F175 CZ atoms) (Figure 4-4F). The PB1-E697K mutation likely disrupts such interactions. PB2 L462 is located at the hydrophobic region of the cap-binding domain of PB2; thus, the PB2-L462F mutation may alter the stability or the conformation of the domain (Figure 4-4F). However, such interpretations should be taken cautiously because the structural resolution of the ICV RNP complex is relatively suboptimal (around 3.9 Å), and the side-chain locations may be inaccurate. Further structure-function studies of IDV RNP will test these hypotheses.

3.2.5 Recognition and transcription of the heterotypic promoter sequence by the IDV polymerase complex

Our previous work showed that the 1-nucleotide difference observed in the conserved 3’ noncoding ends of the vRNA segments between IDV and ICV could contribute to the failure of functional reassortment between these two viruses (*4*). It should be noted that in addition to this polymorphism at position 5 within the 3’ noncoding sequences, the noncoding regions (NCRs) across the seven segments between IDV and ICV are

relatively variable in both sequence and length, especially after the first 11 to 12 nucleotides (Figure 3-5A). These sequence variations as a whole may have a negative impact on the efficient cross-recognition of a heterotypic promoter by the viral RNP complex, resulting in the inhibition of vRNA replication and limiting functional reassortment between IDV and ICV (*21*). As a first step to address this hypothesis, we sought to determine whether the single polymorphism at position 5 between IDV and ICV affected the inefficient cross-recognition of the heterotypic promoter by the viral RNP complex. In this regard, we analyzed the activities of viral RNP complexes when cognate and noncognate promoters were provided in the minigenome replication assay.

Similar to the generation of the HEF segment-based GFP reporter plasmid, we constructed D/OK and influenza virus C/Victoria/2/2012 (C/Vic) M segment-based GFP reporter plasmids in which the full-length 5’ and 3’ noncoding regions of both M segments (containing both conserved and variable sequences) were used to direct the expression of the GFP reporter (Figure 5-5A). HEK-293T cells were cotransfected with plasmids expressing the RNP complex components from either D/OK or C/Vic and a reporter plasmid that contains the 5’ and 3’ noncoding regions of the M segment from one of the two viruses. According to the fluorescence microscopy and Western blot results, the D/OK RNP complex (D-RNP) or the C/Vic RNP complex (C-RNP) initiated the expression of GFP not only from its cognate reporter but also from the noncognate reporter (Figure 3-5B and C). However, the expression levels were visibly different between the cognate and noncognate groups, which showed that D-RNP with the cognate reporter or C-RNP with the cognate reporter produced higher levels of GFP than D-RNP

with the ICV reporter or C-RNP with the IDV reporter, respectively (Figure 3-5B and C). To further confirm these results, we quantified GFP expression by FACS analysis. There were 39.4% GFP-positive cells in the D-RNP-plus-IDV reporter group but only 22.4% GFP-positive cells in the D-RNP-plus-ICV reporter group (Figure 3-5D). Similarly, C-RNP working with the ICV reporter generated 34.9% of the positive GFP expression, while C-RNP working with the IDV reporter generated only 19.7% of the positive GFP expression (Figure 3-5D). These results indicated that IDV RNP or ICV RNP preferred using its cognate promoter to express proteins.

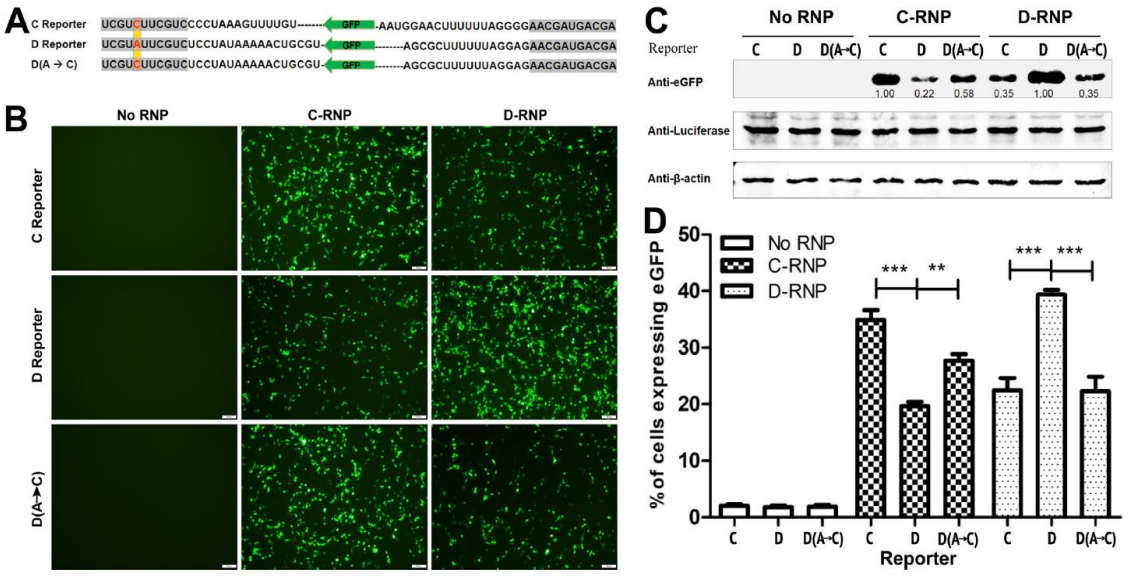

Figure 3-5. Activities of IDV and ICV RNP complexes with the conserved cognate or noncognate noncoding ends of vRNA segments. (A) Diagram showing nucleotide sequences of both the 3' and 5' noncoding regions in the M segment of influenza C and D viruses within the context of the GFP-based reporter. Note that the fifth nucleotide of the 3' noncoding end is different between the M segment sequences of influenza C and D viruses and is in red with

boldface type. “D(A-C)” indicates a mutated IDV reporter in which the fifth nucleotide, A, on the 3’ noncoding end of the D/OK M segment is altered to C, which makes it like the C/Vic M segment 3’ NCR in the first 11 nucleotides. (B to D) Activities of IDV and ICV RNP complexes with the cognate or noncognate promoter were determined by the minigenome replication assay. HEK-293T cells were cotransfected with the ICV or IDV M segment promoter sequence-based GFP reporter plasmid and the plasmids expressing RNP complex components from either D/OK or C/Vic. At 48 h posttransfection, cells were collected, and GFP reporter protein expression was analyzed by fluorescence microscopy (B), Western blotting (C), and FACS analysis (D). Renilla luciferase or β-actin detected by Western blotting was set up as a transfection or loading control. Note that densitometry of Western blot bands was quantified by using ImageJ software (https://imagej.nih.gov/ij/) (C). Specifically, the density of the GFP band (i.e., surrogate of viral RNP activity) was first normalized by the value obtained with the input transfected Renilla luciferase control (i.e., to gauge the transfection variability). Relative viral RNP activity was determined by setting the level of the wild-type group involving C-RNP/C-reporter or D-RNP/D-reporter (containing the respective cognate promoter) to 1.00. The data presented in panels B to D are representative of results from three independent experiments, with each experiment analyzing samples in duplicate.

Since there is only one difference in the first 11 nucleotides of the 3’ NCR between IDV and ICV (*4*, *21*) (Table 3-2), it is very likely that this nucleotide difference affects recognition and transcription of the heterotypic model GFP vRNA by the IDV or ICV polymerase complex. To address this hypothesis, we constructed a mutated IDV reporter plasmid in which the fifth nucleotide, A, on the 3’ NCR of the D/OK M segment was altered to C, which made it like the ICV M segment 3’ NCR in the first 11 nucleotides (Figure 3-5A). It should be noted that the first 11 nucleotides are absolutely conserved in

the 5’ NCR of the M segment between IDV and ICV. Interestingly, this substitution gave rise to significant increases in the expression and replication of the mutant IDV reporter by C-RNP compared to those observed for the wild-type IDV reporter with heterotypic C-RNP in the minireplicon assay (27% versus 19% GFP-positive cells) (Figure 3-5B and D). Conversely, the substitution reduced substantially the activity of the IDV reporter by its cognate D-RNP in comparison to that observed in the minireplicon assay involving the wild-type IDV reporter and D-RNP (22% versus 39.4% GFP-positive cells) (Figure 3-5B and D). Quantitative analysis of GFP expression levels in Western blot assays using ImageJ (https://imagej.nih.gov/ij/) also confirmed the differential activity observed in the cell-based minireplicon assay (Figure 3-5C). For example, the GFP expression level from C-RNP/mutant D reporter containing an A-to-C substitution increased by more than 2-fold compared to that shown from the combination of C-RNP/D reporter. In contrast, the GFP expression level decreased by approximately 3-fold for the D-RNP group when the same mutant D reporter was provided in transfected cells. Altogether, these results revealed that the 1-nucleotide change in the highly conserved noncoding region negatively influences the heterotypic recognition and transcription of vRNAs by the viral RNP complex. The observed heterotypic promoter incompatibility together with other viral factors, such as packaging sequence variation, may contribute to the failure of viable reassortment between IDV and the closely related ICV, which warrants further investigation.

3.3 Discussion

Reverse-genetics systems (RGSs) have already been described for IAV, IBV, and ICV but not yet for IDV. In this study, the first RGS of IDV was successfully developed using a bidirectional seven-plasmid-based system, and the resultant viruses were studied in comparison with the wild-type viruses. We also developed a minigenome replication assay for IDV. Biological characterizations involving mutations collectively demonstrated the robustness and versatility of these two systems, indicating their utility as powerful tools to study structure-function relationships of IDV proteins. The IDV RGS can also be used to elucidate critical determinants that drive IDV to use this agricultural animal as a primary reservoir and amplification host.

Many different ways have been established in the past 2 decades to generate recombinant influenza viruses, including earlier helper virus-dependent methods and later helper virus-independent plasmid-based systems. In helper virus-dependent methods, selection strategies are required because additional helper viruses are used and therefore have to be depleted through drug selection. Owing to this disadvantage, helper virus-dependent methods have been largely replaced by later helper virus-independent plasmid-based methods (*127*). The unidirectional and bidirectional plasmid-based systems have emerged as two predominant helper virus-independent RGSs, which have been previously reported for IAV, IBV, and ICV (*123, 125, 128-131, 133*). In the present study, we succeeded in rescuing recombinant IDVs by using a bidirectional seven-plasmid-based system (Figure 3-1), which is the first RGS reported for IDV. Generally, it is difficult to compare the

generation efficiencies and titers of different influenza virus RGSs. Many factors, such as the cell line selected, transfection efficiency, technical protocol, and virus replication fitness, may determine which strategy should be used. Initially, we failed to generate the recombinant D/OK virus when we directly followed protocols (*123*) that are commonly used for the rescue of influenza A viruses. We realized that the D/OK virus cannot induce significant cytopathic effects and has a much lower replication capacity than influenza A virus in MDCK cells. Moreover, the 293T cell line has weak adhesion to the surfaces of cell culture vessels and is extremely sensitive to tosylsulfonyl phenylalanyl chloromethyl ketone (TPCK)-trypsin, which is required for the cleavage of the HEF protein and probably activation of viral fusion. Therefore, we added a lower concentration of TPCK-trypsin at a later time point, which was optimal to maintain 293T cell viability and, as a result, provided sufficient time for rescue of the recombinant D/OK virus. After making these subtle but critical changes, we could detect the rescued D/OK virus in the supernatant of transfected 293T-MDCK cells at 4 to 5 days posttransfection, which was slower than the rescue of influenza A virus, which could be detected at 2 to 3 days posttransfection (*123*). These findings suggest that rescue strategies for different types or strains of influenza virus should be adjusted according to their replication property and fitness, which will be vital for the successful rescue of IDV or IDV-similar influenza viruses.

Our comparative in vitro growth kinetics studies showed indistinguishable replication fitness of both the parental and RGS-derived viruses, and the RGS viruses can be stably cultured over multiple passages, at both 33°C and 37°C (Figure 3-1 and 2). In addition,

the RGS viruses displayed a receptor-binding capacity indistinguishable from that displayed by the authentic virus (Figure 3-3). These studies clearly suggested that an efficient reverse-genetics system was successfully established and allowed for the genetic manipulation of viral genomes and the generation of mutant viruses, which opens the door for studying the functional importance of viral proteins and molecular aspects of viral replication and pathogenicity.

It has been known that both IDV and ICV contain only one major surface glycoprotein, HEF, which plays multiple critical roles during the virus life cycle (*4, 20*). First, HEF binds to the receptor to initiate virus entry. In agreement with previous reports (*29*), our results showed that IDV HEF could recognize both Neu5,9Ac2 and Neu5Gc9Ac (Figure 3-3), which is different from ICV HEF, which prefers Neu5,9Ac2 over Neu5Gc9Ac as a viral receptor (*20*). HEFs of ICV and IDV have about 53% homology and possess almost identical overall structures (28). One interesting difference between them is that the IDV HEF protein has an open channel in the receptor-binding region, while in the structurally identical region of ICV HEF, there is a salt bridge (*29*). This subtle difference may indicate that IDV has different receptor-binding properties compared to ICV. With the availability of the RGSs, we can directly investigate the diverse receptor-binding properties arising from the subtle genetic differences between IDV and ICV. Second, HEF was a critical determinant of IDV's antigenic diversity. Amino acid substitutions near the HEF receptor-binding region are involved in antigenic variation of influenza viruses (*135*). To understand the molecular basis for IDV lineage-dependent antigenicity, we can use the RGS to introduce select amino acid changes individually or in

combination into the IDV HEF protein and analyze the antigenic properties of these recombinant viruses to identify amino acids determining the antigenicity of IDV. Third, HEF exhibits unique thermodynamic properties. It is known that ICV grows more efficiently at 33°C than at 37°C (*20, 136*). HEF is considered to be an important restriction factor for the temperature sensitivity of ICV (*136*). Interestingly, IDV replicates well at both 33°C and 37°C (*4*) (Figure 3-2). Our previous experiments showed that IDV was able to tolerate a high-temperature environment, and HEF is the primary determinant for the high thermal stability of IDV (*91*). It will be very interesting to use the RGS to determine the amino acids or protein motifs that account for the different thermodynamic properties between ICV HEF and IDV HEF.

During the development of the IDV RGS, we identified several mutations in the viral polymerase complex proteins that rendered the RGS less productive and led to the failed rescue of viable viruses. To investigate the biological significance of these mutations and gain mechanistic insight, we developed a minigenome replication assay for IDV. This system has been widely used to study influenza virus RNP activity by cotransfecting cells with four plasmids encoding PB2, PB1, PA/P3, and NP and a viral promoter-driven reporter plasmid (*128, 137*). Our results of the minigenome replication assay showed that the RNP activity was lost due to the introduction of the L462F mutation into D/OK PB2 (Figure 3-4), which explained why the PB2-L462F mutation caused the failure of RGS in rescuing viruses. The E697K change in PB1 resulted in significantly lower RNP activity than for wild-type PB1 (Figure 3-4). This finding was consistent with the observation that the recombinant IDV containing the PB1-E697K mutation had an extremely low virus

titer (Figure 3-4B). These two mutations on the polymerase complex proteins showed a significant negative impact on RNP activity and, as a result, posed a challenge in rescuing viable IDVs. These data also provide additional justification for exploring conserved polymerase function as a target for anti-influenza drug development.

By using the minigenome replication assay, we further demonstrated that a single nucleotide difference at position 5 of the 3' NCR within the first 11 nucleotides between IDV and ICV resulted in the inefficient cross-recognition of the heterotypic promoter by the viral RNP complex. This functional incompatibility in vRNA replication between IDV and ICV may contribute to the failure of viable reassortment between IDV and ICV, as demonstrated in our previous study. In addition to this single polymorphism, the 3' NCR also shows considerable sequence variation between IDV and ICV in the region toward the segment-specific protein-coding sequence. Their impact on constraining IDV and ICV reassortment should be further investigated. Because productive packaging of vRNAs and successful reassortment between influenza viruses require multiple cis-acting elements and trans-acting factors (*138-140*), we suppose that multiple factors are probably involved in collectively restricting productive reassortment between IDV and the closely related ICV in animal hosts. This hypothesis can be addressed using the robust IDV RGS presented in this study.

3.4 Materials and methods

3.4.1 Cells, viruses, and antibodies

Human embryonic kidney HEK-293T cells (ATCC) and Madin-Darby canine kidney (MDCK) cells (ATCC) were maintained in Dulbecco's modified Eagle medium (DMEM; Gibco, Invitrogen, USA) supplemented with 10% (vol/vol) fetal bovine serum (FBS; PAA Laboratories, Dartmouth, MA, USA) and 100 U/ml penicillin-streptomycin (Life Technologies, Carlsbad, CA, USA). All cells were cultured at 37°C in the presence of 5% CO2. Influenza viruses D/swine/Oklahoma/1314/2011 (D/OK) and D/bovine/Oklahoma/660/2013 (D/660) were propagated in MDCK cells at 37°C. Influenza virus C/Victoria/2/2012 (C/Vic) was grown in MDCK cells at 33°C. Polyclonal rabbit antibody against IDV D/OK was generated in-house by immunizing rabbits with concentrated IDV particles that were inactivated by UV light treatment. Polyclonal rabbit anti-GFP antibody was obtained from Santa Cruz Biotechnology, while monoclonal anti-β-actin antibody was purchased from Sigma-Aldrich. Secondary antibodies such as IRDye 680RD donkey anti-rabbit IgG and IRDye 680RD goat anti-mouse IgG were purchased from Li-Cor.

3.4.2 Construction of plasmids

Viral RNAs were isolated from infectious virus particles with the TRIzol LS reagent (Invitrogen, CA, USA) according to the manufacturer's instructions. RT-PCR was performed with a high-capacity cDNA reverse transcription kit (Thermo Fisher Scientific)

according to the protocol provided by the manufacturer. The primers used to amplify each individual segment in the RT-PCRs are summarized in Table 3-1. After digestion of the PCR products with BsmBI or BsaI, the fragments were purified and cloned into the pHW2000 vector (*123*) (Fig. 3-1A). All inserted cDNAs were sequenced and confirmed (GenScript, NJ, USA) to ensure that there were no unwanted mutations in the constructs.

3.4.3 Transfection and rescue of recombinant viruses

Approximately 20 to 24 h before transfection, cells (~6 x 10^5 HEK-293T cells and ~1.5 x 10^5 MDCK cells) were plated in 2 ml of complete growth medium per well in a 6-well plate. Prior to transfection, cells were 50% to 70% confluent, and the old growth medium was replaced with fresh medium containing 10% FBS without antibiotics. The reverse-genetics plasmids of IDV (1 µg for each segment) were mixed and added into 200 µl of Opti-MEM. Next, 18 µl of polyethylenimine (PEI) was dropped into the premixed diluted plasmids. Mixtures were incubated for 20 min at room temperature and added into different areas of the wells. The culture vessel was gently rocked back and forth and from side to side to evenly distribute the DNA-PEI complexes. At 6 to 9 h posttransfection, the old medium was replaced with 2 ml of fresh DMEM without FBS but containing antibiotics. After another 36 to 42 h of incubation at 37°C, 0.5 ml of DMEM containing 1 µg/ml TPCK-trypsin (Thermo Fisher Scientific) was added to each well. Virus HA titers of ~32 could be detected 3 to 5 days after transfection.

3.4.4 Virus replication assay

Viruses were cultured and measured in MDCK cells in DMEM supplemented with 1 μg/ml TPCK-trypsin and 100 U/ml penicillin-streptomycin. Viral growth kinetics studies were performed on a monolayer of MDCK cells using an inoculum at a multiplicity of infection (MOI) of 0.1 or 0.01. One hour after incubation at 37°C, cells were washed twice with phosphate-buffered saline (PBS), and fresh DMEM with 1 μg/ml TPCK-trypsin and 100 U/ml penicillin-streptomycin was added. Samples were collected at 0, 24, 48, 72, 96, 120, and 144 h postinfection and titrated by a TCID50 assay.

Table 3-1 Primers used in the RT-PCR and cloning experiments

Primer	Sequence (5'–3')
PB2_IDV_BsaI_For	TATTGGTCTCAGGGAAGCATAAGCAGAGGATGTCACTACTATTAAC
PB2_IDV_BsaI_Rev	ATATGGTCTCGTATTAGCAGTAGCAAGAGGATTTTTTCAATG
PB1_IDV_BsmBI_For	TATTCGTCTCAGGGAAGCATAAGCAGAGGATTTTATAAAATGG
PB1_IDV_BsmBI_Rev	ATATCGTCTCGTATTAGCAGTAGCAAGAGGATTTTTCTGTT
P3_IDV_BsaI_For	TATTGGTCTCAGGGAAGCATAAGCAGGAGATTTAGAAATGTCTAG
P3_IDV_BsaI_Rev	ATATGGTCTCGTATTAGCAGTAGCAAGGAGATTTTTAACATTACAAG
HEF_IDV_BsmBI_For	TATTCGTCTCAGGGAAGCATAAGCAGGAGATTTTCAAAGATG
HEF_IDV_BsmBI_Rev	ATATCGTCTCGTATTAGCAGTAGCAAGGAGATTTTTTCTAAGATTC
NP_IDV_BsmBI_For	TATTCGTCTCAGGGAAGCATAAGCAGGAGATTATTAAGCAATATGG
NP_IDV_BsmBI_Rev	ATATCGTCTCGTATTAGCAGTAGCAAGGAGATTTTTTG
M_IDV_BsmBI_For	TATTCGTCTCAGGGAAGCATAAGCAGAGGATATTTTTGACGCAATG
M_IDV_BsmBI_Rev	ATATCGTCTCGTATTAGCAGTAGCAAGAGGATTTTTTCGC
NS_IDV_BsmBI_For	TATTCGTCTCAGGGAAGCATAAGCAGGGGTGTACAATTTCAATATG
NS_IDV_BsmBI_Rev	ATATCGTCTCGTATTAGCAGTAGCAAGGGGTTTTTTCATACTAAAG

3.4.5 Hemagglutination-based competitive inhibition assay

Twenty-five microliters of virus suspensions containing 4 HA units of virus was added to 25 µl of receptor analogs (Neu5,9Ac$_2$ or Neu5Gc9Ac) (Glycohub). The virus-receptor analog mixtures were incubated for 30 min at room temperature. Fifty microliters of 1% turkey red blood cells (RBCs) (Lampire Biological Laboratories, Pipersville, PA, USA) was then added to the mixtures, and results were read after 30 min. PBS was used as a negative control.

Table 3-2. Comparison of the conserved 3'-noncoding ends of the vRNA segments from influenza C and D viruses

Segment	D/OK 3' NC end (3'-5'orientation)	C/Vic 3' NC end (3'-5'orientation)
PB2	UCGUAUUCGUCUCCUA	UCGUCUUCGUCUCCUA
PB1	UCGUAUUCGUCUCCUA	UCGUCUUCGUCUCCUA
P3	UCGUAUUCGUCCUCUA	UCGUCUUCGUCCCCUA
HEF	UCGUAUUCGUCCUCUA	UCGUCUUCGUCCCCUU
NP	UCGUAUUCGUCCUCUA	UCGUCUUCGUCCUCUA
M	UCGUAUUCGUCUCCUA	UCGUCUUCGUCCCCUA
NS	UCGUAUUCGUCCCCAC	UCGUCUUCGUCCCCAU

3.4.6 Minigenome replication assay

A reporter plasmid, pUC57$_{mini}$-D/OK-HEF-Reporter, was synthesized by GenScript. It contains the GFP reporter gene inserted between the 5'- and 3'-end sequences of the viral cRNA of the D/OK HEF segment, and it is flanked by the Pol I terminator and the human

RNA Pol I promoter (Figure 3-4A). All ATG codons before the GFP translation initiation codon in the construct were mutated to CTGs; thus, the translation of GFP used its own start codon (Figure 3-4A). The M segment promoter sequence-based GFP reporter plasmids for both ICV and IDV were generated by conventional PCR and mutagenesis. The reporter plasmid was cotransfected with plasmids expressing RNP complex components (PB2, PB1, P3, and NP) into HEK-293T cells. At 48 h posttransfection, cells were collected, and the GFP reporter protein was detected by fluorescence microscopy and Western blotting. Percentages of GFP-positive cells were quantified by flow cytometry.

3.4.7 Statistical analysis

The data presented in this paper are representative of results from three independent experiments, with each experiment assaying samples in duplicate. Standard-deviation bars indicate the variations among experiments. To analyze the difference between groups, statistical analysis by one-way analysis of variance (ANOVA) followed by Tukey's multiple-comparison test was performed using GraphPad Prism 5.0. Statistically significant differences are indicated in the figures (**, $P < 0.01$; ***, $P < 0.001$).

CHAPTER 4. IDENTIFICATION OF TWO RESIDUES WITHIN THE NUCLEOPROTEIN THAT CRITICALLY AFFECT THE REPLICATION FITNESS OF INFLUENZA D VIRUS

Jieshi Yu,[a]* Chen Huang,[a]* Zizhang Sheng,[b] Dan Wang,[a,c,d] Feng Li[a,c,d]

[a]Department of Biology and Microbiology, South Dakota State University, Brookings, South Dakota, USA. [b]Zuckerman Mind Brian Behavior Institute, Columbia University, New York, New York, USA. [c]BioSNTR, Brookings, South Dakota, USA. [d]SD-CBRC, Brookings, South Dakota, USA. *These authors contributed equally to this work.

Keywords: influenza D virus, reverse-genetics system, replication.

4.1 Introduction

Influenza D virus (IDV), a new genus of the *Orthomyxoviridae* family, was first isolated from clinical ill pigs in 2011 in Oklahoma, USA (*4*). Further epidemiological studies demonstrated that cattle, not pigs, are the primary reservoir of this virus (*21, 38, 40*). To date, IDV has been identified in many countries worldwide, including USA, Canada and Mexico in North America; France, Italy, Ireland, Luxembourg and UK in Europe; China, Japan and Turkey in Asia; and Morocco, Benin, Togo, Kenya and Ethiopia in Africa (*4, 26, 40, 49-53, 62-64, 66-68*). The high seroprevalence of IDV in cattle has been reported in USA (77.5%, n=1992) (*42*), Japan (30.5%, n=1267) (*66*), France (42.7%, n=3326) (*56*), Luxembourg (80.2%, n=450) (*52*), Italy (92.4%, n=420) (*55*), and Ireland (94.6%,

n=1219) (*57*), respectively. The wide circulation and high prevalence of IDV, especially in cattle, highlight the potential threat of IDV to other animal species. Indeed, IDV has also been detected in small ruminants, horses, camels, buffaloes and feral pigs (*23, 24, 26, 48, 54, 56, 57, 63, 68*). These findings suggest that IDV has a global distribution with a broad host range.

Several surveillance and metagenomic studies have shown that IDV detection rates are higher in diseased cattle than that in healthy cattle, and the virus is highly associated with bovine respiratory disease (BRD) complex (*40, 43, 44, 63, 73*). BRD is the most common and costly disease in cattle industry. It is caused by complex interactions between host, multiple pathogens including viruses and bacteria, and environmental factors, leading to 70-80% of the morbidity in USA cattle industry (*43, 78*). The pathogenesis of IDV in cattle has also been validated by experimental infection studies. The results of these studies revealed that IDV caused mild respiratory disease in cattle and could be transmitted between cattle by direct contact or aerosol (*74-77*). In addition, IDV is able to infect ferrets and guinea pigs, both surrogate models for studies of influenza viruses in humans (*4, 82*). IDV infection causes little clinical symptoms but the virus can be transmitted by direct contact in ferrets or guinea pigs (*4, 82*). Moreover, IDV has the capacity to efficiently replicate in the well-differentiated human airway epithelial cells (hAECs), frequently serving as an *in vitro* respiratory epithelium model for emerging respiratory virus studies in humans (*83, 84*). These observations suggest that IDV may have the potential to adapt and transmit to humans. Several serologic studies have demonstrated that antibodies against IDV were detected in humans (*4, 25, 61*). Notably, a

high seroprevalence of IDV was observed among workers with cattle exposure (34 out of 35 persons had IDV antibodies), as reported by a serological study in Florida, USA (*25*). The prevalence of IDV-specific antibodies in humans implies that the virus may infect humans.

Based on the sequences of the hemagglutinin-esterase-fusion (HEF) gene, IDV can be classified into three genetic lineages: D/OK-lineage, D/660-lineage and D/Japan-lineage (*5*). Recently, a new IDV strain isolated from Japan (D/bovine/Yamagata/1/2019) was found to be genetically and antigenically distinguished from the described three lineages, which may be represented as a new IDV lineage (*71*). The D/swine/Oklahoma/1334/2011 (D/OK), D/Bovine/Oklahoma/660/2013 (D/660) and D/bovine/Yamagata/10710/2016 (D/Yamagata) are the representative strains of the D/OK-, D/660-, and D/Japan-lineages, respectively (*5, 21, 38, 64*). They are widely used for the phylogenetic and antigenic studies of IDV. Both the common and lineage-specific antigenicity of IDV were observed (*5, 38*). However, different molecular characteristics among these IDV lineages are not known. The recent reported reverse genetics system of IDV (*141, 142*) should facilitate our understanding of the molecular biology of this emerging influenza virus.

IDV, similar to influenza C virus (ICV), contains seven genome segments and encodes 9 proteins, including the polymerase subunits PB2, PB1, and P3, surface glycoprotein HEF, nucleoprotein (NP), matrix protein M1, ion channel protein M2, and two nonstructural proteins NS1, NS2 (*4, 9, 22, 29, 143, 144*). NP is a multi-functional protein in influenza virus life cycle. As a critical component of ribonucleoprotein (RNP) complex, NP is

essential for viral RNA transcription and replication (*145*). IDV NP contains a bipartite nuclear localization signal (NLS) in the C-terminal tail, which interacts with importin-α7 to mediate nuclear import of NP (*144*). It is reported that some mutations in NP affect the formation of NP homo-oligomers, interaction between polymerase subunits and the binding to viral RNA, which are together associated with the RNP activity (*146-148*). Furthermore, influenza A virus (IAV) NP can act as an elongation factor, while it is dispensable for initiation and termination of viral RNA transcription and replication (*149, 150*). In addition, NP plays a important role in viral replication fitness through some other mechanisms including immune evasion, regulation of apoptosis and autophagy, and interactions with some other host factors (*151-154*).

In the present study, the different viral growth properties were observed and validated between D/OK and D/660 viruses. By using a reverse-genetics system, we found that the NP segment of IDV contributed to the viral replication fitness. Finally, our results demonstrated that amino acids at the positions 247 and 381 of NP critically affected IDV replication efficiency. Interestingly, these two amino acid changes in the NP do not affect IDV RNP activity but may have effect on the late stage of the viral replication cycle, which warrants further examination.

4.2 Results

4.2.1 The D/660 virus was superior to the D/OK virus in replication in different cell lines

To examine and compare the replication fitness of two lineage-representative IDV strains, D/660 and D/OK, we first determined their replication kinetics in MDCK cells that are commonly used for studies of influenza viruses. MDCK cells were infected in parallel with either D/660 or D/OK at a MOI of 0.01 at 37 °C. Aliquots of the tissue culture supernatant were taken at periodic intervals and analyzed for virus replication by using the standard HA assay and TCID50 titration. The data showed that both viruses grew to the peak viral titers at 3 days after infection (Figure 4-1A). Interestingly, we observed that the D/660 virus had ~2.0 $\log_{10}$TCID50/ml or ~ 2.5 $\log_2$HA units, which were substantially higher than the D/OK virus from 2 days post-infection in MDCK cells (Figure 4-1A). The observed growth difference between two viruses was generally maintained during the rest of this five-day experiment.

To confirm the observation, we further compared the replication kinetics of the two viruses in other cell lines. The D/OK and D/660 viruses are respectively isolated from swine and bovine, and able to replicate in a variety of cell lines including human cells (*4, 21*). Therefore, we performed comparisons of the replication abilities of the two viruses in Swine Testis (ST) cells, Madin-Darby Bovine Kidney (MDBK) cells, and Human Rectal Tumor (HRT-18) cells. The results of our experiments showed that the D/660 virus replicated to significantly higher titers than the D/OK virus in all these cell lines (Figure 4-1B to D). The differences of peak viral titers between the D/660 and D/OK viruses were ~2.5 $\log_{10}$TCID50/ml or ~ 3.0 $\log_2$HA units in ST cells (Figure 4-1B), ~2.0 $\log_{10}$TCID50/ml or ~ 3.5 $\log_2$HA units in MDBK cells (Figure 4-1C), and ~2.5

log_{10}TCID50/ml or ~ 3.5 log_2HA units in HRT cells (Figure 4-1D). These data further strengthened our observation that the D/660 virus was superior to the D/OK virus in replication in multiple cell lines.

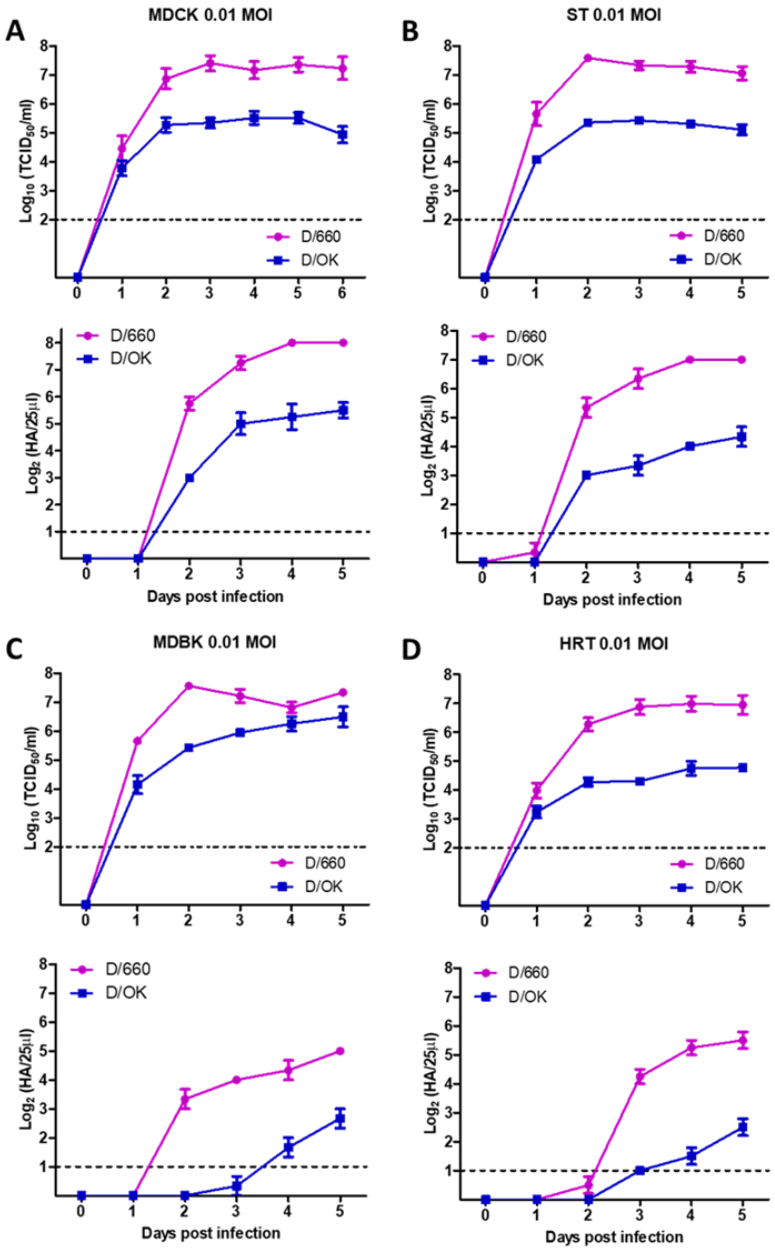

Figure legend in the next page.

Figure 4-1. Replication kinetics of D/660 and D/OK viruses in different cell lines. (A-D) MDCK (A), ST (B), MDBK (C) and HRT-18 (D) cell lines were inoculated with an 0.01 MOI of D/660 or D/OK viruses at the indicated time points. Virus titers were determined by TCID50 per ml in MDCK cells and HA assay. The error bars are representative of three independent experiments.

4.2.2 NP was a key determinant of the replication difference between the D/660 and D/OK viruses

To investigate the underlying mechanisms that attribute to the different viral replication fitness between the D/660 and D/OK viruses, the reverse genetics system was employed to generate chimeric viruses to examine which segment(s) affected the virus replication. As shown in Figure 4-2A, the D/OK virus was used as a genetic backbone, and each of the segment was replaced with its counterpart from the D/660 virus, respectively. MDCK cells were infected with rescued wild-type D/OK virus and other chimeric viruses at a MOI of 0.01, and culture supernatants were collected at the indicated time intervals and assayed for virus replication by using the standard TCID50 experiment. Compared with wild-type D/OK virus, none of the chimeric viruses carrying D/660 PB2, PB1, P3, M or NS segment showed an improved growth kinetics (Figure 4-2B). However, in contrast to the wild-type D/OK virus, when the HEF segment of the D/OK virus was replaced with that of the D/660 virus, the titers of this recombinant virus increased by ~1 $\log_{10}$TCID50/ml (Figure 4-2B). Most importantly, if the NP segment was replaced, the replication titers of the chimeric D/OK virus with the D/660 NP were 2 $\log_{10}$TCID50/ml higher than that of the wild-type D/OK virus (Figure 4-2B). These results suggested that the NP segment might play a critical role in determining the replication capacity of IDV.

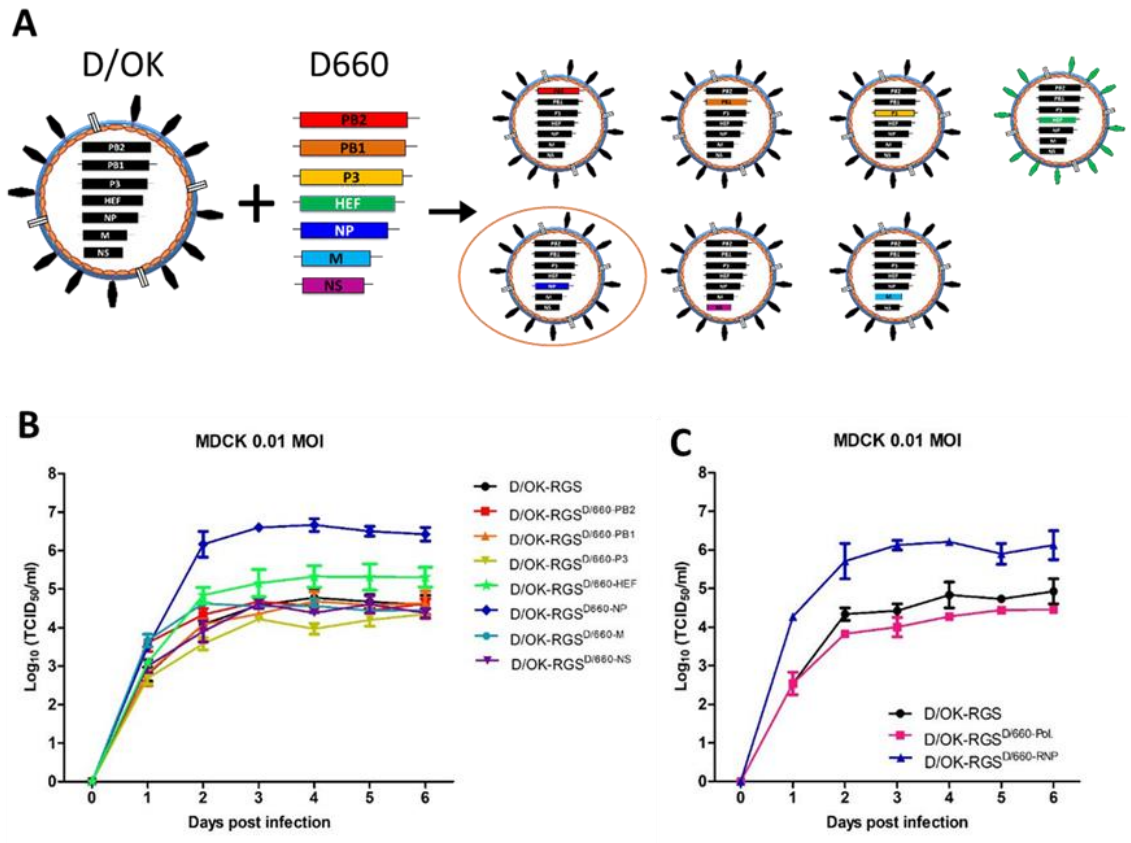

Figure 4-2. NP determines the replication difference between the D/660 and D/OK viruses. (A) Schematic representation of wild-typed D/OK and seven chimeric viruses used in this study. Each segment of D/OK virus was replaced with the corresponding D/660 viral segment, respectively. All of the viruses were generated by RGS and tittered in MDCK cells at the same time. (B) MDCK cells were infected with rescued D/OK or seven chimeric viruses with an MOI of 0.01. (C) MDCK cells were infected with rescued D/OK virus, chimeric D/OK virus expressing D/660 PB1, PB2 and P3 (D/OK-RGS$^{660\text{-pol}}$) or chimeric D/OK virus expressing D/660 PB1, PB2, P3 and NP (D/OK-RGS$^{660\text{-RNP}}$). Viruses were titrated by TCID50 per ml in MDCK cells at the indicated days. The error bars are representative of three independent experiments.

As we know, recruitment of NP with viral RNA-dependent RNA polymerase leads to form a RNP complex, which is critical for the viral transcription and replication. To further investigate whether the polymerase subunits or RNP components work together to contribute to the replication difference between the two virus strains, we rescued the D/OK chimeric viruses carrying D/660 polymerase (PB2, PB1 and P3) or carrying the four components of RNP complex (PB2, PB1, P3 and NP) from the D/660 virus strain. We found that the D/OK chimeric virus carrying the D/660 polymerase grew at a rate similar to the wild type D/OK virus, while if the RNP (polymerase plus the NP protein) was replaced, the virus titer was significantly changed (2 log10TCID50/ml) (Figure 4-2C). These results further confirmed that NP is a key determinant of the replication difference between the D/660 and D/OK viruses.

4.2.3 Two residues in positions 247 and 381 within the NP protein were key determinants of the replication fitness of IDV

By alignment of NP protein seqeunces, five different amino acid residues, P74L, S132T, E247D, K381E and A462T, were observed between the D/660 and D/OK viruses (Figure 4-3A). Structure studies indicated that NP formed a tetramer in solution (*144*). In the structure modeling of the IDV NP, the residue 74 was close to the RNA binding groove, the residue 132 was in the interior of the body domain, and the residue 381 was in the body domain but outside of functional sites. The amino acids 247 and 462 were buried and closed to the tetramer interface (Figure 4-3B).

To explore which residue(s) within the IDV NP protein contribute to viral replication fitness, the D/OK RGS was used to generate recombinant D/OK viruses with mutations in NP protein. MDCK cells were infected with these mutant viruses at an MOI of 0.01, and virus titers were measured by the TCID50 titration (Figure 4-3C). The virus with the A462T or S132T mutation had little effect on viral growth property (Figure 4-3C). However, the virus with E247D mutation replicated approximately 1 $\log_{10}$TCID50/ml higher than the wild type D/OK virus. Importantly, the virus containing the NP-K381E change displayed 2 log10TCID50/ml higher titers when compared to the wild-type D/OK virus at the indicated time points, which possesses a replication kinetics similar to the chimeric D/OK virus containing the D/660 NP (Figure 4-3C). These results suggested that residues in position 247 and 381 of the NP were possible determinants for the observed difference in replication kinetics between D/OK and D/660 viruses.

To confirm the critical roles of these two residues in IDV replication, loss-of-function mutations were introduced into the D/660 NP segment. Compared to the chimeric D/OK virus carrying the wild-type D/660 NP, viruses with mutant D/660 NP, D/660-NP-D247E and D/660-NP-E381K replicated to 1 and 2 log10TCID50/ml lower titers, respectively (Figure 4-4D). The replication levels of viruses carrying D/660 NP-L74P, T132S and T462A mutations were similar to the virus containing wild-type D/660 NP segment (Figure 4-4D). Taken together, our data demonstrated that the mutations in positions 247 and 381 of the NP protein attributed to the different replication properties between the D/660 and D/OK viruses.

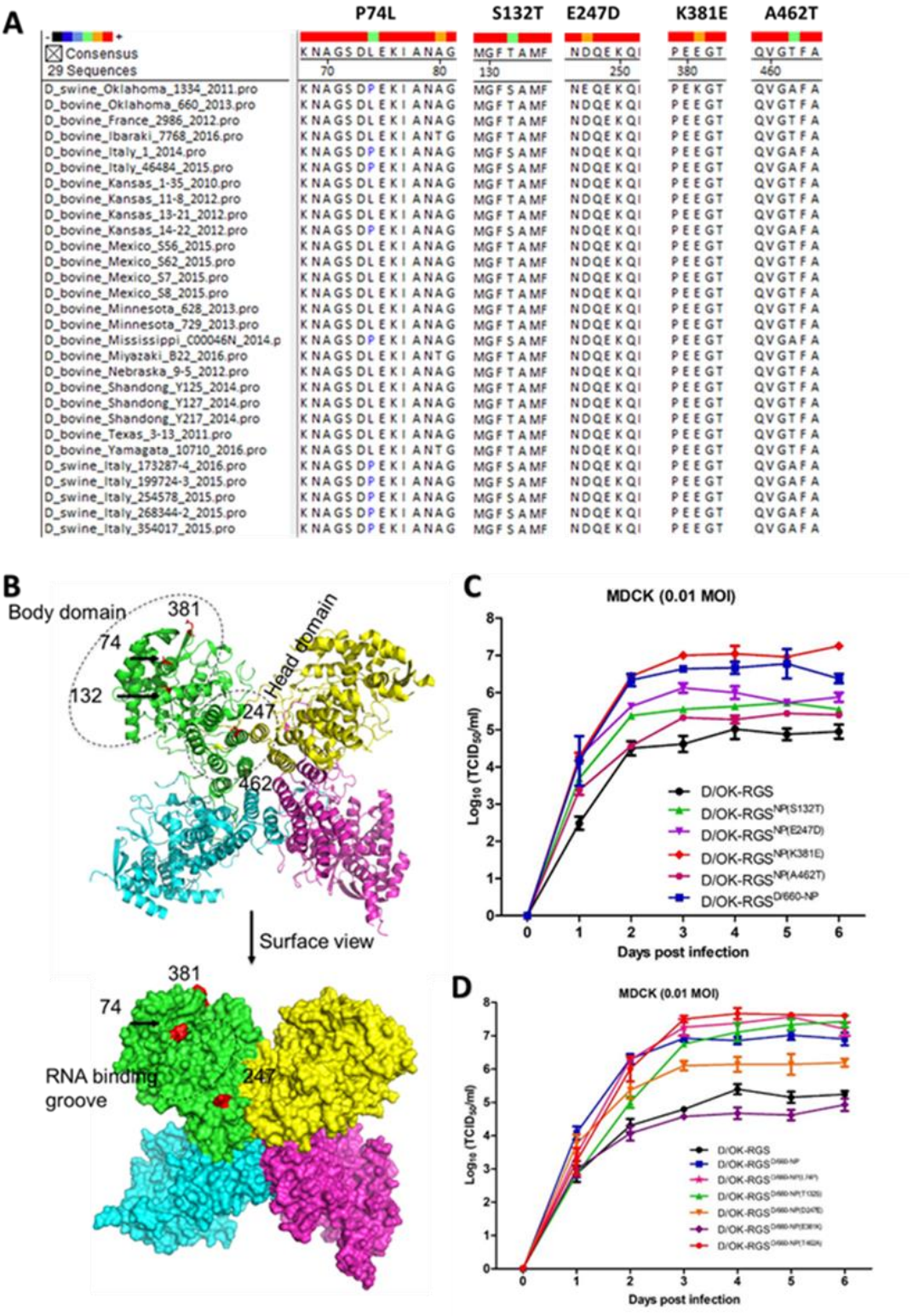

Figure legend in the next page.

Figure 4-3. Two residues in positions 247 and 381 within the NP protein were key determinants of the replication fitness of IDV. (A) Alignment of the IDV NP protein. Five different amino acid residues are identified between the D/OK and D660 virus strains, which are highlighted in the above alignments. (B) Structural modeling of the IDV NP depicting cartoon and surface representations. The four subunits of the NP tetramer are colored differently. The locations of 5 amino acid differences between D/OK virus and virus are noted by red color. (C) The chimeric D/OK virus containing D/660 NP or four recombinant D/OK viruses each carrying a single-point mutation (S132T, E247P, K381E and A462T) in NP were generated by RGS. (D) Single-point mutant viruses (L74P, T132S, P247E, E381K and T462A) in NP were generated by using chimeric D/OK virus containing D/660 NP as a backbone. MDCK cells were infected at MOI of 0.01 and the supernatants were harvested at the indicated days post infection and assayed for viral infectivity by TCID50 experiment. The error bars represent the standard error of the mean of three independent experiments.

4.2.4 Amino acid changes in NP had no effect on IDV RNP activity but might affect virus replication in the late stage of the viral life cycle

As a critical component of RNP complex, NP provides a structural framework for viral transcription and replication. Numerous publications reported that mutations in the NP could affect the RNP activity by regulating its homo-oligomerization, viral RNA binding, and polymerase assembly (*146-148*). To investigate the effects of NP mutations on the RNP activity, minigenome replication assay was performed in HEK-293T cells, which were co-transfected the GFP reporter plasmid with the plasmids expressing the polymerase complex (PB2, PB1 and P3) and wild-type or mutant NP plasmids. The percentage of positive cells expressing GFP (Figure 4-4A and 4B) was measured by

FACS. Unexpectedly, the percentage of GFP-positive cells was similar among groups with the wild-type and mutant NP proteins (Figure 4-4A and 4B). Moreover, all the gain-of-function mutations in D/OK-NP and loss-of-function mutations in D/660-NP had no effect on GFP expression measured by Western-blot analysis in the mini-genome replication assay (Figure 4-4C). The expression of NP and β-actin was set up as a transfection or loading control. By quantifying the Western-blot bands, we found that the ratios of GFP to NP (Figure 4-4D) and NP to β-actin (Figure 4-4E) were similar in the indicated mutants. These data suggested that genetic variants of NP had no effect on IDV RNP activity.

To further investigate the mechanisms of the NP that are responsible for the replication fitness of IDV, droplet digital PCR (dd PCR) was performed to test if the NP affected IDV replication in the early stage of its life cycle. MDCK cells were infected with the D/OK or D/660 virus at the same MOI of 0.01. The infected cells were collected at indicated time points, and the total mRNA was extracted for RT and dd PCR. Interestingly, as shown in the Figure 4-4F, the relative viral mRNA copies of the D/OK virus (with lower replication capacity) were significantly higher than that of the D/660 virus (with higher replication capacity) at the early stage (prior to 16 hours post-infection) of the viral life cycle. Nevertheless, 16 hours after infection, the relative viral mRNA copies of the D/660 virus dramatically increased while the relative viral mRNA copies of the D/OK virus increased significantly lower than that of the D/660 virus (Figure 4-4F). These results indicated that the amino acid changes in NP might affect IDV replication in the late stage of the viral life cycle.

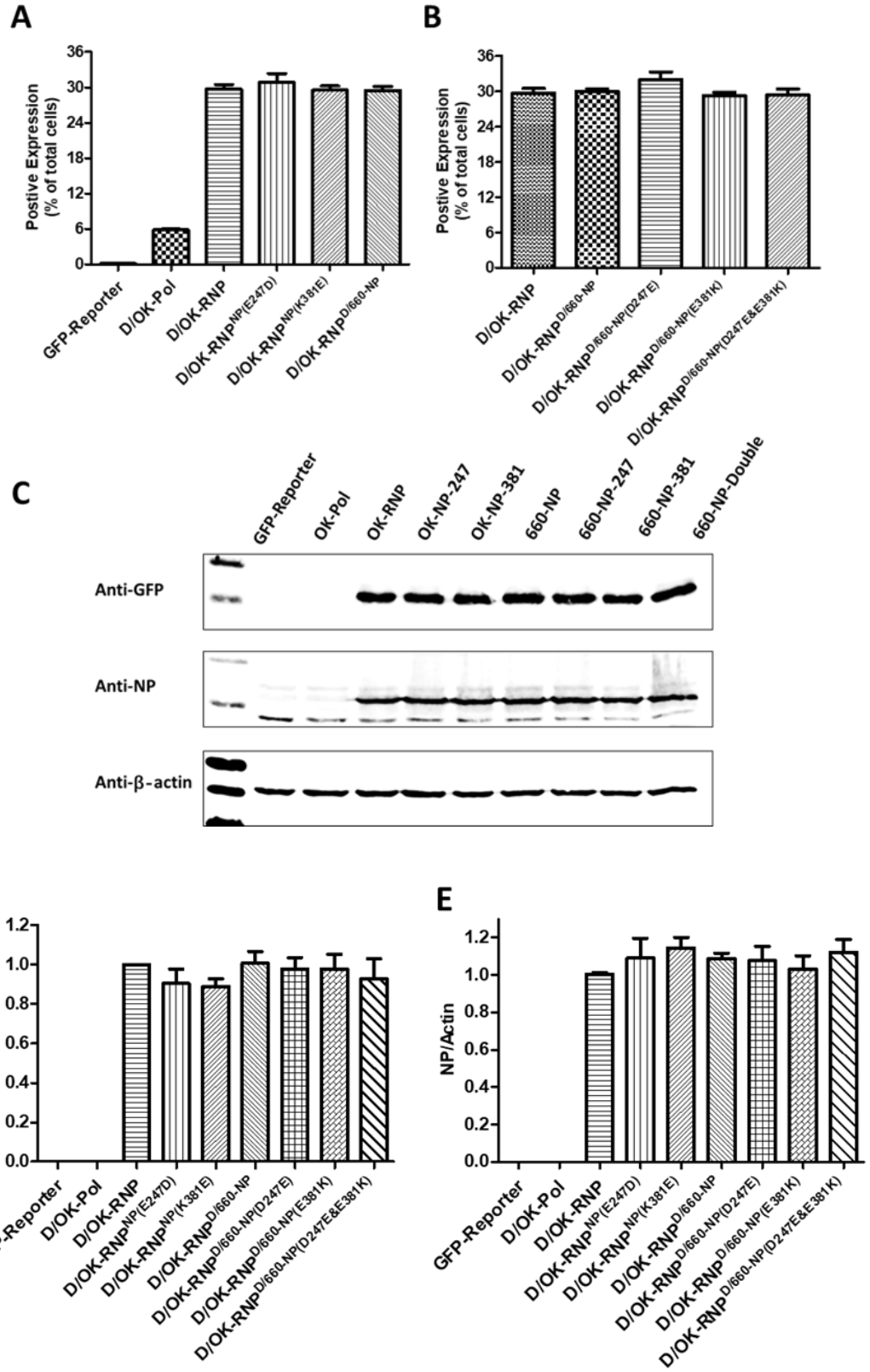
A
Postive Expression (% of total cells)
36
30
24
18
12
6
0
GFP-Reporter
D/OK-Pol
D/OK-RNP
D/OK-RNP NP(E247D)
D/OK-RNP NP(K381E)
D/OK-RNP D/660-NP
B
Postive Expression (% of total cells)
D/OK-RNP
D/OK-RNP D/660-NP
D/OK-RNP D/660-NP(D247E)
D/OK-RNP D/660-NP(E381K)
D/OK-RNP D/660-NP(D247E&E381K)
C
GFP-Reporter
OK-Pol
OK-RNP
OK-NP-247
OK-NP-381
660-NP
660-NP-247
660-NP-381
660-NP-Double
Anti-GFP
Anti-NP
Anti-β-actin
D
GFP/NP
1.2
1.0
0.8
0.6
0.4
0.2
0.0
GFP-Reporter
D/OK-Pol
D/OK-RNP
D/OK-RNP NP(E247D)
D/OK-RNP NP(K381E)
D/OK-RNP D/660-NP
D/OK-RNP D/660-NP(D247E)
D/OK-RNP D/660-NP(E381K)
D/OK-RNP D/660-NP(D247E&E381K)
E
NP/Actin
1.2
1.0
0.8
0.6
0.4
0.2
0.0
GFP-Reporter
D/OK-Pol
D/OK-RNP
D/OK-RNP NP(E247D)
D/OK-RNP NP(K381E)
D/OK-RNP D/660-NP
D/OK-RNP D/660-NP(D247E)
D/OK-RNP D/660-NP(E381K)
D/OK-RNP D/660-NP(D247E&E381K)

Figure 4-4 continued

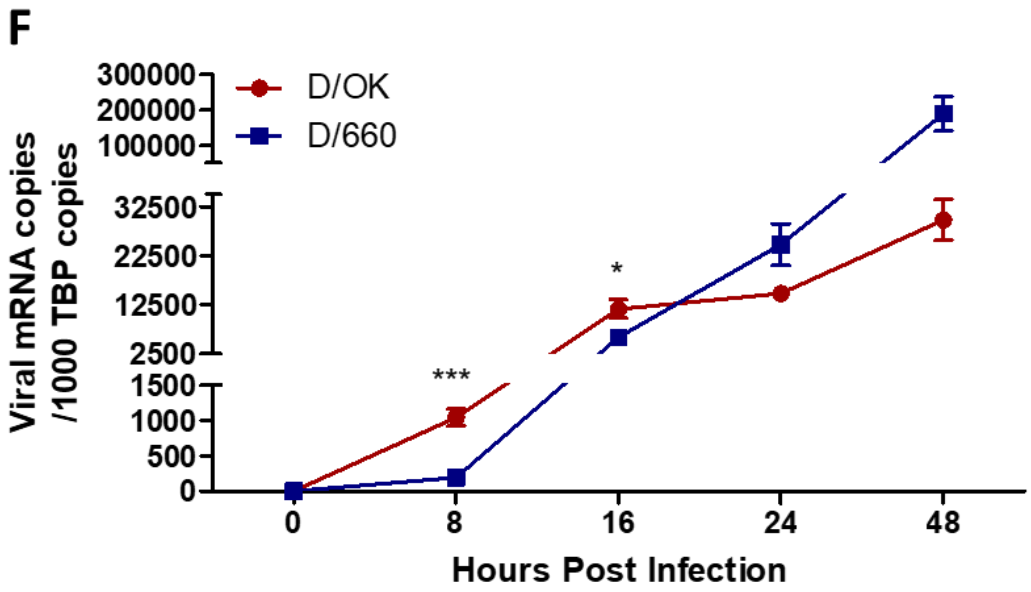

Figure 4-4. Amino acid changes in NP had no effect on IDV RNP activity but might affect virus replication in the late stage of the viral life cycles. (A-C) Activity of the D/OK wild-type RNP complex or the RNP complex with the indicated D/OK-NP or D/660-NP mutation was measured by a minigenome replication assay. Briefly, Polymerase complex components derived from D/OK virus together with their wild-type NP gene or mutant NP genes were co-transfected with GFP reporter plasmid into HEK-293T cells. Fourth-eight hours later, GFP reporter protein expression was estimated and analyzed by FACS analysis (A and B) and Western blotting (C). NP and β-actin detected by Western blotting was set up as a transfection or loading control. (D and E) The densitometry of Western blot bands was quantified by ImageJ software. The ratios of GFP to NP (D) and NP to β-actin (E) were normalized by D/OK-RNP and set arbitrarily as 1. The error bars are representative of three independent experiments. (E) Detection of relative viral mRNA copies of IDVs by ddPCR in early stage. MDCK cells were infected with D/660 or D/OK virus at an MOI of 0.01. Total RNAs were extracted at the indicated hours post-infection. The mRNA level of viral segment NP was measured by ddPCR and presented as viral mRNA copies

per 1000 TBP copies. The mRNA level of TBP was detected as an internal control. The error bars are means and SD from three independent experiments. Statistical analysis was performed by Student's t test. *, $P<0.05$; ***, $P<0.001$.

4.3 Discussion

Here we observed replication differences between the two lineage-representative IDV strains, D/660 and D/OK, in different cell lines. Specifically, using chimeric viruses generated by RGS, we demonstrate that NP segment determined the replication fitness of IDV. Furthermore, we identified that positions 247 and 381 within the NP protein critically affect IDV replication in late stage of the viral life cycle.

As intracellular pathogens, influenza viruses exploit host cellular proteins and biological pathways to complete their life cycle. Different influenza virus strains displayed distinct replication efficiency in different cells, which can be associated with viral entry, replication, release, and host immune response (*155-157*). Considering the D/660 and D/OK IDV strains isolated from cattle and swine respectively, cellular tropism may result in the distinct replication kinetics. In this regard, four cell lines from different species, including canine (MDCK), swine (ST), bovine (MDBK) and human (HRT-18G), were used to compared cellular tropism between D/660 and D/OK virus strains *in vitro*. Data in figure 4-1 showed that the D/660 virus replicates more efficiently than the D/OK virus in all cell lines, indicating that viral factors, not host cellular factors might contribute to the distinct replication efficiency of IDV.

Influenza D virus contains seven segments encoding 9 proteins, PB2, PB1, P3, HEF, NP, M (DM1, DM2), and NS (NS1, NS2). PB2. PB1, P3 and NP together with viral RNA forms the RNP complex, which serves as a core machinery for replication and transcription, as well as for transportation and assembly of the genomes into budding virions (*158, 159*). In RNP complex, PB1 is an RNA-dependent RNA polymerase (*160*) and P3 (named PA in IAV and IBV) is an endonuclease (*161, 162*). PB2 is essential for viral transcription by binding the 5′ cap RNA fragment cleaved from host pre-mRNAs (*163*). Thus, Natural polymorphisms or genetically engineered mutations targeting enzyme activities or the interaction of individual RNP complex unit can affect influenza viral replication efficiency. For example, several amino acid mutations of PB2, including 627K, 591K, 701N, were identified to be responsible for the adaptation of avian H5N1 virus to mammalians (*163-165*). H5N1 virus containing these mutants increased its replicative efficiency in mouse model or human cells. Ozawa et al. reported that PB1-F2-stop12L mutant exhibited more replication efficiency than wild-type pandemic (H1N1) 2009 influenza virus in MDCK cells (*166*). As the only major glycoprotein in the surface of ICV and IDV, HEF contains receptor binding, receptor destroying and membrane fusion activities (*20*), determining the virus formation, virion stability and host tropism (*91, 167, 168*). M1 protein of influenza virus is an essential component for virion assembly (*169*). It is reported that the A24T mutant in M1 protein of ICV changed virus morphology from a mainly filamentous to spherical appearance. In addition, M1 contains RNA-binding domains and regulates viral replication by interaction with RNP complex (*170*). NS1 was shown to be an inhibitor of interferon innate immune response and enhance viral replication (*171, 172*). Moreover, some specific mutants in NS1 are

associated with virulence and host adaptation (*173-175*). To investigate which segment(s) contribute to different grow kinetics between the two virus strains, D/OK RGS was used to generate chimeric viruses carrying each segment, polymerase or RNP complex of the D/660 virus. Our data demonstrated that the NP determined the replication difference between the D/660 and D/OK virus strains.

We further identified two amino acids of NP were critical for IDV replication. NP with 247D or 381E significantly enhanced viral replication capacities *in vitro*. To date, crystal structure of IDV NP is available and amino acid differences between the two IDV strains are noted in Fig 4-3B (*144*). Similar with other three types of influenza virus, NP of IDV forms a small oligomer (dimer, trimer or tetramer) and contains some functional domains for RNA binding, PB2 binding and nucleus transportation (*147, 176, 177*). We can see that the residue 247 is buried and closed to the tetramer interface, while the amino acid 381 locates in the surface of body domain but outside of functional sites. However, it is too difficult to predict the function of the two residues of NP based on their location. A number of studies reported mutants of influenza virus NP affected viral replication by targeting RNP activity (*148*). For instance, residues S165, R416 and E339 of IAV NP have been identified to be associated with NP oligomerization (*146, 147, 178*). Mutant K470R in H5N1 Influenza A Virus NP increases the viral growth in MDCK cells and virulence in mouse model (*179*). In this regard, we examined RNP activities of wild type or recombinant viruses with mutants by the minigenome replication assay. Intriguingly, both gain of functional mutants in D/OK virus and loss of functional mutants in D/660 virus exhibited no effect on RNP activities. In addition, by alignment NP sequences of

existing IDV strains, the position 247 and 381 are occupied by E and K only in the NP of D/swine/Oklahoma/1334/2011 strain, while D and E are present in all other IDV strains. Further investigation is needed to better understand the underlying mechanism that drive swine D/OK depart from all other influenza D viruses including D/660 in these two critical residues of NP protein.

.

In conclusion, our data demonstrated that the D/660 virus had a higher replication capacity than the D/OK virus in multiple cell lines. We further identified that genetic variants at the 247 and 381 residues of NP contributed to the distinct viral replication capacity between the two virus strains. Interestingly, the two residues of NP had no effect on RNP activities. These findings may provide some novel insights into NP function on IDV replication.

4.4 Materials and Methods

4.4.1 Cells and viruses

Five cell lines, Madin-Darby canine kidney (MDCK) cells (ATCC), Swine testicle (ST) cells (ATCC), Madin-Darby bovine kidney (MDBK) cells (ATCC), HRT-18G cells (ATCC) and Human embryonic kidney HEK-293T cells (ATCC) were used in this study. All cell lines were cultured and maintained in Dulbecco's modified Eagle medium (DMEM; Gibco, Invitrogen, USA) with 10% (vol/vol) fetal bovine serum (FBS; PAA Laboratories, Dartmouth, MA, USA) and 100 U/ml penicillin-streptomycin (Life Technologies, Carlsbad, CA, USA) at 37 ° C with 5% CO2. Serum-free DMEM

supplemented with 1 μg/ml TPCK-trypsin (Sigma - Aldrich, St Louis) and 100 U/ml penicillin-streptomycin was used as the infectious medium. Two influenza D virus strains, D/bovine/Oklahoma/660/2013 (D/660) and D/swine/Oklahoma/1314/2011 (D/OK), were propagated and titrated by 50% tissue culture infective doses (TCID50)/ml in MDCK cells at 37°C. Viruses were stored at -80°C until further use.

4.4.2 Antibodies and regents

The rabbit antisera for NP of influenza D virus were prepared in-house. Polyclonal antibody against eGFP and monoclonal anti-β-actin antibody was purchased from Santa Cruz Biotechnology and Sigma-Aldrich, respectively. Goat anti-mouse and donkey anti-rabbit IRDye 680RD secondary antibodies were obtained from Li-cor.

4.4.3 Plasmid construction and reverse genetics

The rescued recombinant influenza D/swine/Oklahoma/1314/2011 (D/OK) virus strain by reverse genetics system was described in our previous publication (*141*). Briefly, the dual promoter vector pHW2000 was used to produce vRNA by human Pol I promoter and the murine Pol I terminator from one strand and viral mRNA by the CMV promoter and the BGH poly(A) signal from the opposite strand. The seven pHW2000 plasmids encoding seven genomic segments (PB2, PB1, P3, HEF, NP, M, and NS) of IDV were co-transfected into cocultured HEK-293T–MDCK cells. Five days later, supernatants were collected, and the recombinant virus was passaged and titrated by TCID50/ml in MDCK cells at 37°C. The gain of functional site mutants (S132T, E247D, K381E, A462T) in NP

of the D/OK virus strain and loss of functional mutants (L74P, T132S, D247E, E381K, T462A) in NP of the D/660 virus strain were constructed by using wild type D/OK or D/660 NP as template following the site directed mutagenesis protocol.

4.4.4 Viral replication kinetics assay

MDCK, ST, MDBK or HRT-18G cells were seeded in 12-well plates in the concentration of 1×10^5 cells/ml. After 14-16 h, cells were washed by phosphate-buffered saline (PBS) and inoculated with influenza D virus at a multiplicity of infection (MOI) of 0.01. After 1 h incubation, cells were washed with PBS twice, and corresponding infectious medium was added. Supernatants were collected at the indicated days post-infection and virus titers were measured by TCID50 assay in MDCK cells.

4.4.5 Minigenome replication assay

The construction of plasmid containing GFP reporter gene was described previously (*141*). For the minigenome replication assay, HEK-293T cells seeded in 12-well plates with a 70-90% confluent were co-transfected plasmids encoding GFP reporter gene and influenza D/OK polymerase components (PB2, PB1 and P3) with wild type NP or mutants by PEI transfection reagent. Forty-eight hours later, HEK-293T cells were collected and fixed by 2% Paraformaldehyde (PFA). The percentage of positive cells expressing GFP and mean of fluorescence intensity (MFI) were determined by flow

cytometry (FACS). Cells were lysed and the expression of GFP, NP and β-actin were measured by Western Blot analysis.

4.4.6 Structural modeling

The model of influenza D virus NP was constructed by Modeler. The NP structure from D/bovine/France/2986/2012 was chosen as the template (sequence identity: 98%-99%). The sequences of IDV NP were then aligned using Muscle. The location of 5 residue differences between the swine D/OK virus and the bovine D660 virus were colored red.

4.4.7 Droplet Digital PCR

MDCK cells were seeded in 12-well plates and infected with bovine D/660 and swine D/OK virus at an MOI of 0.01. After 0, 8, 16, 24 or 48-h post-infection, cells was lysed with TRIzol Reagent (Invitrogen, CA, USA) and extracted according to the manufacturer's instructions. A high-capacity cDNA reverse transcription kit (Thermo Fisher Scientific) and Oligo dT (18) primer were used for reverse transcription reactions following the manufacturer's protocol. The ddPCR analysis was performed on Bio-Rad QX200 ddPCR system with the reaction condition following our previous study (*180*). Gene-specific primers and probe for IDV NP segment-drived mRNA were used for determining viral replication. The mRNA levels of NP were normalized to TATA-Box binding protein (TBP) and presented as viral mRNA copies per 1000 TBP copies.

4.4.8 Statistical analysis

At least three independent experiments were performed for all data presented in this study. Results were analyzed by one-way analysis of variance (ANOVA) followed by Tukey's multiple-comparison test using GraphPad Prism 5.0 software. Statistically significant differences are noted in the figures (*, $P<0.05$; **, $P<0.01$; ***, $P<0.001$).

CHAPTER 5. CONCLUSIONS AND FUTURE DIRECTIONS

Influenza D virus (IDV) utilizes cattle as a primary reservoir. Increased outbreaks in pigs and serological and genetic evidences of human infection have raised a concern about the potential of IDV adapting and transmitting to humans. Here, we directly compared IDV's stability to that of other influenza types (A, B, and C) following prolonged incubation at high temperatures or in a low-pH environment. We found that IDV is the most stable among four types of influenza viruses. Importantly, we demonstrated that the hemagglutinin-esterase fusion (HEF) protein, which drives the fusion between viral and host cell membranes, is the primary determinant for the high thermal and acid stability of IDV. Considering that there is a link between the acid stability of the hemagglutinin protein of influenza A virus and its cross-species transmission, further investigation of the mechanism of HEF-directed viral tolerance to high temperature and low pH may offer novel insights into tissue tropism and cross-species transmission of influenza viruses.

We developed a plasmid-based IDV reverse-genetics system that can generate infectious viruses with replication kinetics similar to those of wild-type viruses following transfection of cultured cells. Further characterization demonstrated that viruses rescued from the described RGS resembled the parental viruses in biological and receptor-binding properties. We also developed and validated an IDV minireplicon reporter system that specifically measures viral RNA polymerase activity. In summary, the reverse-genetics system and minireplicon reporter assay described in this study should be of value in

identifying viral determinants of replication fitness, cross-species transmissibility and pathogenicity of the novel influenza D viruses.

IDV has evolved to three genetic lineages: D/OK-lineage, D/660-lineage and D/Japan-lineage, according to the sequences of the HEF gene. The D/OK, D/660 and D/Yamagata are three lineage-representative strains, respectively. The phylogenesis and antigenicity of IDV strains from different lineages have been well compared and characterized. However, The underlying mechanisms that attribute to the variability of the biological characteristics between IDV lineages are not fully understood. Here, we reported a significantly phenotypic divergence between the D/OK and the D/660 viruses in replication fitness. We found the D/660 virus replicated to significantly higher titers than the D/OK virus regardless of the cell types. By using the reverse genetics system, we generated recombinant chimeric D/OK viruses in that each of its RNA segments was replaced with its corresponding segment from the D660 virus, and observed that only the replication fitness of the chimeric swine D/OK virus containing the D660 NP segment was significantly increased. Finally, we identified two positions 247 and 381 within the NP protein were key determinants of the replication difference between the D/OK and D660 viruses. Interestingly, we have observed that theses amino acid changes in the NP might alter the functionality of NP in the late stage of the replication cycle but not affected IDV RNP activity in the mini-genome replication studies, which warrants further investigation. In the present study, we demonstrated that genetic variations of the NP had a substantial impact on IDV replication fitness. In light of the fact that we have developed a robust reverse genetics system for influenza D virus as reported in this dissertation, it

will facilitate future studies towards understanding the cross-species transmission mechanism at the molecular level, and developing a safe and effective vaccine that can be used to control and prevent of influenza D virus infection of animals and humans.

LIST OF REFERENCES

1. E. C. Hutchinson, Influenza Virus. *Trends Microbiol* **26**, 809-810 (2018).
2. R. A. Medina, A. Garcia-Sastre, Influenza A viruses: new research developments. *Nat Rev Microbiol* **9**, 590-603 (2011).
3. Y. Matsuzaki *et al.*, Frequent reassortment among influenza C viruses. *J Virol* **77**, 871-881 (2003).
4. B. M. Hause *et al.*, Isolation of a novel swine influenza virus from Oklahoma in 2011 which is distantly related to human influenza C viruses. *PLoS Pathog* **9**, e1003176 (2013).
5. T. Odagiri *et al.*, Antigenic heterogeneity among phylogenetic clusters of influenza D viruses. *J Vet Med Sci* **80**, 1241-1244 (2018).
6. W. Chen *et al.*, A novel influenza A virus mitochondrial protein that induces cell death. *Nat Med* **7**, 1306-1312 (2001).
7. M. Hatta, Y. Kawaoka, The NB protein of influenza B virus is not necessary for virus replication in vitro. *J Virol* **77**, 6050-6054 (2003).
8. M. Matrosovich, G. Herrler, H. D. Klenk, Sialic Acid Receptors of Viruses. *Top Curr Chem* **367**, 1-28 (2015).
9. E. Kesinger *et al.*, Influenza D virus M2 protein exhibits ion channel activity in Xenopus laevis oocytes. *PLoS One* **13**, e0199227 (2018).
10. W. S. Ryu, Molecular Virology of Human Pathogenic Viruses. *Molecular Virology of Human Pathogenic Viruses*, 1-423 (2017).
11. T. Noda *et al.*, Architecture of ribonucleoprotein complexes in influenza A virus particles. *Nature* **439**, 490-492 (2006).
12. S. Nakatsu *et al.*, Complete and Incomplete Genome Packaging of Influenza A and B Viruses. *mBio* **7**, (2016).
13. S. Nakatsu *et al.*, Influenza C and D Viruses Package Eight Organized Ribonucleoprotein Complexes. *J Virol* **92**, (2018).

14. R. G. Webster, W. J. Bean, O. T. Gorman, T. M. Chambers, Y. Kawaoka, Evolution and ecology of influenza A viruses. *Microbiol Rev* **56**, 152-179 (1992).
15. S. W. Yoon, R. J. Webby, R. G. Webster, Evolution and ecology of influenza A viruses. *Curr Top Microbiol Immunol* **385**, 359-375 (2014).
16. M. de Graaf, R. A. Fouchier, Role of receptor binding specificity in influenza A virus transmission and pathogenesis. *EMBO J* **33**, 823-841 (2014).
17. J. Tan, G. Asthagiri Arunkumar, F. Krammer, Universal influenza virus vaccines and therapeutics: where do we stand with influenza B virus? *Curr Opin Immunol* **53**, 45-50 (2018).
18. M. Koutsakos, T. H. Nguyen, W. S. Barclay, K. Kedzierska, Knowns and unknowns of influenza B viruses. *Future Microbiol* **11**, 119-135 (2016).
19. J. Kauppila *et al.*, Influenza C virus infection in military recruits--symptoms and clinical manifestation. *J Med Virol* **86**, 879-885 (2014).
20. M. Wang, M. Veit, Hemagglutinin-esterase-fusion (HEF) protein of influenza C virus. *Protein Cell* **7**, 28-45 (2016).
21. B. M. Hause *et al.*, Characterization of a novel influenza virus in cattle and Swine: proposal for a new genus in the Orthomyxoviridae family. *mBio* **5**, e00031-00014 (2014).
22. S. Su, X. Fu, G. Li, F. Kerlin, M. Veit, Novel Influenza D virus: Epidemiology, pathology, evolution and biological characteristics. *Virulence* **8**, 1580-1591 (2017).
23. M. Quast *et al.*, Serological evidence for the presence of influenza D virus in small ruminants. *Vet Microbiol* **180**, 281-285 (2015).
24. H. Nedland *et al.*, Serological evidence for the co-circulation of two lineages of influenza D viruses in equine populations of the Midwest United States. *Zoonoses Public Health* **65**, e148-e154 (2018).
25. S. K. White, W. Ma, C. J. McDaniel, G. C. Gray, J. A. Lednicky, Serologic evidence of exposure to influenza D virus among persons with occupational contact with cattle. *J Clin Virol* **81**, 31-33 (2016).

26. E. Salem *et al.*, Serologic Evidence for Influenza C and D Virus among Ruminants and Camelids, Africa, 1991-2015. *Emerg Infect Dis* **23**, 1556-1559 (2017).
27. A. Varki, Multiple changes in sialic acid biology during human evolution. *Glycoconj J* **26**, 231-245 (2009).
28. A. Varki, R. Schauer, in *Essentials of Glycobiology*, nd *et al.*, Eds. (Cold Spring Harbor (NY), 2009).
29. H. Song *et al.*, An Open Receptor-Binding Cavity of Hemagglutinin-Esterase-Fusion Glycoprotein from Newly-Identified Influenza D Virus: Basis for Its Broad Cell Tropism. *PLoS Pathog* **12**, e1005411 (2016).
30. R. Liu *et al.*, Influenza D virus diverges from its related influenza C virus in the recognition of 9-O-acetylated N-acetyl- or N-glycolyl-neuraminic acid-containing glycan receptors. *Virology* **545**, 16-23 (2020).
31. H. Zhang, Tissue and host tropism of influenza viruses: importance of quantitative analysis. *Sci China C Life Sci* **52**, 1101-1110 (2009).
32. S. Ge, Z. Wang, An overview of influenza A virus receptors. *Crit Rev Microbiol* **37**, 157-165 (2011).
33. F. Ni, I. N. Mbawuike, E. Kondrashkina, Q. Wang, The roles of hemagglutinin Phe-95 in receptor binding and pathogenicity of influenza B virus. *Virology* **450-451**, 71-83 (2014).
34. N. M. Bouvier, P. Palese, The biology of influenza viruses. *Vaccine* **26 Suppl 4**, D49-53 (2008).
35. L. H. Pinto, R. A. Lamb, The M2 proton channels of influenza A and B viruses. *J Biol Chem* **281**, 8997-9000 (2006).
36. J. Fontana, A. C. Steven, At low pH, influenza virus matrix protein M1 undergoes a conformational change prior to dissociating from the membrane. *J Virol* **87**, 5621-5628 (2013).
37. D. Dou, R. Revol, H. Ostbye, H. Wang, R. Daniels, Influenza A Virus Cell Entry, Replication, Virion Assembly and Movement. *Front Immunol* **9**, 1581 (2018).
38. E. A. Collin *et al.*, Cocirculation of two distinct genetic and antigenic lineages of proposed influenza D virus in cattle. *J Virol* **89**, 1036-1042 (2015).

39. C. C. Sreenivasan, M. Thomas, R. S. Kaushik, D. Wang, F. Li, Influenza A in Bovine Species: A Narrative Literature Review. *Viruses* **11**, (2019).
40. L. Ferguson *et al.*, Influenza D virus infection in Mississippi beef cattle. *Virology* **486**, 28-34 (2015).
41. J. Luo *et al.*, Serological evidence for high prevalence of Influenza D Viruses in Cattle, Nebraska, United States, 2003-2004. *Virology* **501**, 88-91 (2017).
42. S. Silveira *et al.*, Serosurvey for Influenza D Virus Exposure in Cattle, United States, 2014-2015. *Emerg Infect Dis* **25**, 2074-2080 (2019).
43. N. Mitra, N. Cernicchiaro, S. Torres, F. Li, B. M. Hause, Metagenomic characterization of the virome associated with bovine respiratory disease in feedlot cattle identified novel viruses and suggests an etiologic role for influenza D virus. *J Gen Virol* **97**, 1771-1784 (2016).
44. M. Zhang *et al.*, Respiratory viruses identified in western Canadian beef cattle by metagenomic sequencing and their association with bovine respiratory disease. *Transbound Emerg Dis* **66**, 1379-1386 (2019).
45. E. S. Bailey *et al.*, First sequence of influenza D virus identified in poultry farm bioaerosols in Sarawak, Malaysia. *Trop Dis Travel Med Vaccines* **6**, 5 (2020).
46. B. E. Martin *et al.*, Feral Swine in the United States Have Been Exposed to both Avian and Swine Influenza A Viruses. *Appl Environ Microbiol* **83**, (2017).
47. Z. Feng *et al.*, Influenza A subtype H3 viruses in feral swine, United States, 2011-2012. *Emerg Infect Dis* **20**, 843-846 (2014).
48. L. Ferguson *et al.*, Influenza D Virus Infection in Feral Swine Populations, United States. *Emerg Infect Dis* **24**, 1020-1028 (2018).
49. M. F. Ducatez, C. Pelletier, G. Meyer, Influenza D virus in cattle, France, 2011-2014. *Emerg Infect Dis* **21**, 368-371 (2015).
50. C. Chiapponi *et al.*, Detection of Influenza D Virus among Swine and Cattle, Italy. *Emerg Infect Dis* **22**, 352-354 (2016).
51. H. Dane *et al.*, Detection of influenza D virus in bovine respiratory disease samples, UK. *Transbound Emerg Dis* **66**, 2184-2187 (2019).
52. C. J. Snoeck *et al.*, Influenza D Virus Circulation in Cattle and Swine, Luxembourg, 2012-2016. *Emerg Infect Dis* **24**, 1388-1389 (2018).

53. O. Flynn *et al.*, Influenza D Virus in Cattle, Ireland. *Emerg Infect Dis* **24**, 389-391 (2018).
54. S. Gorin *et al.*, Assessment of Influenza D Virus in Domestic Pigs and Wild Boars in France: Apparent Limited Spread within Swine Populations Despite Serological Evidence of Breeding Sow Exposure. *Viruses* **12**, (2019).
55. C. Rosignoli *et al.*, Influenza D virus infection in cattle in Italy. *Large Animal Review* **23**, 123-128 (2017).
56. J. Oliva *et al.*, Serological Evidence of Influenza D Virus Circulation Among Cattle and Small Ruminants in France. *Viruses* **11**, (2019).
57. T. O'Donovan, L. Donohoe, M. F. Ducatez, G. Meyer, E. Ryan, Seroprevalence of influenza D virus in selected sample groups of Irish cattle, sheep and pigs. *Ir Vet J* **72**, 11 (2019).
58. E. Foni *et al.*, Influenza D in Italy: towards a better understanding of an emerging viral infection in swine. *Sci Rep* **7**, 11660 (2017).
59. C. Chiapponi *et al.*, Detection of a New Genetic Cluster of Influenza D Virus in Italian Cattle. *Viruses* **11**, (2019).
60. S. E. Lauterbach *et al.*, Assessing exhibition swine as potential disseminators of infectious disease through the detection of five respiratory pathogens at agricultural exhibitions. *Vet Res* **50**, 63 (2019).
61. C. M. Trombetta *et al.*, Influenza D Virus: Serological Evidence in the Italian Population from 2005 to 2017. *Viruses* **12**, (2019).
62. W. M. Jiang *et al.*, Identification of a potential novel type of influenza virus in Bovine in China. *Virus Genes* **49**, 493-496 (2014).
63. S. L. Zhai *et al.*, Influenza D Virus in Animal Species in Guangdong Province, Southern China. *Emerg Infect Dis* **23**, 1392-1396 (2017).
64. S. Murakami *et al.*, Influenza D Virus Infection in Herd of Cattle, Japan. *Emerg Infect Dis* **22**, 1517-1519 (2016).
65. H. Mekata *et al.*, Molecular epidemiological survey and phylogenetic analysis of bovine influenza D virus in Japan. *Transbound Emerg Dis* **65**, e355-e360 (2018).
66. T. Horimoto *et al.*, Nationwide Distribution of Bovine Influenza D Virus Infection in Japan. *PLoS One* **11**, e0163828 (2016).

67. A. Yilmaz *et al.*, First report of influenza D virus infection in Turkish cattle with respiratory disease. *Research in Veterinary Science*, (2020).
68. S. Murakami *et al.*, Influenza D Virus Infection in Dromedary Camels, Ethiopia. *Emerg Infect Dis* **25**, 1224-1226 (2019).
69. M. Fusade-Boyer *et al.*, Risk Mapping of Influenza D Virus Occurrence in Ruminants and Swine in Togo Using a Spatial Multicriteria Decision Analysis Approach. *Viruses* **12**, (2020).
70. K. Asha, B. Kumar, Emerging Influenza D Virus Threat: What We Know so Far! *J Clin Med* **8**, (2019).
71. S. Murakami *et al.*, Influenza D Virus of New Phylogenetic Lineage, Japan. *Emerg Infect Dis* **26**, 168-171 (2020).
72. J. Lee *et al.*, Comparison of Pathogenicity and Transmissibility of Influenza B and D Viruses in Pigs. *Viruses* **11**, (2019).
73. T. F. Ng *et al.*, A metagenomics and case-control study to identify viruses associated with bovine respiratory disease. *J Virol* **89**, 5340-5349 (2015).
74. B. M. Hause *et al.*, An inactivated influenza D virus vaccine partially protects cattle from respiratory disease caused by homologous challenge. *Vet Microbiol* **199**, 47-53 (2017).
75. L. Ferguson *et al.*, Pathogenesis of Influenza D Virus in Cattle. *J Virol* **90**, 5636-5642 (2016).
76. E. Salem *et al.*, Pathogenesis, Host Innate Immune Response, and Aerosol Transmission of Influenza D Virus in Cattle. *J Virol* **93**, (2019).
77. X. Zhang *et al.*, Pathogenesis of co-infections of influenza D virus and Mannheimia haemolytica in cattle. *Vet Microbiol* **231**, 246-253 (2019).
78. D. Mosier, Review of BRD pathogenesis: the old and the new. *Anim Health Res Rev* **15**, 166-168 (2014).
79. R. M. Skelton *et al.*, Contribution of Host Immune Responses Against Influenza D Virus Infection Toward Secondary Bacterial Infection in a Mouse Model. *Viruses* **11**, (2019).
80. H. Tse *et al.*, Clinical and virological factors associated with viremia in pandemic influenza A/H1N1/2009 virus infection. *PLoS One* **6**, e22534 (2011).

81. J. Oliva *et al.*, Murine Model for the Study of Influenza D Virus. *J Virol* **94**, (2020).

82. C. Sreenivasan *et al.*, Replication and Transmission of the Novel Bovine Influenza D Virus in a Guinea Pig Model. *J Virol* **89**, 11990-12001 (2015).

83. M. Holwerda *et al.*, Determining the Replication Kinetics and Cellular Tropism of Influenza D Virus on Primary Well-Differentiated Human Airway Epithelial Cells. *Viruses* **11**, (2019).

84. J. Zhou *et al.*, Differentiated human airway organoids to assess infectivity of emerging influenza virus. *Proc Natl Acad Sci U S A* **115**, 6822-6827 (2018).

85. E. Kindler *et al.*, Efficient replication of the novel human betacoronavirus EMC on primary human epithelium highlights its zoonotic potential. *mBio* **4**, e00611-00612 (2013).

86. T. Kuiken *et al.*, Host species barriers to influenza virus infections. *Science* **312**, 394-397 (2006).

87. D. B. Smith, E. R. Gaunt, P. Digard, K. Templeton, P. Simmonds, Detection of influenza C virus but not influenza D virus in Scottish respiratory samples. *J Clin Virol* **74**, 50-53 (2016).

88. E. S. Bailey, J. Y. Choi, J. Zemke, M. Yondon, G. C. Gray, Molecular surveillance of respiratory viruses with bioaerosol sampling in an airport. *Trop Dis Travel Med Vaccines* **4**, 11 (2018).

89. J. Y. Choi *et al.*, Aerosol Sampling in a Hospital Emergency Room Setting: A Complementary Surveillance Method for the Detection of Respiratory Viruses. *Front Public Health* **6**, 174 (2018).

90. L. K. Borkenhagen *et al.*, Surveillance for respiratory and diarrheal pathogens at the human-pig interface in Sarawak, Malaysia. *PLoS One* **13**, e0201295 (2018).

91. J. Yu *et al.*, The Hemagglutinin-Esterase Fusion Glycoprotein Is a Primary Determinant of the Exceptional Thermal and Acid Stability of Influenza D Virus. *mSphere* **2**, (2017).

92. C. J. Russell, M. Hu, F. A. Okda, Influenza Hemagglutinin Protein Stability, Activation, and Pandemic Risk. *Trends Microbiol* **26**, 841-853 (2018).

93. Q. Wang, X. Tian, X. Chen, J. Ma, Structural basis for receptor specificity of influenza B virus hemagglutinin. *Proc Natl Acad Sci U S A* **104**, 16874-16879 (2007).

94. I. A. Wilson, J. J. Skehel, D. C. Wiley, Structure of the haemagglutinin membrane glycoprotein of influenza virus at 3 A resolution. *Nature* **289**, 366-373 (1981).

95. A. D. Mesecar, K. Ratia, Viral destruction of cell surface receptors. *Proc Natl Acad Sci U S A* **105**, 8807-8808 (2008).

96. J. Dubois, O. Terrier, M. Rosa-Calatrava, Influenza viruses and mRNA splicing: doing more with less. *mBio* **5**, e00070-00014 (2014).

97. R. A. Lamb, C. J. Lai, P. W. Choppin, Sequences of mRNAs derived from genome RNA segment 7 of influenza virus: colinear and interrupted mRNAs code for overlapping proteins. *Proc Natl Acad Sci U S A* **78**, 4170-4174 (1981).

98. C. M. Horvath, M. A. Williams, R. A. Lamb, Eukaryotic coupled translation of tandem cistrons: identification of the influenza B virus BM2 polypeptide. *EMBO J* **9**, 2639-2647 (1990).

99. A. Pekosz, R. A. Lamb, Influenza C virus CM2 integral membrane glycoprotein is produced from a polypeptide precursor by cleavage of an internal signal sequence. *Proc Natl Acad Sci U S A* **95**, 13233-13238 (1998).

100. S. Hongo *et al.*, Influenza C virus CM2 protein is produced from a 374-amino-acid protein (P42) by signal peptidase cleavage. *J Virol* **73**, 46-50 (1999).

101. B. Bogdanow *et al.*, The dynamic proteome of influenza A virus infection identifies M segment splicing as a host range determinant. *Nat Commun* **10**, 5518 (2019).

102. M. L. Reed *et al.*, Amino acid residues in the fusion peptide pocket regulate the pH of activation of the H5N1 influenza virus hemagglutinin protein. *J Virol* **83**, 3568-3580 (2009).

103. S. E. Galloway, M. L. Reed, C. J. Russell, D. A. Steinhauer, Influenza HA subtypes demonstrate divergent phenotypes for cleavage activation and pH of fusion: implications for host range and adaptation. *PLoS Pathog* **9**, e1003151 (2013).

104. L. R. Hoffman, I. D. Kuntz, J. M. White, Structure-based identification of an inducer of the low-pH conformational change in the influenza virus hemagglutinin: irreversible inhibition of infectivity. *J Virol* **71**, 8808-8820 (1997).

105. C. M. Carr, C. Chaudhry, P. S. Kim, Influenza hemagglutinin is spring-loaded by a metastable native conformation. *Proc Natl Acad Sci U S A* **94**, 14306-14313 (1997).

106. R. M. DuBois *et al.*, Acid stability of the hemagglutinin protein regulates H5N1 influenza virus pathogenicity. *PLoS Pathog* **7**, e1002398 (2011).

107. S. Herfst *et al.*, Airborne transmission of influenza A/H5N1 virus between ferrets. *Science* **336**, 1534-1541 (2012).

108. M. Imai *et al.*, Experimental adaptation of an influenza H5 HA confers respiratory droplet transmission to a reassortant H5 HA/H1N1 virus in ferrets. *Nature* **486**, 420-428 (2012).

109. M. Russier *et al.*, Molecular requirements for a pandemic influenza virus: An acid-stable hemagglutinin protein. *Proc Natl Acad Sci U S A* **113**, 1636-1641 (2016).

110. H. Zaraket, O. A. Bridges, C. J. Russell, The pH of activation of the hemagglutinin protein regulates H5N1 influenza virus replication and pathogenesis in mice. *J Virol* **87**, 4826-4834 (2013).

111. M. Lipsitch *et al.*, Viral factors in influenza pandemic risk assessment. *Elife* **5**, (2016).

112. T. Takahashi *et al.*, The low-pH stability discovered in neuraminidase of 1918 pandemic influenza A virus enhances virus replication. *PLoS One* **5**, e15556 (2010).

113. M. Ohuchi, R. Ohuchi, K. Mifune, Demonstration of hemolytic and fusion activities of influenza C virus. *J Virol* **42**, 1076-1079 (1982).

114. F. Formanowski, S. A. Wharton, L. J. Calder, C. Hofbauer, H. Meier-Ewert, Fusion characteristics of influenza C viruses. *J Gen Virol* **71 (Pt 5)**, 1181-1188 (1990).

115. W. Mothes, A. L. Boerger, S. Narayan, J. M. Cunningham, J. A. Young, Retroviral entry mediated by receptor priming and low pH triggering of an envelope glycoprotein. *Cell* **103**, 679-689 (2000).

116. M. Cote, Y. M. Zheng, S. L. Liu, Receptor binding and low pH coactivate oncogenic retrovirus envelope-mediated fusion. *J Virol* **83**, 11447-11455 (2009).

117. N. R. Sharma *et al.*, Hepatitis C virus is primed by CD81 protein for low pH-dependent fusion. *J Biol Chem* **286**, 30361-30376 (2011).

118. G. Simmons *et al.*, Inhibitors of cathepsin L prevent severe acute respiratory syndrome coronavirus entry. *Proc Natl Acad Sci U S A* **102**, 11876-11881 (2005).

119. K. Schornberg *et al.*, Role of endosomal cathepsins in entry mediated by the Ebola virus glycoprotein. *J Virol* **80**, 4174-4178 (2006).

120. T. Krey, H. J. Thiel, T. Rumenapf, Acid-resistant bovine pestivirus requires activation for pH-triggered fusion during entry. *J Virol* **79**, 4191-4200 (2005).

121. B. Kumar *et al.*, The emerging influenza virus threat: status and new prospects for its therapy and control. *Arch Virol* **163**, 831-844 (2018).

122. A. Stevaert, L. Naesens, The Influenza Virus Polymerase Complex: An Update on Its Structure, Functions, and Significance for Antiviral Drug Design. *Med Res Rev* **36**, 1127-1173 (2016).

123. E. Hoffmann, G. Neumann, Y. Kawaoka, G. Hobom, R. G. Webster, A DNA transfection system for generation of influenza A virus from eight plasmids. *Proc Natl Acad Sci U S A* **97**, 6108-6113 (2000).

124. E. de Wit *et al.*, Efficient generation and growth of influenza virus A/PR/8/34 from eight cDNA fragments. *Virus Res* **103**, 155-161 (2004).

125. A. Mostafa, P. Kanrai, J. Ziebuhr, S. Pleschka, Improved dual promotor-driven reverse genetics system for influenza viruses. *J Virol Methods* **193**, 603-610 (2013).

126. G. Neumann, K. Fujii, Y. Kino, Y. Kawaoka, An improved reverse genetics system for influenza A virus generation and its implications for vaccine production. *Proc Natl Acad Sci U S A* **102**, 16825-16829 (2005).

127. O. G. Engelhardt, Many ways to make an influenza virus--review of influenza virus reverse genetics methods. *Influenza Other Respir Viruses* **7**, 249-256 (2013).

128. S. Pleschka *et al.*, A plasmid-based reverse genetics system for influenza A virus. *J Virol* **70**, 4188-4192 (1996).
129. E. Fodor *et al.*, Rescue of influenza A virus from recombinant DNA. *J Virol* **73**, 9679-9682 (1999).
130. E. Hoffmann *et al.*, Rescue of influenza B virus from eight plasmids. *Proc Natl Acad Sci U S A* **99**, 11411-11416 (2002).
131. B. Crescenzo-Chaigne, S. van der Werf, Rescue of influenza C virus from recombinant DNA. *J Virol* **81**, 11282-11289 (2007).
132. E. de Wit *et al.*, A reverse-genetics system for Influenza A virus using T7 RNA polymerase. *J Gen Virol* **88**, 1281-1287 (2007).
133. K. Pachler, J. Mayr, R. Vlasak, A seven plasmid-based system for the rescue of influenza C virus. *J Mol Genet Med* **4**, 239-246 (2010).
134. N. Hengrung *et al.*, Crystal structure of the RNA-dependent RNA polymerase from influenza C virus. *Nature* **527**, 114-117 (2015).
135. B. F. Koel *et al.*, Substitutions near the receptor binding site determine major antigenic change during influenza virus evolution. *Science* **342**, 976-979 (2013).
136. E. Takashita *et al.*, Intrinsic temperature sensitivity of influenza C virus hemagglutinin-esterase-fusion protein. *J Virol* **86**, 13108-13111 (2012).
137. W. Zhu *et al.*, A reporter system for assaying influenza virus RNP functionality based on secreted Gaussia luciferase activity. *Virol J* **8**, 29 (2011).
138. C. Li, M. Hatta, S. Watanabe, G. Neumann, Y. Kawaoka, Compatibility among polymerase subunit proteins is a restricting factor in reassortment between equine H7N7 and human H3N2 influenza viruses. *J Virol* **82**, 11880-11888 (2008).
139. C. Isel, S. Munier, N. Naffakh, Experimental Approaches to Study Genome Packaging of Influenza A Viruses. *Viruses* **8**, (2016).
140. M. Gerber, C. Isel, V. Moules, R. Marquet, Selective packaging of the influenza A genome and consequences for genetic reassortment. *Trends Microbiol* **22**, 446-455 (2014).
141. J. Yu *et al.*, Development and Characterization of a Reverse-Genetics System for Influenza D Virus. *J Virol* **93**, (2019).

142. H. Ishida *et al.*, Establishment of a Reverse Genetics System for Influenza D Virus. *J Virol*, (2020).

143. Q. Peng *et al.*, Structural insight into RNA synthesis by influenza D polymerase. *Nat Microbiol* **4**, 1750-1759 (2019).

144. A. Donchet *et al.*, The structure of the nucleoprotein of Influenza D shows that all Orthomyxoviridae nucleoproteins have a similar NPCORE, with or without a NPTAIL for nuclear transport. *Sci Rep* **9**, 600 (2019).

145. A. Portela, P. Digard, The influenza virus nucleoprotein: a multifunctional RNA-binding protein pivotal to virus replication. *J Gen Virol* **83**, 723-734 (2002).

146. W. H. Chan *et al.*, Functional analysis of the influenza virus H5N1 nucleoprotein tail loop reveals amino acids that are crucial for oligomerization and ribonucleoprotein activities. *J Virol* **84**, 7337-7345 (2010).

147. Q. Ye, R. M. Krug, Y. J. Tao, The mechanism by which influenza A virus nucleoprotein forms oligomers and binds RNA. *Nature* **444**, 1078-1082 (2006).

148. I. Mena *et al.*, Mutational analysis of influenza A virus nucleoprotein: identification of mutations that affect RNA replication. *J Virol* **73**, 1186-1194 (1999).

149. A. Honda, K. Ueda, K. Nagata, A. Ishihama, RNA polymerase of influenza virus: role of NP in RNA chain elongation. *J Biochem* **104**, 1021-1026 (1988).

150. L. Turrell, J. W. Lyall, L. S. Tiley, E. Fodor, F. T. Vreede, The role and assembly mechanism of nucleoprotein in influenza A virus ribonucleoprotein complexes. *Nat Commun* **4**, 1591 (2013).

151. R. Wang *et al.*, Autophagy Promotes Replication of Influenza A Virus In Vitro. *J Virol* **93**, (2019).

152. D. Dornfeld, P. P. Petric, E. Hassan, R. Zell, M. Schwemmle, Eurasian Avian-Like Swine Influenza A Viruses Escape Human MxA Restriction through Distinct Mutations in Their Nucleoprotein. *J Virol* **93**, (2019).

153. C. M. Deeg *et al.*, In vivo evasion of MxA by avian influenza viruses requires human signature in the viral nucleoprotein. *J Exp Med* **214**, 1239-1248 (2017).

154. N. R. Meyerson *et al.*, Nuclear TRIM25 Specifically Targets Influenza Virus Ribonucleoproteins to Block the Onset of RNA Chain Elongation. *Cell Host Microbe* **22**, 627-638 e627 (2017).

155. R. Youil *et al.*, Comparative study of influenza virus replication in Vero and MDCK cell lines. *J Virol Methods* **120**, 23-31 (2004).

156. A. Mehle, J. A. Doudna, A host of factors regulating influenza virus replication. *Viruses* **2**, 566-573 (2010).

157. M. N. Matrosovich, T. Y. Matrosovich, T. Gray, N. A. Roberts, H. D. Klenk, Human and avian influenza viruses target different cell types in cultures of human airway epithelium. *Proc Natl Acad Sci U S A* **101**, 4620-4624 (2004).

158. S. Boivin, S. Cusack, R. W. Ruigrok, D. J. Hart, Influenza A virus polymerase: structural insights into replication and host adaptation mechanisms. *J Biol Chem* **285**, 28411-28417 (2010).

159. W. Zheng, Y. J. Tao, Structure and assembly of the influenza A virus ribonucleoprotein complex. *FEBS Lett* **587**, 1206-1214 (2013).

160. O. Poch, I. Sauvaget, M. Delarue, N. Tordo, Identification of four conserved motifs among the RNA-dependent polymerase encoding elements. *EMBO J* **8**, 3867-3874 (1989).

161. A. Dias *et al.*, The cap-snatching endonuclease of influenza virus polymerase resides in the PA subunit. *Nature* **458**, 914-918 (2009).

162. E. Fodor *et al.*, A single amino acid mutation in the PA subunit of the influenza virus RNA polymerase inhibits endonucleolytic cleavage of capped RNAs. *J Virol* **76**, 8989-9001 (2002).

163. D. Guilligay *et al.*, The structural basis for cap binding by influenza virus polymerase subunit PB2. *Nat Struct Mol Biol* **15**, 500-506 (2008).

164. M. Hatta *et al.*, Growth of H5N1 influenza A viruses in the upper respiratory tracts of mice. *PLoS Pathog* **3**, 1374-1379 (2007).

165. J. Steel, A. C. Lowen, S. Mubareka, P. Palese, Transmission of influenza virus in a mammalian host is increased by PB2 amino acids 627K or 627E/701N. *PLoS Pathog* **5**, e1000252 (2009).

166. M. Ozawa *et al.*, Impact of amino acid mutations in PB2, PB1-F2, and NS1 on the replication and pathogenicity of pandemic (H1N1) 2009 influenza viruses. *J Virol* **85**, 4596-4601 (2011).

167. S. Szepanski, H. J. Gross, R. Brossmer, H. D. Klenk, G. Herrler, A single point mutation of the influenza C virus glycoprotein (HEF) changes the viral receptor-binding activity. *Virology* **188**, 85-92 (1992).

168. T. Zurcher, G. Luo, P. Palese, Mutations at palmitylation sites of the influenza virus hemagglutinin affect virus formation. *J Virol* **68**, 5748-5754 (1994).

169. Y. Muraki *et al.*, A mutation on influenza C virus M1 protein affects virion morphology by altering the membrane affinity of the protein. *J Virol* **81**, 8766-8773 (2007).

170. T. Liu, Z. Ye, Restriction of viral replication by mutation of the influenza virus matrix protein. *J Virol* **76**, 13055-13061 (2002).

171. M. Mibayashi *et al.*, Inhibition of retinoic acid-inducible gene I-mediated induction of beta interferon by the NS1 protein of influenza A virus. *J Virol* **81**, 514-524 (2007).

172. M. U. Gack *et al.*, Influenza A virus NS1 targets the ubiquitin ligase TRIM25 to evade recognition by the host viral RNA sensor RIG-I. *Cell Host Microbe* **5**, 439-449 (2009).

173. Z. Li *et al.*, The NS1 gene contributes to the virulence of H5N1 avian influenza viruses. *J Virol* **80**, 11115-11123 (2006).

174. J. Ping *et al.*, Genomic and protein structural maps of adaptive evolution of human influenza A virus to increased virulence in the mouse. *PLoS One* **6**, e21740 (2011).

175. M. Selman, S. K. Dankar, N. E. Forbes, J. J. Jia, E. G. Brown, Adaptive mutation in influenza A virus non-structural gene is linked to host switching and induces a novel protein by alternative splicing. *Emerg Microbes Infect* **1**, e42 (2012).

176. A. K. Ng *et al.*, Structure of the influenza virus A H5N1 nucleoprotein: implications for RNA binding, oligomerization, and vaccine design. *FASEB J* **22**, 3638-3647 (2008).

177. A. K. Ng *et al.*, Structural basis for RNA binding and homo-oligomer formation by influenza B virus nucleoprotein. *J Virol* **86**, 6758-6767 (2012).

178. L. Turrell, E. C. Hutchinson, F. T. Vreede, E. Fodor, Regulation of influenza A virus nucleoprotein oligomerization by phosphorylation. *J Virol* **89**, 1452-1455 (2015).

179. L. Chen *et al.*, Amino Acid Substitution K470R in the Nucleoprotein Increases the Virulence of H5N1 Influenza A Virus in Mammals. *Front Microbiol* **8**, 1308 (2017).

180. Z. Sheng *et al.*, Identification and characterization of viral defective RNA genomes in influenza B virus. *J Gen Virol* **99**, 475-488 (2018).